

Washington University in St. Louis

Washington University Open Scholarship

All Theses and Dissertations (ETDs)

January 2009

Identification and Characterization of a Xylosylphosphotransferase of *Cryptococcus neoformans*

Morgann Reilly

Washington University in St. Louis

Follow this and additional works at: <https://openscholarship.wustl.edu/etd>

Recommended Citation

Reilly, Morgann, "Identification and Characterization of a Xylosylphosphotransferase of *Cryptococcus neoformans*" (2009). *All Theses and Dissertations (ETDs)*. 292.

<https://openscholarship.wustl.edu/etd/292>

This Dissertation is brought to you for free and open access by Washington University Open Scholarship. It has been accepted for inclusion in All Theses and Dissertations (ETDs) by an authorized administrator of Washington University Open Scholarship. For more information, please contact digital@wumail.wustl.edu.

WASHINGTON UNIVERSITY IN ST. LOUIS

Division of Biology and Biomedical Sciences
Molecular Microbiology and Microbial Pathogenesis Program
Department of Molecular Microbiology

Dissertation Examination Committee:

Tamara L. Doering, Chair

Daniel E. Goldberg

David B. Haslam

Stuart A. Kornfeld

Jennifer K. Lodge

IDENTIFICATION AND CHARACTERIZATION OF A
XYLOSYLPHOSPHOTRANSFERASE OF *CRYPTOCOCCUS NEOFORMANS*

by

Morgann Claire Reilly

A dissertation presented to the
Graduate School of Arts and Sciences
of Washington University in
partial fulfillment of the
requirements for the degree
of Doctor of Philosophy

December 2009

Saint Louis, Missouri

ABSTRACT OF THE DISSERTATION

Cryptococcus neoformans is an environmental yeast and an opportunistic pathogen capable of causing a meningoencephalitis in human hosts. The organism produces an extensive polysaccharide capsule that is unique among pathogenic fungi and absolutely required for its virulence. Work in the Doering laboratory on the capsule and other glycoconjugates of *C. neoformans* has focused on the identification of glycosyltransferases, enzymes that catalyze the transfer of a sugar moiety from an active donor to a specific acceptor, creating a particular linkage. Previous work demonstrated that xylose residues, derived from the nucleotide sugar UDP-xylose, are necessary for cryptococcal virulence. An assay to detect xylosyltransferase activity was developed in the laboratory using a radiolabeled UDP-xylose donor, a dimannose acceptor, and protein fractions from *C. neoformans* as the source of enzymatic activity. Using this assay, several discrete xylosyltransferase activities have been detected, including one that depends on the presence of manganese cations as a cofactor. The identification and characterization of the protein responsible for this activity has been the focus of these dissertation studies. The product of the manganese-dependent xylosyltransferase activity was analyzed by mass spectrometry and NMR and found to be xylose- α -phosphate-6-mannose- α -1,3-mannose, indicating that the enzyme responsible is, unexpectedly, a xylosylphosphotransferase (Xpt1p). There are no reports in the literature of similar glycan structures, suggesting that Xpt1p is a novel enzyme capable of generating a unique sugar linkage. The locus encoding Xpt1p activity was identified based on limited

homology to a known mammalian glycosylphosphotransferase and confirmed by activity studies of a deletion mutant. Xpt1p was subsequently shown to prefer the donor and acceptor molecules UDP-xylose and mannose, respectively. It was further found to play a role in the glycosylation of cellular proteins, in particular the synthesis of *O*-linked glycan structures, and has been suggested to exist in a multimeric protein complex. This thesis details these studies of Xpt1p and considers the future directions of this research. Altogether, this work has broadened our understanding of glycan synthesis in general and the synthesis of cryptococcal glycans in particular.

ACKNOWLEDGEMENTS

My graduate career has been longer than most and somewhat unusual in that I spent a significant amount of time in two labs during my time at Washington University. Therefore, there are many people I would like and need to thank for their support over the last eight and a half years.

I will begin at the beginning by thanking Joseph St. Geme for taking me into his lab as a naïve first-year graduate student and for later respecting my decision to remain at Washington University when the lab moved to another institution. The St. Geme lab was a great place to work and I would like to acknowledge all my labmates: Amy Buscher, Deborah Cholon, Shane Cotter, Susan Grass, Twyla Juehne, Thomas Kehl-Fie, Sven Laarmann, Nicholas Piotrowski, Amanda Sheets, Lucas Starnes, Soila Sukupolvi-Petty, and Neil Surana. I would especially like to thank Amy for teaching me how to run a well-controlled experiment; Shane for reminding me of the bigger picture; Thomas, my Saturday morning work-buddy; and Luke, my lab brother. My first lab came with a first thesis proposal and therefore a first thesis committee, so I would like to thank Virginia Miller (chair), Michael Caparon, Tamara Doering, Daniel Goldberg, David Haslam, and Andrew Pekosz for their time.

I would like to further thank Tamara Doering for welcoming me into her lab as a hardened fourth-year student when I was struggling to figure out whether I even wanted to continue in science and for having faith in my project even when I did not. I would like to acknowledge all the members of the Doering lab whom I worked with over the years:

Indrani Bose, Cara Griffith, Brian Haynes, Elizabeth Held, Myong-Ju Kim, Stacey Klutts, Pardeep Kumar, Hong Liu, Colleen Skau, Michal Skowrya, Matthew Williams, Meng Yang, and Aki Yoneda. I would particularly like to thank Stacey, without whom I would know nothing about protein purification; and Aki, my lab sister. Of course, I also need to thank the members of my current thesis committee, David Haslam (chair), Jacques Baenziger, Daniel Goldberg, Stuart Kornfeld, and Jennifer Lodge for their guidance over the years. I would also like to include William Goldman and Maurine Linder, both of whom served as chairs of my committee for a time before leaving take chairman positions other universities.

Finally, I would like to thank my friends and family who made it possible to come through this in the end. First, my grad school friends, for helping to make St. Louis a home for me: Kelly Barton, Heather Christensen, Holly Epple, Scott Hughes, Thomas Kehl-Fie, Colin Kietzman, Ellen Langer, N'Goundo Magassa, Julian Meeks, Celeste Newby, Julie O'Neal, Jason Rosch, Regina Rowe, Lucas Starnes, Justin Weinbaum, and Aki Yoneda. I also thank the friends I knew before grad school, for reminding me that there was more to life than research: Marina Chow, Emily Manning, Louisa Pyle, Tara Simms, Brazee Smith, Julie Stoltz, Sara Streett, Lia Thomas, and Elizabeth Walters. Last, but certainly not least, I thank my family, who I suspect think I'm a little crazy for having done this, but who love and support me all the same: my parents, Dianne and Gary Reilly; my sister, Guinevere Reilly; and my grandparents, Arthur and Una Nolder.

TABLE OF CONTENTS

Title page	i
Abstract.....	ii
Acknowledgements	iv
Table of contents.....	vi
List of figures.....	ix
List of tables	xii

Chapter 1. *Cryptococcus neoformans* and the biosynthesis of fungal and yeast glycans

Cryptococcus and cryptococcosis.....	2
Fungal glycan synthesis	7
Precursors for glycan synthesis.....	7
Glycosyltransferases	9
Protein glycosylation.....	12
Glycolipids.....	23
Cell wall polymers	28
Intracellular glycans	32
Exopolysaccharides.....	34
Xylose in the cryptococcal cell	37
Synthesis of UDP-Xyl.....	37
Xylosyltransferases	39

Acknowledgements	42
Abbreviations used	42
References	43

Chapter II. A novel xylosylphosphotransferase activity discovered in *Cryptococcus neoformans*

Abstract	63
Introduction	64
Experimental procedures	67
Results	79
Discussion	97
Acknowledgements	100
Abbreviations used	100
References	101

Chapter III. A xylosylphosphotransferase of *Cryptococcus neoformans* functions in protein glycosylation

Abstract	108
Introduction	109
Experimental procedures	112
Results	120
Discussion	133

Acknowledgements	136
Abbreviations used	136
References	137

Chapter IV. Multimerization of a xylosylphosphotransferase in *Cryptococcus neoformans*

Abstract	145
Introduction	146
Experimental procedures	149
Results	155
Discussion	162
Acknowledgements	164
Abbreviations used	164
References	165

Chapter V. Future directions and conclusions

Future directions	168
Conclusions	175
Acknowledgements	176
Abbreviations used	176
References	177

LIST OF FIGURES

Chapter 1. *Cryptococcus neoformans* and the biosynthesis of fungal and yeast glycans

Figure 1. Images of <i>C. neoformans</i>	6
Figure 2. <i>N</i> -linked glycosylation in <i>S. cerevisiae</i> : core synthesis and transfer....	14
Figure 3. <i>N</i> -linked glycosylation in <i>S. cerevisiae</i> : ER core processing and Golgi processing of core-type structures.....	15
Figure 4. <i>N</i> -linked glycosylation in <i>S. cerevisiae</i> : Golgi processing of highly mannosylated structures	17
Figure 5. <i>O</i> -linked glycosylation in <i>S. cerevisiae</i>	19
Figure 6. <i>S. cerevisiae</i> GPI-anchor synthesis and addition to protein.....	21
Figure 7. GIPC synthesis in <i>S. cerevisiae</i>	25
Figure 8. Glycosylceramide synthesis in fungi	27
Figure 9. Repeating units of GXM and GXMGal capsular polysaccharides in <i>C. neoformans</i>	35
Figure 10. Synthesis of UDP-Xyl.....	38

Chapter II. A novel xylosylphosphotransferase activity discovered in *Cryptococcus neoformans*

Supplemental Figure 1. Plasmid for RNA interference in <i>C. neoformans</i>	73
Figure 1. Xylosyltransferase activities of <i>C. neoformans</i>	80
Figure 2. Xylosyltransferase activities in <i>CXT1</i> and <i>CXT2</i> mutants	81

Figure 3. Xpt1p product composition	83
Figure 4. Xpt1p product structure.....	85
Figure 5. RNA interference targeting of the <i>XPT1</i> gene	88
Figure 6. Deletion of <i>XPT1</i>	90
Figure 7. Competition of Xpt1p activity.....	91
Figure 8. Donor substrates of Xpt1p.....	93
Figure 9. Xylosyltransferase activities of Xpt1p-HA	94
Figure 10. Acceptor substrates of Xpt1p	96

Chapter III. A xylosylphosphotransferase of *Cryptococcus neoformans* functions in protein glycosylation

Figure 1. Xylosyltransferase activities in <i>C. neoformans</i>	121
Figure 2. Xylosyltransferase activities in the <i>C. neoformans</i> species complex	122
Figure 3. Capsule morphology in wild-type and <i>xpt1Δ</i> mutant cells	124
Figure 4. Protein glycosylation studies of <i>xpt1Δ</i> mutant	126
Figure 5. <i>O</i> -linked glycan profiles.....	128
Figure 6. Filtered scans showing Xyl-P-Man structures.....	129
Figure 7. Fragmentation of Xyl-P-Man <i>O</i> -glycans	130-131
Figure 8. Xpt1p-HA localization.....	132

Chapter IV. Multimerization of a xylosylphosphotransferase in *Cryptococcus neoformans*

Figure 1. Xylosyltransferase activities of <i>C. neoformans</i>	154
Figure 2. Molecular weight calculations for the manganese-dependent xylosyltransferase activity.....	157
Figure 3. Deletion and complementation of <i>XPT1</i>	159
Figure 4. Immunoblot of Xpt1p-HA.....	160
Figure 5. Xylosyltransferase activities of Xpt1p-HA	161

LIST OF TABLES

Chapter II. A novel xylosylphosphotransferase activity discovered in *Cryptococcus neoformans*

Supplemental Table 1. Primers used in these studies.....	67
Table 1. <i>C. neoformans</i> strains used in these studies.....	68
Table 2. Known glycosylphosphotransferases from other organisms	87

Chapter III. A xylosylphosphotransferase of *Cryptococcus neoformans* functions in protein glycosylation

Table 1. <i>C. neoformans</i> strains used in these studies.....	112
---	-----

Chapter IV. Multimerization of a xylosylphosphotransferase in *Cryptococcus neoformans*

Table 1. <i>C. neoformans</i> strains used in these studies.....	146
Table 2. Partial purification of the manganese-dependent xylosyltransferase activity from CAP67 <i>cxt1</i> Δ <i>cxt2</i> Δ	155
Supplemental Table 1. Affinity resins tested during protein purification studies	156

CHAPTER I

CRYPTOCOCCUS NEOFORMANS* AND THE BIOSYNTHESIS OF FUNGAL AND YEAST GLYCANS

Morgann C. Reilly

Department of Molecular Microbiology, Washington University School of Medicine,
St. Louis, MO 63110, USA.

* *Portions of this chapter were previously published; reprinted with permission:*

Reilly M.C., and Doering T.L. 2009. Biosynthesis of fungal and yeast glycans. In: Moran A.P., Holst O., Brennan P.J., von Itzstein M. (editors), *Microbial Glycobiology*. Elsevier Inc., San Diego: 393-412.

Klutts J.S., Yoneda A., Reilly M.C., Bose I., and Doering T.L. 2006. Glycosyltransferases and their products: cryptococcal variations on fungal themes. *FEMS Yeast Research* 6: 499-512.

This introduction sets the stage for the main focus of my thesis, a unique xylosylphosphotransferase that I discovered in the fungal pathogen *Cryptococcus neoformans*. The first section introduces the organism and the disease it causes. This is followed by an overview of the glycan and glycoconjugate structures found in fungi and their biosynthetic pathways. Finally, I introduce the research of the Doering laboratory and the reasons behind our particular interest in the xylosyltransferases of *C. neoformans*.

CRYPTOCOCCUS AND CRYPTOCCOSIS

Cryptococcus neoformans is a free-living, saprophytic yeast of the fungal phylum *Basidiomycota*. Unlike other members of the genus, *C. neoformans* regularly infects mammalian hosts and is considered an opportunistic pathogen of humans. Originally classified as a single species that could be differentiated into four serotypes (A-D), *C. neoformans* is now referred to as a species complex consisting of separate species and varieties (1): *C. neoformans* var. *grubii* (serotype A), *C. neoformans* var. *neoformans* (serotype D), and *C. gattii* (originally serotypes B and C). *C. neoformans* var. *grubii* and var. *neoformans* have been isolated worldwide from soil and avian excreta, and are often associated with disease in the immunocompromised population. In contrast, *C. gattii* is most often found in the tropical and sub-tropical regions of the world in association with certain trees, and characteristically infects immunocompetent individuals. Unless specified, the term *C. neoformans* when used here will collectively refer to members of all four historically defined serotypes.

Humans are colonized by *C. neoformans* via the inhalation of basidiospores or small yeast cells (2). During the primary infection of the lungs, the organism is typically isolated within a granuloma by the host immune system or eradicated completely without any symptomatic evidence of infection (3). If segregated within a granuloma, *C. neoformans* may reactivate at a later time following a change in the host's immune status. Although healthy individuals rarely exhibit symptoms of infection, serological studies indicate that a majority of adults have anti-cryptococcal antibodies and that most individuals are exposed in early childhood (4, 5). Depending on variables such as inoculum, isolate virulence, and host factors, the organism may disseminate (either acutely or following a period of latency) to extra-pulmonary sites throughout the human body. Although *C. neoformans* can cause localized infections in most organs, it demonstrates a particular tropism for the central nervous system (2). This can result in a meningoencephalitis that is fatal if left untreated.

The global incidence of cryptococcosis has risen markedly over the last several decades as a result of the HIV epidemic as well as the increasing use of immunosuppressive therapies in medicine (4). Existing anti-fungal regimens (amphotericin B, flucytosine, and fluconazole) have a limited ability to clear a *C. neoformans* infection and can have toxic side-effects (6). Thus even in developed countries the mortality from HIV-associated cryptococcal meningitis remains high, at 10-30%; in developing nations, where patients tend to present for treatment later and resources are more limited, cryptococcosis accounts for 13-44% of all deaths in HIV-infected patients (3). It has recently been estimated that the annual global burden of cryptococcal infections is nearly 1×10^6

cases, with fatalities numbering over 6×10^5 (7). As these statistics clearly indicate, the need to study this ‘opportunistic’ pathogen should not be underestimated.

C. neoformans has evolved a number of traits that allow it to survive within its mammalian hosts. The three classic virulence-associated phenotypes of *C. neoformans* are its ability to grow at higher (mammalian body) temperatures, the production of melanin, and the generation of a polysaccharide capsule. Although the idea of temperature tolerance as a virulence factor is unconventional, it should be remembered that the vast majority of fungal species are environmental organisms. Even *C. neoformans*, which can reproduce asexually in the human body (8), cannot mate at higher temperatures (9). It is fundamentally an environmental yeast: studies have demonstrated that *C. neoformans* is better able to withstand inhospitable growth conditions or the presence of anti-fungal agents at 25°C rather than 37°C (10, 11). Yet members of the *C. neoformans* species complex can survive at these higher temperatures, making them the only members of their genus to act as pathogens. Numerous loci have been identified in serial analysis of gene expression (SAGE; (12)) or DNA microarray (13) surveys as being transcriptionally regulated in response to temperature. Studies have demonstrated the role of various cell signaling molecules in temperature tolerance, including Ras1p (14), Mpk1 (15), Rac1p (16), and Cdc24 (17). In addition, a number of proteins involved in stress response pathways, such as thiol peroxidases (18), manganese superoxide dismutase (19), and trehalose-6-phosphate synthase (20), have been shown to be temperature-regulated. In order to survive in an environment as different from the soil as a mammalian host, *C. neoformans*

has evolved such that many cellular pathways are regulated in response to changes in the yeast's ambient temperature.

C. neoformans is also distinguished from other members of the *Cryptococcus* genus by the production of melanin (a negatively charged pigment) when grown on media containing diphenolic compounds (21, 22). Melanin has been found to play a protective role both in the environment and in the host. In the environment, melanin protects the cell against temperature fluctuations (23), the ionizing radiation of ultra-violet light (24), heavy metal toxicity (25), and hydrolytic enzymes like those found in bird guano (26). Non-melanizing mutants of *C. neoformans* show inhibited growth at 37°C (27), do not accumulate in brain tissues (28), and fail to produce lethal infections in mice (29). Phenotypes associated with melanin production include resistance to antibody-mediated phagocytosis (30) and protection from oxidation (31) as well as the inhibition of tumor necrosis factor alpha (TNF α) production and lymphoproliferation (32). Despite its link to virulence, there has been some debate as to whether or not melanin is generated by *C. neoformans* during infection (33, 34). It may be that oxidation resistance (35), and possibly other traits previously linked to melanin production, can be attributed to the activities of laccase, the enzyme that generates melanin (36). Whether directly or indirectly, however, melanization is linked to virulence in *C. neoformans*.

The most prominent virulence factor of *C. neoformans* is its extracellular capsule, which can be clearly seen in Figure 1. The capsule is primarily composed of two polysaccharide structures along with some mannoproteins (the structure and synthesis of these glycans is described in the following section). The cryptococcal capsule contributes sig-

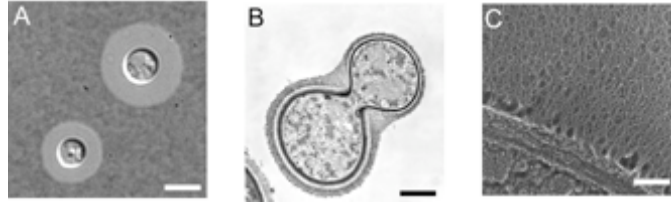


Figure 1. Images of *C. neoformans*. Panel A, differential interference contrast micrograph of cells that were mixed with India ink after induction of capsule formation by growth in low-iron medium. Bar, 3 μ M. Panel B, thin-section micrograph of a budding cell fixed in the presence of ruthenium red dye. Bar, 1 μ M. Panel C, quick-freeze, deep-etch image of the edge of a cell, with an arc of cell wall separating the cell interior (lower left) from the capsule fibers emanating outwards (upper right). Bar, 0.15 μ M. Figure from (142).

nificantly to the organism's evasion of the host's immune response by interfering with elements of both cellular and humoral immunity. The capsule polysaccharides are able to prevent the host from developing an antibody response (37, 38). In the absence of opsonins, macrophages will not phagocytose encapsulated *C. neoformans* (39), thereby inhibiting lymphocyte proliferation (40). Increased interleukin-10 (IL-10) production by monocytes in response to *C. neoformans* suppresses expression of class II major histocompatibility complex (MHC) molecules on monocytes, the proliferative T-cell response, and cytokine production (41, 42). Both TNF α and IL-1 β production are inhibited by the capsule polysaccharides (43); leukocyte migration in response to infection is diminished (44) and the maturation and activation of dendritic cells is limited (45). Thus the capsule plays a major role in the survival of *C. neoformans* in its hosts.

FUNGAL GLYCAN SYNTHESIS

Fungi produce a remarkable range of glycans and glycoconjugates. Here, I present an overview of fungal glycan biosynthesis, beginning with the precursor molecules utilized in the various biosynthetic pathways and proceeding to individual classes of glycoconjugates. The carbohydrate structures of the model yeast *Saccharomyces cerevisiae*, which have been extensively investigated, serve as the core of this section, with attention drawn to known variations on the biosynthetic processes as they occur in *C. neoformans* and other fungal species. Some of the glycosynthesis pathways of fungi present variations on general eukaryotic themes, while others are specific to these organisms. The latter is emphasized in the cases of pathogenic fungi given that unique aspects of biosynthesis may allow for the development of selective anti-fungal chemotherapies.

Precursors for glycan synthesis

In both eukaryotes and prokaryotes, glycan synthesis requires sugar donor molecules. These active precursors are usually either nucleotide triphosphate sugars or dolichol-phosphate sugars, depending on the synthetic context. For the purpose of this background discussion, the focus will be on mannose (Man), one of the more common monosaccharides in fungal glycans and a moiety about which much is known. Specific discussion of xylose (Xyl) precursors is included in final section of this chapter.

Nucleotide-linked sugar synthesis and localization. The activated nucleotide sugar donor of Man, GDP-Man, is synthesized from GTP and Man-1-phosphate (Man-1-P) in a reaction catalysed by GDP-mannose pyrophosphorylase. The Man-1-P is derived

either from the phosphorylation of Man obtained from the environment or originates within the cell when generated from other sugar phosphates or via other metabolic processes.

GDP-Mannose, like many other nucleotide sugars, is made in the cytosol. This presents a topological problem for cells that produce most of their glycoconjugates in the organelles of the secretory pathway. The cellular solution to this dilemma is to produce specific nucleotide sugar transporters (NSTs) to move these charged donor molecules across the membrane of the endoplasmic reticulum (ER) or Golgi apparatus. The NSTs are multi-membrane spanning proteins that act as antiporters, importing nucleotide sugars into an organelle in exchange for the corresponding nucleotide monophosphate. For example, the Golgi-localized GDP-Man transporter (Vrg4p in *S. cerevisiae*; (46)) imports GDP-Man in exchange for GMP; the latter is derived from the cleavage of the GDP produced when Man is transferred from the nucleotide sugar to a growing glycoconjugate.

The *S. cerevisiae* protein Vrg4p is essential, as are its homologs in the pathogens *Candida albicans* and *Candida glabrata* (47, 48). In contrast, *Cryptococcus neoformans*, a basidiomycetous fungal pathogen of humans with two functional GDP-Man transporters, is able to survive, albeit with poor growth, even in the absence of both proteins (49). Importantly, higher eukaryotes have no such proteins as NSTs: mammalian Golgi mannosylation uses lipid-linked Man as the donor for comparable secretory protein modification (see below). These transporters in pathogenic fungi thus represent potential drug targets. The occurrence and specificity of NSTs for other nucleotide sugars are discussed in several excellent reviews ((50-52).

Dolichol-linked sugar synthesis. Dolichol-linked sugars are critical donors of monosaccharide residues in the synthesis of eukaryotic glycan structures (reviewed in (53)). Again using Man as an example, dolichol phosphate mannose (Dol-P-Man) is formed on the cytosolic leaflet of the ER membrane by the enzyme dolichol phosphate mannose synthase (Dpm1p), which catalyses the transfer of Man from cytosolic GDP-Man to membrane-associated dolichol monophosphate (Dol-P). *S. cerevisiae* and the plant pathogen *Ustilago maydis* encode a Dpm1p with a hydrophobic region that localizes the protein to the ER. In contrast, the model fission yeast *Schizosaccharomyces pombe* encodes a Dpm1p without a transmembrane domain. To mediate the same reaction, the *S. pombe* Dpm1p therefore requires the presence of two additional proteins, Dpm2p and Dpm3p, which are thought to stabilize and localize the catalytic subunit (53). The lipid moiety of Dol-P-Man allows an unidentified flippase to translocate the active sugar donor to the luminal leaflet of the ER membrane where it is appropriately situated to participate in reactions of glycan synthesis. Dolichol may also be used as a platform for the assembly of larger biosynthetic intermediates; these compounds are discussed below in the context of protein glycosylation.

Glycosyltransferases

Glycosyltransferases catalyse the specific transfer of a monosaccharide moiety from an activated sugar donor to a distinct acceptor molecule in a particular linkage. Common sugar donors include nucleotide monophosphosugars, nucleotide diphosphosugars and dolichol-linked sugars. As will be discussed below, both saccharides as well

as non-saccharides, such as proteins and lipids, can serve as acceptor molecules. In eukaryotes, the reactions catalysed by glycosyltransferases often take place within the endoplasmic reticulum (ER)-Golgi pathway. Resident glycosyltransferases of these organelles exist as type II membrane proteins with a short N-terminal cytoplasmic domain, a membrane-spanning domain, a stem region, and a globular C-terminal luminal domain.

The transfer of a glycosyl moiety from one molecule to another can occur via either an inverting or retaining mechanism. In inverting glycosyltransferases, the deprotonated hydroxyl group of the acceptor attacks the C1 anomeric carbon of the sugar donor to form a glycosidic bond, resulting in an inversion of the configuration at C1 (54). The mechanism of retaining glycosyltransferases, in which a glycosidic bond is formed between the donor and acceptor while retaining the C1 configuration, is less clear. Glycosyltransferases typically require metal ion cofactors. Binding of the cofactor and/or the sugar donor molecule results in a conformational change in the protein. A number of these enzymes contain one or more flexible loop regions that re-order upon binding of the sugar donor to generate the acceptor-binding site. Once the glycosyl unit has transferred from the donor to the acceptor molecule, the saccharide product is released and the loop reverts to its native conformation, releasing any remaining moieties of the donor molecule (54).

Traditionally, glycosyltransferases were classified on the basis of their donor, acceptor, and product specificity, and identified by an Enzyme Commission (EC) number (55). With the availability of thousands of putative glycosyltransferase sequences from genome studies, a new classification scheme for these enzymes was proposed that did not

require knowledge of biochemical function. Instead, these enzymes are divided into families based on similarities in amino acid sequence to one or more founding members that have been biochemically characterized (56). A database of enzymes involved in carbohydrate metabolism (CAZy, carbohydrate active enzymes) organized according to this classification scheme is maintained by the Glycobiology unit at AFMB-CNRS in Marseille, France, and can be found on the internet at <http://www.cazy.org/index.html>. As of November 2009, the CAZy database contained 92 glycosyltransferase families that included 64 confirmed and putative enzymes from the *C. neoformans* var. *neoformans* JEC21 genome project.

The primary amino acid sequences of glycosyltransferases are typically very diverse, although the predicted proteins exhibit overall structural similarities. All glycosyltransferases contain distinct donor and acceptor binding domains connected by a linker region that forms the active site. On the basis of broader structural patterns, glycosyltransferases have been primarily divided into two superfamilies, GT-A and GT-B. The GT-A enzymes have two dissimilar domains: an N-terminal sugar donor-binding domain composed of several β -strands that are each flanked by α -helices to form a Rossmann-like fold, and a C-terminal acceptor binding domain made up largely of mixed β -sheets (54). Members of the GT-A family frequently have a three-residue DXD, EXD or equivalent motif that is involved in the binding of a metal ion (often Mg^{2+} or Mn^{2+}), although not all GT-A enzymes require such a cofactor and some lack this motif. Enzymes of the GT-B superfamily typically have two Rossmann-like folds that allow the acceptor molecule to bind at the N-terminus while the C-terminal domain is involved in binding the sugar do-

nor (54). Although some GT-B enzymes utilize metal ion cofactors, most do not and thus GT-Bs lack a DXD motif or its equivalent, further distinguishing them from GT-A molecules. Members of the GT-B superfamily do, however, exhibit a pattern of proline (Pro) and glycine (Gly) residues located within the donor-binding domain (57). In addition to the defined GT-A and GT-B superfamilies, there are a growing number of glycosyltransferases that do not fall into either of these categories on the basis of structural motifs or amino acid sequence (58-60). Although a number of authors have suggested the creation of additional glycosyltransferase superfamilies to accommodate these outliers, a consensus within the field has not yet been reached.

The formation of glycoconjugates often requires several glycosyltransferases working sequentially to generate the desired linear or branched structures. These glycosyltransferases may form large protein complexes, as with the *S. cerevisiae* M-Pol II enzyme complex discussed below (see '*N*-linked glycan synthesis' section). Functional redundancy of glycosyltransferases is also typical, as demonstrated by the *S. cerevisiae* PMT and Mnt families of mannosyltransferases that act in the *O*-linked glycosylation of proteins (see '*O*-linked glycan synthesis' section).

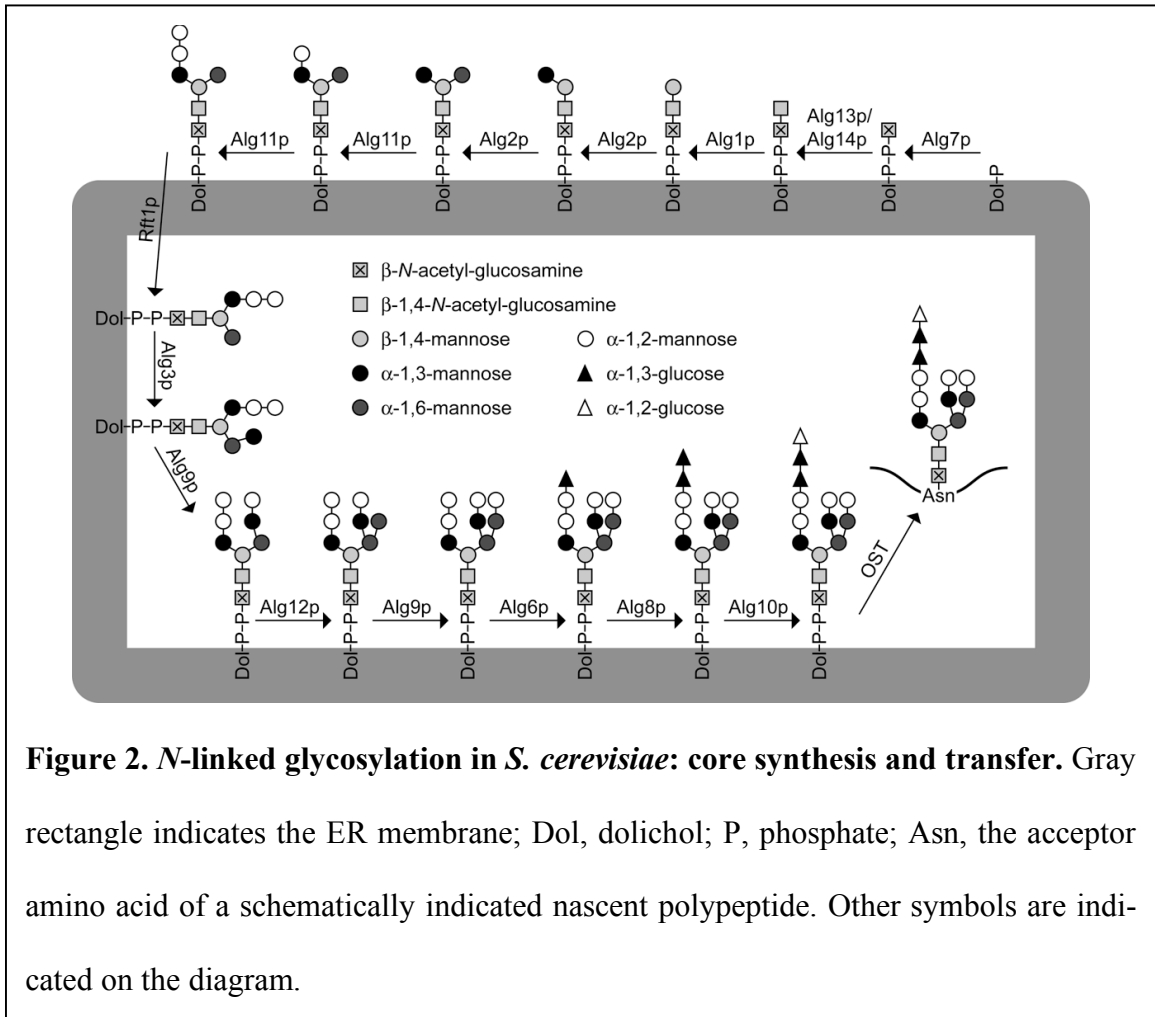
Protein glycosylation

The carbohydrate modifications of a glycoprotein can contribute to the final conformation, stability, function, and localization of the polypeptide. Glycans are typically associated with fungal proteins in one of three ways: *N*-glycosylation (where the glycan is linked to an asparagine (Asn) residue), *O*-glycosylation (where the glycan is linked to

the hydroxy group of serine (Ser) or threonine (Thr)), and GPI anchors (where the glycolipid is linked to a C-terminal amino acid). The transfer of these carbohydrate structures is initiated during or soon after the translocation of nascent polypeptide chains into the ER lumen. The core glycans are further elaborated by the actions of glycosidases and glycosyltransferases in the ER and Golgi as the protein traverses the secretory pathway, yielding a diverse array of structures.

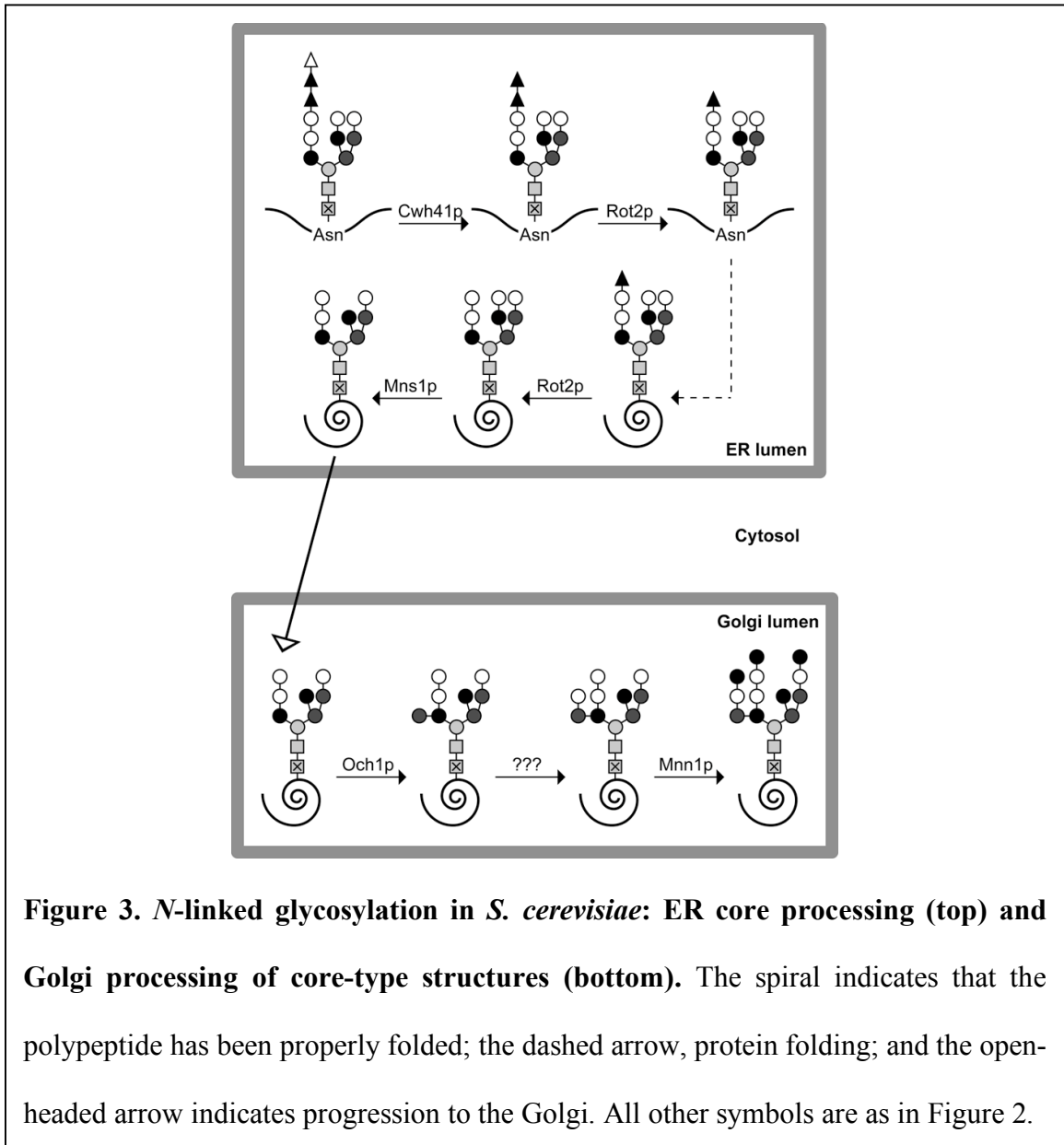
N-linked glycan synthesis. *N*-glycosylation begins with the assembly of a dolichol-linked oligosaccharide precursor at the cytoplasmic leaflet of the ER membrane (Figure 2; recently reviewed in (61)). In *S. cerevisiae*, the glycosylphosphotransferase Alg7p first transfers *N*-acetylglucosamine (GlcNAc)-P from UDP-GlcNAc to membrane-bound Dol-P to form Dol-PP-GlcNAc. A second GlcNAc residue is added by the dimer Alg13p/Alg14p (62, 63), and the structure is further modified by a series of mannosyltransferases (Alg1p, Alg2p and Alg11p) which add five mannose residues derived from GDP-Man (64). The resulting Dol-PP-GlcNAc₂Man₅ molecule is then translocated by the flippase Rft1p to the luminal leaflet of the ER (65).

Synthesis of the *N*-glycan precursor continues with the transfer of four Man residues from Dol-P-Man to the oligosaccharide core by the mannosyltransferases Alg3p, Alg12p, and Alg9p. Finally, the Dol-PP-GlcNAc₂Man₉ structure is capped with three glucose residues (from Dol-P-Glc) via the actions of the glucosyltransferases Alg6p, Alg8p, and Alg10p. The resulting Dol-PP-GlcNAc₂Man₉Glc₃ structure contains the complete core glycan that can be transferred from its dolichol anchor to a protein. This polypeptide modification occurs at the Asn residue of the sequence motif Asn-X-Ser/Thr



(where X is any amino acid except for Pro) and is catalysed by the oligosaccharyltransferase (OST) protein complex. In *S. cerevisiae*, the OST is comprised of at least eight proteins; the highly conserved Stt3p harbors the transferase activity of the complex and the other proteins mediate association of the diverse reaction substrates (66).

Following transfer of the $\text{GlcNAc}_2\text{Man}_9\text{Glc}_3$ core to the nascent polypeptide, two luminal glucosidases act upon the core glycan (Figure 3, top): α -glucosidase I (encoded by *CWH41*) removes the terminal α -1,2-Glc while α -glucosidase II (encoded by *ROT2*)



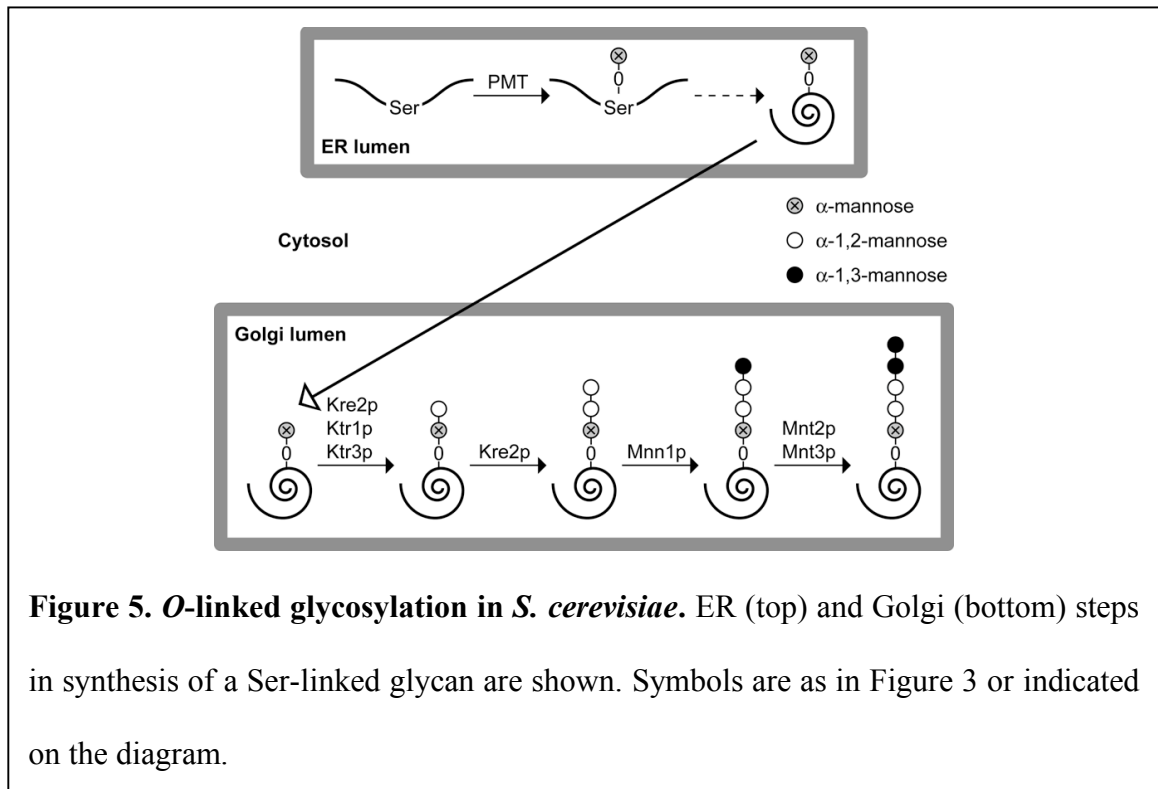
removes the distal α -1,3-Glc to yield $\text{GlcNAc}_2\text{Man}_9\text{Glc}$ (reviewed in (67)). In this monoglucosylated state, the unfolded polypeptide is recognized by molecular chaperones that assist in glycoprotein folding. (The role of N-linked glycans in protein quality control in the ER is an extensive subject that is beyond the scope of this chapter; the topic is thor-

oughly addressed in a review by (68).) Once the glycoprotein has achieved its proper conformation, it is released by the molecular chaperones and Rot2p removes the final Glc residue from the *N*-linked oligosaccharide. In *S. cerevisiae*, the resulting structure is further trimmed by the mannosidase Mns1p, which removes a single α -1,2-Man residue. The folded protein, with its GlcNAc₂Man₈ modification, is then transferred from the ER to the Golgi.

Fungi do not generate the ‘complex-type’ *N*-glycans typical of mammalian systems (69). Instead, the core oligosaccharide structures of *N*-linked glycans are either minimally modified (‘core-type’) or receive extensive modifications (‘highly mannosylated’). In *S. cerevisiae*, protein modifications involve Man addition exclusively. When a GlcNAc₂Man₈ modified polypeptide arrives in the Golgi apparatus, Och1p adds a single α -1,6-Man to the structure. A glycoprotein that will retain a core-type *N*-linked glycan structure is further modified at this new Man by an α -1,2-mannosyltransferase (the protein responsible has not yet been identified) that adds a single Man and by subsequent capping of secondary branches by the α -1,3-mannosyltransferase, Mnn1p (Figure 3, bottom). In contrast to these modest alterations, highly mannosylated *N*-linked glycans receive extensive modifications beyond the actions of Och1p (Figure 4). First, the enzyme complex mannan polymerase I (M-Pol I) modifies the new Man with a linear branch of α -1,6-linked Man that is upwards of ten residues in length; a second mannan polymerase complex (M-Pol II) extends this branch with up to fifty more α -1,6-Man residues. These α -1,6-Man are elaborated by the addition of α -1,2-Man by Mnn2p or Mnn5p, and Man-P by the oligomer Mnn4p/Mnn6p. Finally, the secondary branches of these extensive Man

pombe and *Kluyveromyces lactis*, a yeast used in industry, do not appear to have a functional homolog of the mannosidase Mns1p, such that proteins are transferred from the ER to the Golgi with intact GlcNAc₂Man₉ structures. The greatest diversity with regard to the number and linkages of Man residues occurs within the Golgi apparatus, where elaboration of the linear α -1,6-Man branch can create a structure of up to two hundred Man residues. Here, the model mold *Neurospora crassa* and several members of the *Aspergillus* genus are unusual in their incorporation of galactofuranose residues into some *N*-linked glycan structures (71-73).

***O*-linked glycan synthesis.** Fungal *O*-glycosylation is initiated in the ER lumen with the transfer of a Man residue from Dol-P-Man to a Ser or Thr residue by protein *O*-mannosyltransferases (PMTs; Figure 5, top). Unlike *N*-glycosylation, no consensus sequence dictating which residues in a polypeptide will be *O*-glycosylated has been elucidated. Seven PMTs have been identified in *S. cerevisiae*. These integral membrane proteins exhibit 50-80% homology and are classified into three major subfamilies based on similarities in hydrophathy profiles: the PMT1 family (Pmt1p and Pmt5), the PMT2 family (Pmt2p, Pmt3p and Pmt6p) and the PMT4 family (Pmt4p) (detailed in (74, 75). Members of the PMT1 and PMT2 families dimerize with one another while Pmt4p forms homomeric complexes; the resulting Pmt complexes exhibit varying substrate specificities. In *S. cerevisiae*, PMT activity is essential, although redundancy in the proteins allows viability of some single and double mutants (discussed in (75)). Attesting to the importance of *O*-glycosylation in fungi, strains with PMT defects exhibit alterations in growth, cell wall integrity, morphology, development, and virulence. These effects may be a di-



direct consequence of glycan loss or may be due to the role of these modifications in mediating protein stability, localization, or function.

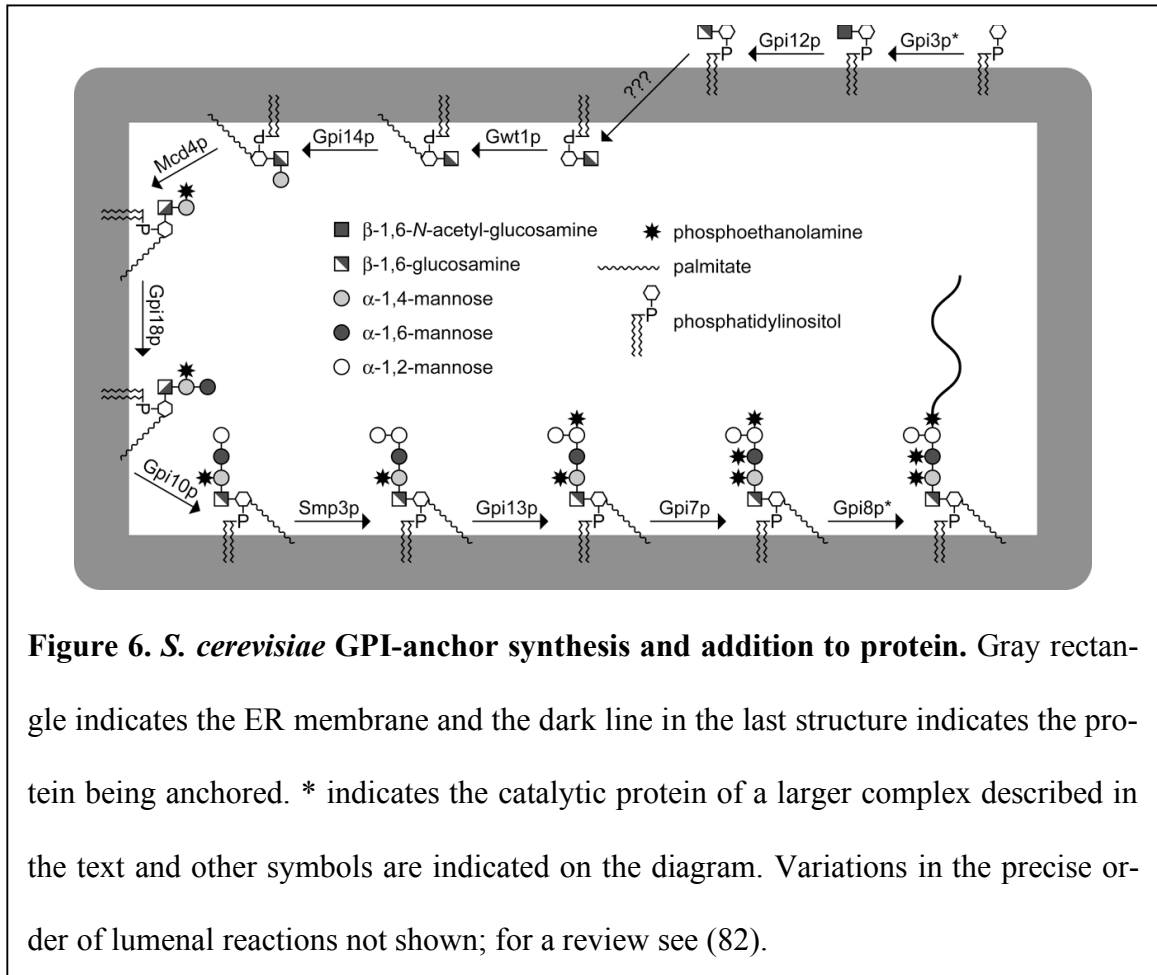
Echoing the progress of *N*-glycosylation, the core Man of *O*-glycans that is added to protein in the ER is elaborated in the Golgi apparatus, where one to six Man residues derived from GDP-Man may be added to extend the linear chain (Figure 5, bottom). Mannose may be added in α -1,2-linkages through the actions of the KTR family (Ktr1p, Ktr3p and Kre2p) or in α -1,3-linkages by the MNN1 family (Mnn1p, Mnt2p and Mnt3p). *S. cerevisiae* also links Man-P to the second Man in some *O*-glycan structures (76).

The process of *O*-glycosylation described above for *S. cerevisiae* is thought to proceed similarly in other fungal species, although some variations have been identified. For example, while all fungi have members of each of the three PMT subfamilies identi-

fied in *S. cerevisiae*, many do not exhibit the same extent of redundancy. In contrast to *S. cerevisiae*, *C. albicans* has only five PMTs; other species, including *S. pombe* and the filamentous fungus *Aspergillus nidulans*, encode just one enzyme in each subfamily (77). The genome of *C. neoformans* contains a single homologue each of *PMT1*, *PMT2*, and *PMT4*; *PMT2* is an essential gene while deletion of either *PMT1* or *PMT4* leads to serious defects in the morphology and integrity of the cell(78, 79).

Variation in *O*-glycan structures suggests that *O*-glycan synthesis in many fungi involves enzymes beyond those identified in *S. cerevisiae*, which tends to utilize a simple repertoire of sugars. For example, *S. pombe* adds Gal residues to the non-reducing end of short α -1,2-Man chains (80). Studies of the environmental yeast *Cryptococcus laurentii* have defined three *O*-linked glycans: [Gal- α (1 \rightarrow 6)]₁₀-Gal- β -Man; Man- α (1 \rightarrow 2)-Man- α (1 \rightarrow 2)-Man; and Man- α (1 \rightarrow 2)-Man- α (1 \rightarrow 6)-Man- α (1 \rightarrow 3)[Xyl- β (1 \rightarrow 2)]-Man. Biochemical studies have allowed detection of enzyme activities potentially involved in most of the synthetic steps required to generate these structures (reviewed in (81)). In contrast, simple *O*-glycans containing only α -1,2-Man residues are found in *C. albicans* and the methylotrophic yeast *Pichia pastoris* (80).

GPI anchor synthesis. A third major form of protein glycosylation that occurs in fungi is the addition of glycosylphosphatidylinositol (GPI) anchors (for a detailed review, see (82)). The basic structure of GPI anchors is conserved across all eukaryotes. In fungi, these glycoconjugates undergo several unique processing events, including remodeling of the GPI lipid to ceramide (Cer) and transfer of anchored polypeptides from the GPI moiety to covalent linkage with cell wall glycans.



Synthesis of the GPI anchor begins in the cytoplasmic leaflet of the ER membrane, where GlcNAc is transferred from UDP-GlcNAc to phosphatidylinositol (PI) (Figure 6). This process is catalysed in *S. cerevisiae* by the transmembrane protein Gpi3p in association with five other polypeptides that form the GPI-GlcNAc transferase complex. The resulting GlcNAc-PI is then de-*N*-acetylated by Gpi12p to yield GlcN-PI and transferred to the luminal leaflet of the ER membrane by an unidentified flippase. Once in the lumen, the inositol moiety is palmitoylated by Gwt1p. This is followed by the addition of up to four Man residues (from Dol-P-Man) and up to three phosphoethanolamine

(EtnP) moieties. The presence of EtnP on the third Man is absolutely required for the association of the GPI anchor with a protein. Therefore, both Gpi13p (which adds this EtnP) and Smp3p (which adds the fourth Man, whose presence is required for the actions of Gpi13p) are essential. This is not the case in mammalian cells, which require only three Man residues for EtnP addition.

There is no specific amino acid sequence that directs GPI anchorage of a protein, but the residues at and near the addition site (termed the ' ω ' site) have been analysed in detail. The C-terminus of a protein that will receive a GPI anchor consists of a sequence of ten polar amino acids preceding ω ; a Gly, alanine (Ala), Ser, Asn, aspartic acid (Asp), or Cys at ω ; a Gly, Ala, or Ser at $\omega+1$; six or more moderately polar amino acids; and a final stretch of hydrophobic residues that form a transmembrane region. This pattern is recognized by GPI transamidase, a complex of five membrane proteins. The catalytic protein of this complex, Gpi8p, displaces the GPI signal sequence from the target protein (which is initially anchored to the ER membrane by its C-terminal hydrophobic sequence) and transfers the protein molecule to the GPI structure.

Both the lipid and glycan components of *S. cerevisiae* GPI anchors are subject to modification. Lipid remodeling promotes the efficient transport and membrane localization of anchored proteins. These steps occur in the ER, beginning with the deacylation of inositol by Bst1p. One fatty acid of the diacylglycerol moiety is then removed by Per1p and replaced with a longer fatty acid by Gup1p; a similar replacement may occur at the other fatty acid chain of the diacylglycerol. In a fungal-specific process, most GPI diacylglycerol moieties are replaced by phytoceramide, though the enzymes responsible

have not yet been identified. Further modifications occur following the transport of the GPI-associated protein from the ER to the Golgi apparatus, such as the replacement of the phytoceramide with other Cer species (83). The glycan portion of GPIs are also sometimes modified by the addition of another α -1,2- or α -1,3-Man to the fourth Man of the anchor by an unknown mannosyltransferase.

Glypiated proteins in fungi frequently undergo one final transformation, whereby the polypeptide and most of the GPI glycan are transferred from the anchor to a covalent linkage with cell wall glucans. This process has been demonstrated in multiple fungi, including *C. albicans*, *S. pombe*, *Aspergillus niger*, *C. glabrata* and *C. neoformans* as well as in *S. cerevisiae*, and serves to localize proteins to the cell wall. This transglycosylation process does not occur outside of the fungal kingdom and has yet to be defined in terms of enzymology and regulation .

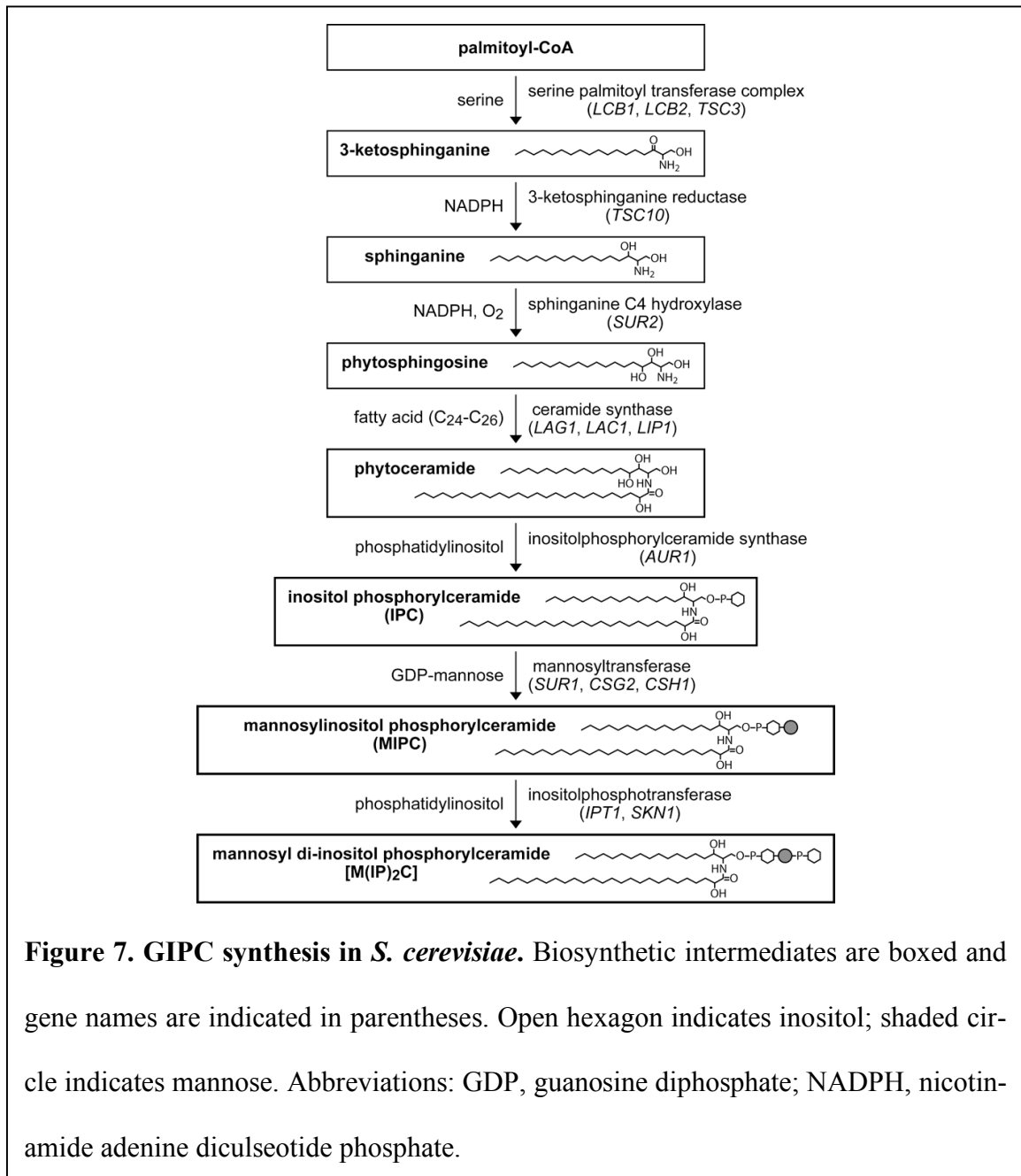
The structure and biosynthesis of GPIs in fungi other than *S. cerevisiae* appears for the most part to be well-conserved. Still, work by Franzot and Doering (84) determined that a range of fatty acids beyond palmitate can modify the inositol group in both *C. neoformans* and *S. cerevisiae*. Fontaine and colleagues (85) have also reported that the glycan portion of *Aspergillus fumigatus* GPI anchors consistently contains a fifth Man residue (Man₅GlcN), one more than typically found in *S. cerevisiae*.

Glycolipids

The major glycolipids in fungi are glycosphingolipids. These glycoconjugates function as essential components of the yeast cell membrane, contributing to its fluidity

and permeability. Fungal glycosphingolipids consist of one or more monosaccharide residues joined to Cer, a fatty acid linked to a sphingosine (a long-chain aliphatic amino alcohol). Glycosphingolipids can be divided into two classes: one in which the glycosyl moiety is linked to Cer via inositol phosphate (glycosylinositol phosphorylceramide or GIPC) and another in which the glycosyl moiety is linked directly to Cer (glycosylceramide). GIPCs occur as free membrane lipids and as membrane anchors of covalently bound proteins (see discussion of GPI anchors above) while glycosylceramides are associated with the fungal cell wall and are thought to play a role in cell cycle and differentiation (86). Importantly, there are significant differences between the structures, and thus the biosynthetic pathways, of fungal glycosphingolipids and those of mammals. This suggests that glycosphingolipid synthesis has potential as a target for antifungal compounds.

GIPC synthesis. Synthesis of *S. cerevisiae* glycosphingolipids (Figure 7) begins in the ER with the actions of the serine palmitoyltransferase (SPT) complex. This complex catalyzes the condensation of palmitoyl-CoA and serine to generate 3-ketosphinganine. The ketone group of 3-ketosphinganine is reduced in an NADPH-dependent reaction by Tsc10p to produce sphinganine, and this molecule can then be hydroxylated by Sur2p to form phytosphingosine. The ceramide synthase complex (Lip1p in combination with either Lac1p or Lag1p) next adds a very long chain fatty acid (C₂₄-C₂₆) to phytosphingosine, generating phytoceramide. Alternatively, sphinganine may first be acylated by the ceramide synthase complex to form dihydroceramide and subsequently hydroxylated by Sur2p to form phytoceramide.



Phytoceramide made in the ER is transported to the Golgi where, in a synthetic step unique to fungi, inositol phosphate is transferred by IPC synthase (Aur1p) from phosphatidylinositol to the Cer. The resulting inositol phosphorylceramide (IPC) is then

acted upon by one of two mannosylation complexes (Sur1p and Csg2 or Csh1p and Csg2) that catalyses the transfer of Man from GDP-Man to form mannosylinositol phosphorylceramide (MIPC). Finally, a second inositol phosphate can be transferred from phosphatidylinositol to form mannosyl di-inositol phosphorylceramide (M(IP)₂C) in a reaction that requires the products of the *IPT1* and *SKN1* genes. From the Golgi, GIPCs are transported to the outer leaflet of the plasma membrane. The reactions of GIPC synthesis are reviewed elsewhere (87, 88).

Some fungal species have evolved variations on the GIPC synthesis pathway outlined above. For example, while the proteins Lcb1p, Lcb2p, and Tsc3p are necessary for optimal activity of the SPT complex in *S. cerevisiae*, other fungal species do not appear to require Tsc3p. With regard to variations in structure, the pathogen *Sporothrix shenckii* synthesizes glucosaminyl IPC in addition to MIPC (89), and several fungi, including *C. neoformans* and *A. fumigatus*, generate derivatives of MIPC with additional sugar residues such as Man, Xyl, galactofuranose, and glucosamine (89, 90). *C. albicans* incorporates additional phosphate residues into GIPCs: Man-P is added to the Man of MIPC and afterwards modified with a linear chain of β -linked Man residues, generating a surface molecule referred to as phospholipomannan (PLM) (91). Significantly, *C. albicans* yeast that are deficient in this pathway are unable to avoid macrophage lysis *in vitro* and exhibit reduced pathogenicity in animal models of candidiasis (92).

Glycosylceramide synthesis. The generation of glycosylceramides proceeds as described above for GIPCs through the generation of phytosphingosine (Figure 7, third step). The pathways then diverge upon the addition of a shorter fatty acid (C₁₆-C₁₈) by the

sylceramide galactosyltransferases form GalGlcCer in the plant pathogen *Magnaporthe griseae* (95) or Gal₃GlcCer in *N. crassa* (96). In addition, the lipid portions of fungal glycosylceramides may be varied, as by the actions of a fatty acid Δ^3 -desaturase (93). Creative studies by (97) in which endogenous *GCSI* of *P. pastoris* was replaced with homologs from other fungi demonstrated the ability of these enzymes to glycosylate sphingolipids with longer chain fatty acids (C₂₄-C₂₆); similar structures containing elongated fatty acids were seen when *GCSI* homologs were expressed in *S. cerevisiae* (which cannot synthesize GlcCer *de novo*). The utilization of these compounds, which in *S. cerevisiae* are generally directed to GIPC synthesis, further increases glycosylceramide diversity. Broader investigation of fungal glycolipids will undoubtedly expose additional variations on this synthetic theme.

Cell wall polymers

The fungal cell wall is a complex and dynamic structure of glycans and glycoproteins. It is primarily composed of polymers of Glc, Man, and GlcNAc (glucans, mannans, and chitin, respectively), with extensive cross-linking between these elements. Both the degree of interconnection and the distribution of the wall components depend on the fungal species, developmental stage, and growth conditions. An overview of the synthesis of the major glycan components of fungal cell walls (reviewed in detail in (98, 99)) is presented.

β -1,3-glucan synthesis. The dominant fungal cell wall component is β -1,3-glucan, a polymer of ~1,500 Glc residues that is branched via β -1,6-linkages (99). This

polymer is notably absent in mammals yet required for viability in yeast, a combination that has led to the development of effective anti-fungal drugs targeting its synthesis (100). Despite its relevance, there is much that is not understood about the synthesis of β -1,3-glucan, including whether this process requires a primer molecule and how polymer length is regulated. The Glc donor for synthesis is likely cytoplasmic UDP-Glc, which is utilized by plasma membrane bound enzymes under the regulatory control of GTP-binding proteins. The catalytic subunits of the activity in *S. cerevisiae* are believed to be Fks1p and Gsc2p. These integral membrane proteins localize to the plasma membrane at sites of polar growth and enable nascent glucan chains to be transported across the membrane for incorporation into the cell wall. In *S. cerevisiae*, Fks1p is the dominant β -1,3-glucan synthase, and is expressed during mitotic growth, while Gsc2p is active under conditions of nutritional or environmental stress. A third homolog, Fks3p, may be involved in cell wall construction during developmental processes such as mating and spore formation.

Genome analysis has identified sequences encoding multiple FKS homologs in fungi including *C. albicans*, *S. pombe*, the cotton pathogen *Ashbya gossypii*, and members of the *Saccharomyces* genus. In contrast, only a single, essential *FKSI* has been identified in *Yarrowia lipolytica*, *C. neoformans*, the dimorphic pathogen *Coccidioides posadasii*, and the AIDS-defining pathogen *Pneumocystis carinii*. Excellent reviews of β -1,3-glucan synthesis are found in (99, 101). An unusual variation related to β -1,3-glucan is the linear β -1,3-/ β -1,4-glucan found in *A. fumigatus* (102). Although not previously described in fungi, this glycan represents 10% of total β -glucan in that organism.

β-1,6-glucan synthesis. β-1,6-glucan interconnects other cell wall components in *S. cerevisiae*, thus playing a central role in cell wall structure. The degree of polymerization of this glucan is generally lower than that of β-1,3-glucan, with ~350 Glc residues/chain. The structure is highly branched by the introduction of β-1,3-linkages; the frequency of these branches ranges from 7% of the backbone residues in *C. albicans* to ten-fold that frequency in *S. pombe*, suggesting species-dependent variation in branching or cross-linking activities (99). The synthesis of β-1,6-glucans (reviewed in (103)) presents numerous questions, starting with its localization. Genetic manipulation of *S. cerevisiae* and analysis of the resulting levels of β-1,6-glucan has implicated a broad array of genes in this pathway, including genes encoding proteins of the secretory pathway and at the cell surface. Supporting the resulting hypothesis that β-1,6-glucan is made intracellularly, immuno-EM studies have detected this polymer in the Golgi and secretory vesicles of *S. pombe* (104), but the degree of polymerization and form of the glucan represented by this localization is not clear. Cell-free synthesis of β-1,6-glucan has been achieved in crude membrane preparations from *S. cerevisiae* (105); continued effort in this biochemical direction should help clarify this intriguing research area.

Synthesis of other cell wall glucans. Beyond the β-glucans described above, many fungal cell walls also include α-glucans. These compounds do not occur in *S. cerevisiae* or *C. albicans*, but are highly abundant (up to 95% of the glucans) in the cell wall of other yeasts, such as the pathogens *Paracoccidioides brasiliensis* and *Blastomyces dermatitidis*. Synthesis of α-1,3-glucan has been studied in *S. pombe*, where it exists as a linear polymer of ~200 Glc residues/chain (106). This compound is synthesized by the

product of a single essential gene, *AGSI* (alpha-glucan synthase 1), which may further join polymer chains by linkers of α -1,4-glucan (107). Three homologs of Ags1p are required for *S. pombe* spore wall maturation.

Similar to *S. pombe*, an *AGS* gene family is also found in *A. fumigatus*, with data suggesting the homologs have distinct roles in growth, development, and virulence (108). Simpler synthetic machinery is present in *H. capsulatum* and *C. neoformans*, where a single *AGSI* gene is required for normal virulence (109, 110). α -1,3-glucan plays a special role in the latter pathogen, where it is required for association of the fungal capsule with the cell wall (111).

Chitin synthesis. Chitin is a polymer of β -1,4-linked GlcNAc, typically composed of more than 1,000 residues, which self-associates to form microfibrils. This relatively minor but critical component of the cell wall is deposited at the bud neck of yeast and at fungal septa in a highly regulated manner, and can be deacetylated to form another cell wall polymer, chitosan. Chitin is generated from UDP-GlcNAc by synthases that translocate the polymeric product through the plasma membrane (112). In accordance with their function, these enzymes are integral proteins of the cytoplasmic leaflet of the plasma membrane. Because chitin synthesis primarily occurs at sites of active growth and cell wall remodeling, it is both temporally and spatially regulated. In *S. cerevisiae* three chitin synthases (Chs1p, Chs2p, and Chs3p) have been described, which play specific roles in cell growth: Chs1p repairs the site of daughter cell separation from the parent, Chs2p forms chitin in the septum during cell division, and Chs3p makes chitin at the bud neck, the lateral cell wall, and spore cell walls. Interestingly, the activity of Chs3p is regulated

by subcellular localization: it is stored in small microsomal vesicles (chitosomes) that deliver it to the plasma membrane as needed. Multiple gene products have been implicated in the regulation and localization of chitin synthesis in *S. cerevisiae*, but describing them is beyond the scope of this chapter; useful reviews of chitin synthesis include (113, 114).

Most fungi have multiple chitin synthase genes, which appear to have distinct although occasionally overlapping functions (reviewed in (114)). *S. cerevisiae* offers a relatively simple case, compared to the eight Chs proteins in *C. neoformans* (115), or the seven in *A. fumigatus* (116). These enzymes have been classified based on sequence motifs and homology; notably, some families are restricted to filamentous fungi. Deletion of the genes encoding many of these enzymes yields striking phenotypic changes, including altered morphology, stress resistance, or virulence in animal and plant pathogens (115). Some fungi secrete deacetylases that modify chitin to chitosan, a more soluble cationic polymer. The genes encoding two such enzymes in *S. cerevisiae* (*CDA1* and *CDA2*) are expressed only during sporulation and contribute to spore wall formation. In contrast, chitosan is a normal cell wall component of *C. neoformans* and the three cryptococcal chitin deacetylases are required for normal cell integrity and bud separation (117).

Intracellular glycans

Glycogen and trehalose are the main stores of glucose in *S. cerevisiae*. Glycogen functions as a reserve carbohydrate that is synthesized and stored under nutrient-rich conditions and then degraded during periods of nutrient deprivation. Trehalose has been postulated to serve as a chemical chaperone that protects proteins and membranes from

stress-induced denaturation (reviewed in (118)). Synthesis of both glycogen and trehalose is reviewed extensively elsewhere (119).

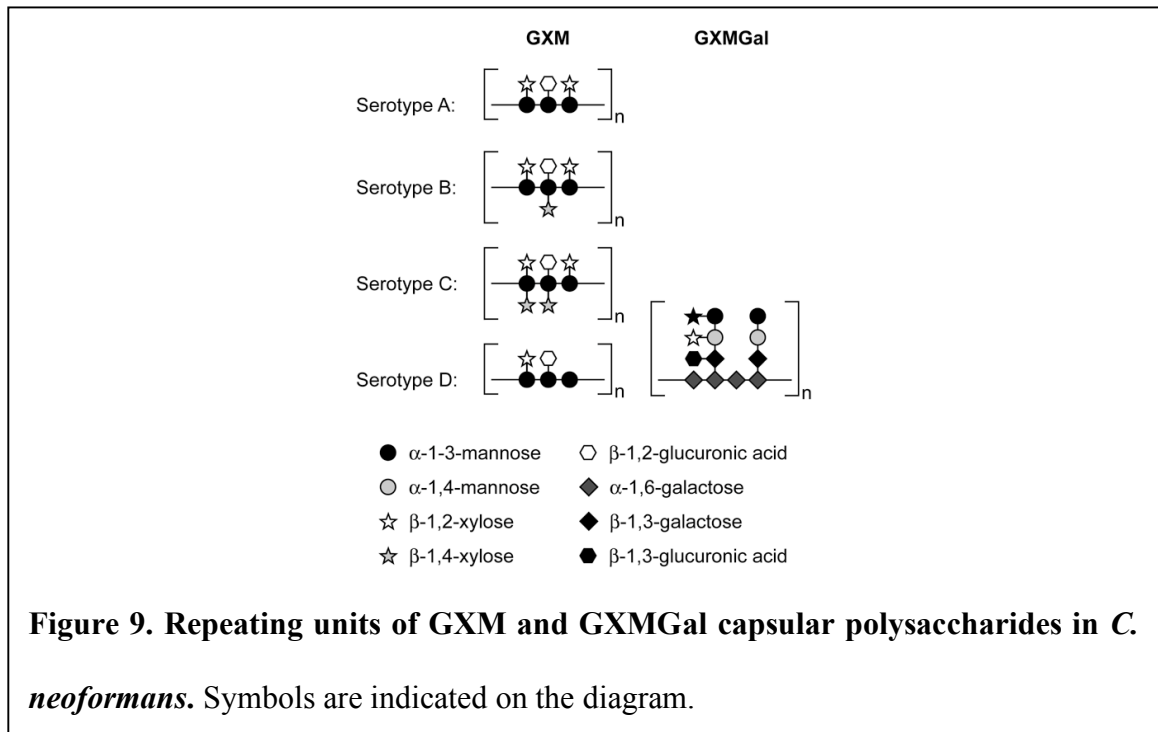
Glycogen synthesis. Glycogen is a branched polymer of up to 100,000 Glc residues that is distributed throughout the fungal cytosol. Synthesis (reviewed in (119, 120)) occurs in the cytosol, beginning with the actions of the protein glycogenin (either Glg1p or Glg2p in *S. cerevisiae*). Interestingly, glycogenin itself serves as the primer for glycogen polymerization: Glg1p and Glg2p are each capable of utilizing UDP-Glc as a donor for auto-glucosylation at one of several tyrosine (Tyr) residues, generating a short α -1,4-Glc chain. Although Glg1p and Glg2p are capable of auto-glucosylating, the proteins exist as a dimer *in vivo* and the reaction is believed to occur intermolecularly. The protein-linked chain of up to ten Glc residues generated by glycogenin is elongated by the action of Gsy1p or the more dominant Gsy2p (glycogen synthase isoforms 1 and 2, respectively), which adds Glc in an α -1,4-linkage to the non-reducing end of the initial oligomer. Following elongation, the linear α -1,4-glucans are ramified by Glc3p, a branching enzyme that adds seven α -1,4-Glc residues in an α -1,6-linkage. In a departure from the glycogen synthesis pathway of *S. cerevisiae*, the glycogenin and glycogen synthase enzymes of *N. crassa* are each encoded by just one protein (121).

Trehalose synthesis. Trehalose is an unusual disaccharide of glucose linked ‘head to head’ in an α -1,1-linkage, and notably is absent from mammalian cells. Trehalose synthesis in *S. cerevisiae* proceeds by two sequential reactions: first, trehalose-phosphate synthase (Tps1p) catalyses the transfer of Glc from UDP-Glc to Glc-6-phosphate, forming trehalose-6-phosphate. In a subsequent reaction, trehalose-6-phosphate phosphatase

(Tps2p) acts on this product to generate free trehalose. Together these enzymes form a complex with two other proteins, Tps3p and Tsl1p, which are thought to have regulatory functions. *C. neoformans* strains that lack Tps1p and Tps2p are temperature sensitive and a *tps1* mutant is avirulent (20).

Exopolysaccharides

The processes described earlier in this section broadly apply to all fungi. Some fungi, however, are unique in their generation of additional extracellular glycan structures (exopolysaccharides). One example is the extensive polysaccharide capsule of *C. neoformans*, the organism's main virulence factor (reviewed in (122)). This structure consists primarily of two polysaccharides: glucuronoxylomannogalactan (GXMGal; polymer size of $\sim 1 \times 10^5$ Da) and glucuronoxylomannan (GXM; polymer size of $\sim 1-7 \times 10^6$ Da). Both polymers are composed of repeating subunits (Figure 9). GXMGal has a linear backbone of α -1,6-linked Gal residues with oligomeric side-chains of Gal, glucuronic acid (GlcA), Man, and Xyl ((123); similar polymers are reported in other cryptococcal species. The GXM polysaccharide has a linear backbone of α -1,3-Man residues that are 6-*O*-acetylated (124) and are substituted with residues of Xyl (linked β -1,2 and β -1,4), and GlcA (linked β -1,2). The pattern of GXM modifications varies among different serotypes of *C. neoformans* (Figure 9) and between related species. For example, studies of *Cryptococcus flavescens* reveal a similar high molecular mass polymer that is substituted more frequently with GlcA (125). This polymer is also substituted at the 6-position of Man with chains consisting of Man- β (1 \rightarrow 4)-Xyl or Man- β (1 \rightarrow 4)-Xyl- β (1 \rightarrow 4)-Xyl.



The cryptococcal polysaccharides are of interest because of their unique structures and the role of the capsule in disease. Studies of mutant *C. neoformans* that are deficient in secretion suggest that GXM biosynthesis begins within the cell, with products exported via the secretory pathway, but the nature of these products remains to be established (126). Little is known about specific enzymes involved in synthesis of capsule polymers. A mannosyltransferase activity capable of modifying $\text{Xyl}\alpha\text{-CH}_3$ has been described in membrane preparations of *C. laurentii* (127); this could potentially be involved in the formation of GXM structures like those of *C. flavescens* described above, although the linkage formed has not been determined. Recently, a β -1,2-xylosyltransferase that participates in synthesis of both GXM and GXMGal has been purified and cloned from *C. neoformans* (128, 129). Intriguingly, this enzyme is also required for cryptococcal GIPC

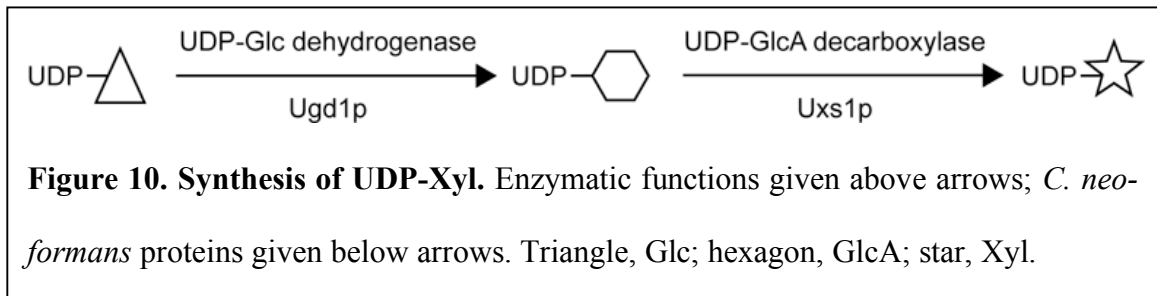
synthesis (130), raising the possibility that the two biosynthetic pathways are linked. The enzymes required for other capsule biosynthetic steps are not yet known. Once capsule polymers are made and exported they become associated with the cell surface in a process that is dependent on cell wall α -1,3-glucan (110, 111), but the mechanism of this association has not been defined. Future investigations are clearly required to determine the biosynthetic pathways of cryptococcal capsule polysaccharides.

XYLOSE IN THE CRYPTOCOCCAL CELL

Studies in the Doering laboratory address various aspects of glycan synthesis in the cryptococcal cell. This includes the generation of nucleotide sugar donor molecules in the cytoplasm (131-133) and their subsequent transport into the ER and Golgi (49). Research has also addressed the assembly of glycan polymers (128, 129, 134, 135) and, in the case of the capsule polysaccharides, their export to the cell surface (126). Our particular interest in the Xyl residues of cellular glycans stemmed from studies addressing the synthesis of UDP-Xyl (the sole source of Xyl residues in the cell; (136)); from this, our work naturally extended to the study of the xylosyltransferases involved in the assembly of cellular glycans. As noted in the preceding Fungal Glycan Synthesis section, Xyl residues have been detected in the *O*-linked glycans of the related yeast, *C. laurentii* (81), in the GIPCs of *C. neoformans* (90), and in the cryptococcal capsular polysaccharides, GXM and GXMGal (124, 137). With each of these glycans, the fungal structures differ significantly from those generated by humans, making them potentially interesting drug targets.

Synthesis of UDP-Xyl

UDP-Xyl is derived from UDP-GlcA through the actions of an UDP-glucuronic acid decarboxylase (see Figure 10). In *C. neoformans* this enzyme was identified based on its homology to a putative aminoarabinose synthesis protein encoded by the bacterium *Salmonella typhimurium* (131) and was named Uxs1p (UDP-xylose synthase 1). Expression of the coding sequence of *UXS1* in *Escherichia coli* allowed for detection of an ac-



tivity that converted UDP-GlcA to UDP-Xyl (131). The activity of Uxs1p is not essential to *C. neoformans* as the corresponding locus could be deleted and the resulting mutant strain (*uxs1Δ*) showed no difference in growth compared to the wild-type parental strain (133, 138)). In *uxs1Δ* cells, levels of UDP-Xyl fell below the limit of detection while UDP-GlcA accumulated to high levels because it could no longer be converted to UDP-Xyl (133).

The *uxs1Δ* strain was still able to generate capsule as assessed by India Ink staining, but the polysaccharide coating surrounding the *uxs1Δ* cells appeared thinner than that of wild-type (138). Studies performed using transmission electron microscopy found that the capsule fibers of an *uxs1Δ* strain appeared truncated and thickened compared to wild-type (133). Analysis of GXM purified from the *uxs1Δ* strain confirmed an absence of Xyl residues in GXM, but found no other apparent change in either the structure (ratio of Man and GlcA residues) or modification (acetylation patterns) of the polysaccharide. The loss of Xyl residues in the capsule's structure led to differences in the binding pattern of most monoclonal anti-capsular antibodies (138, 139).

Studies performed using the *uxs1Δ* strain demonstrated that the mutant strain was able to bind complement component 3 (C3) factor more quickly than wild-type (139).

This was unexpected as earlier studies comparing complement binding among the different serotypes of *C. neoformans* found C3b capture increased in correlation with the number of Xyl residues found in GXM (140). Although accelerated C3 deposition did not translate to increased interactions with polymorphonuclear neutrophils (PMNs) following pre-opsonization (139), the *uxs1*Δ strain was avirulent in a tail vein injection model of cryptococcal infection and could not be isolated from the animal following inoculation (138). It was this loss of virulence in the *uxs1*Δ strain that directed our interest towards the synthesis of Xyl-containing glycans in the cryptococcal cell.

Xylosyltransferases

An assay was developed in our laboratory to detect xylosyltransferase activities that might be involved in the synthesis of capsule or other cellular glycans. The assay utilized a radiolabeled UDP-[¹⁴C]Xyl donor and a Man-α(1→3)-Man oligosaccharide as the substrate; this dimannose resembles the backbone of GXM and the side-chains of GXMGal as well as some *O*-glycan and GIPC structures. With this assay, a single dominant activity was detected in the membrane proteins of *C. neoformans* (128). This activity was enriched using a combination of ion exchange, gel filtration, and affinity resins, eventually leading to the isolation of a ~90 kDa protein. The protein was identified as Cap3p (one of five homologs to the acapsular-associated protein Cap10) and renamed Cxt1p for cryptococcal xylosyltransferase 1. Interestingly, even though detection of the Cxt1p activity was not dependent on the inclusion of metal ions in the reaction, the muta-

tion of DXD sites within the protein resulted in a dramatic reduction of xylosyltransferase activity (128).

The product of Cxt1p was identified as a trisaccharide with Xyl linked to the reducing Man of the acceptor substrate: Man- α (1 \rightarrow 3)[Xyl- β (1 \rightarrow 2)]-Man (128). This motif resembled elements of several cryptococcal glycans. Although no differences in the capsule of a *cxt1* Δ strain could be detected by immunofluorescence using monoclonal antibodies, structural analysis indicated a ~30% reduction in Xyl residues in GXM while GXMGal demonstrated almost a complete loss of all Xyl residues (129). Studies of *C. neoformans* glycolipid structures found that the major GIPC of *cxt1* Δ cells also lacked its normal Xyl residue and was truncated (130). Intriguingly, growth of *C. neoformans* in murine lungs was attenuated in the absence of *CXT1* in an inhalational model of infection (129) yet no difference in infectivity was seen in the mutant using an intravenous model (141).

Work in the Doering laboratory on the xylosyltransferases of *C. neoformans* has continued beyond the study of Cxt1p. In *cxt1* Δ cell lines, a minor amount of residual activity was observed (129) and has since been correlated with *CAP5* (another of the *CAP10* homologues in the genome) and renamed *CXT2*.¹ A third xylosyltransferase activity was seen following the addition of metal ions to the xylosyltransferase reaction outlined above; it is this activity that is explored in this dissertation.

The following chapters detail the detection, identification, and characterization of a cation-dependent xylosylphosphotransferase activity in *C. neoformans* that modifies

¹ J.S. Klutts and T.L. Doering, in preparation

Man substrates. The next chapter describes the initial observation of this activity, the product analysis that identified it as a novel enzyme able to link xylose-phosphate to Man, and the identification of the corresponding gene. Chapter III further explores the occurrence of this enzyme in cryptococcal strains and describes studies that determined its involvement in the synthesis of *O*-linked protein glycans. Additional work presented in Chapter IV suggests that this enzyme functions in association with other proteins. This is followed by a chapter that briefly considers the future directions of this research. My studies have identified and characterized a completely novel glycoactive enzyme and, in conjunction with other investigations of the xylosyltransferases of *C. neoformans*, have contributed significantly to our understanding of the unique glycobiology of this environmental yeast and opportunistic pathogen.

ACKNOWLEDGEMENTS

The author thanks Tamara Doering, Aki Yoneda, and Maurizio del Poeta for comments on the manuscript.

ABBREVIATIONS USED

Cer, ceramide; C3, complement component 3; Dol, dolichol; Dol-P, dolichol-phosphate; ER, endoplasmic reticulum; EtnP, phosphoethanolamine; Gal, galactose; GIPC, glycosylinositol phosphorylceramide; Glc, glucose; GlcA, glucuronic acid; GlcNAc, N-acetylglucosamine; GPI, glycosylphosphatidylinositol; GXM, glucuronoxylomannan; GXMGal, glucuronoxylomannogalactan; IL, interleukin; Man, mannose; Man-P, mannose-phosphate; MHC, major histocompatibility complex; MIPC, mannosylinositol phosphorylceramide; M-Pol, mannan polymerase complex; NST, nucleotide sugar transporter; OST, oligosaccharyltransferase; PI, phosphatidylinositol; PLM, phospholipomannan; PMNs, polymorphonuclear neutrophils; PMT, protein *O*-mannosyltransferase; SAGE, serial analysis of gene expression; SPT, serine palmitoyltransferase; TNF; tumor necrosis factor; Xyl, xylose.

REFERENCES

1. Lin, X., and J. Heitman. 2006. The biology of the *Cryptococcus neoformans* species complex. *Annu. Rev. Microbiol.* 60: 69-105.
2. Casadevall, A., and J. Perfect. 1998. *Cryptococcus neoformans*. American Society for Microbiology.
3. Bicanic, T., and T.S. Harrison. 2005. Cryptococcal meningitis. *Br. Med. Bull.* 72: 99-118.
4. Chen, L.C., D.L. Goldman, T.L. Doering, L. Pirofski, and A. Casadevall. 1999. Antibody response to *Cryptococcus neoformans* proteins in rodents and humans. *Infect. Immun.* 67: 2218-2224.
5. Goldman, D.L., H. Khine, J. Abadi, D.J. Lindenberg, L. Pirofski, R. Niang, and A. Casadevall. 2001. Serologic evidence for *Cryptococcus neoformans* infection in early childhood. *Pediatrics* 107: E66.
6. Ma, H., and R.C. May. 2009. Virulence in *Cryptococcus* species. *Adv. Appl. Microbiol.* 67: 131-190.
7. Park, B.J., K.A. Wannemuehler, B.J. Marston, N. Govender, P.G. Pappas, and T.M. Chiller. 2009. Estimation of the current global burden of cryptococcal meningitis among persons living with HIV/AIDS. *AIDS* 23: 525-530.
8. Heere, L.J., T.A. Mahvi, and M.M. Annable. 1975. Effect of temperature on growth and macromolecular biosynthesis in *Cryptococcus* species. *Mycopathologia* 55: 105-113.

9. Dong, H., and W. Courchesne. 1998. A novel quantitative mating assay for the fungal pathogen *Cryptococcus neoformans* provides insight into signalling pathways responding to nutrients and temperature. *Microbiology* 144 (Pt 6): 1691-1697.
10. Howard, D.H. 1961. Sep. Some factors which affect the initiation of growth of *Cryptococcus neoformans*. *J. Bacteriol.* 82: 430-435.
11. Madeira-Lopes, A. 1986. Thermal death potentiation by amphotericin B in *Cryptococcus neoformans* and its dependence on pre-incubation temperature. *J. Med. Vet. Mycol.* 24: 35-40.
12. Steen, B.R., T. Lian, S. Zuyderduyn, W.K. MacDonald, M. Marra, S.J. Jones, and J.W. Kronstad. 2002. Temperature-regulated transcription in the pathogenic fungus *Cryptococcus neoformans*. *Genome Res.* 12: 1386-1400.
13. Kraus, P.R., M.J. Boily, S.S. Giles, J.E. Stajich, A. Allen, G.M. Cox, F.S. Dietrich, J.R. Perfect, and J. Heitman. 2004. Identification of *Cryptococcus neoformans* temperature-regulated genes with a genomic-DNA microarray. *Eukaryot Cell* 3: 1249-1260.
14. Alspaugh, J.A., R. Pukkila-Worley, T. Harashima, L.M. Cavallo, D. Funnell, G.M. Cox, J.R. Perfect, J.W. Kronstad, and J. Heitman. 2002. Adenylyl cyclase functions downstream of the Galpha protein Gpa1 and controls mating and pathogenicity of *Cryptococcus neoformans*. *Eukaryot Cell* 1: 75-84.
15. Kraus, P.R., D.S. Fox, G.M. Cox, and J. Heitman. 2003. The *Cryptococcus neoformans* MAP kinase Mpk1 regulates cell integrity in response to antifungal drugs and loss of calcineurin function. *Mol. Microbiol.* 48: 1377-1387.

16. Vallim, M.A., C.B. Nichols, L. Fernandes, K.L. Cramer, and J.A. Alspaugh. 2005. A Rac homolog functions downstream of Ras1 to control hyphal differentiation and high-temperature growth in the pathogenic fungus *Cryptococcus neoformans*. *Eukaryot. Cell.* 4: 1066-1078.
17. Nichols, C.B., Z.H. Perfect, and J.A. Alspaugh. 2007. A Ras1-Cdc24 signal transduction pathway mediates thermotolerance in the fungal pathogen *Cryptococcus neoformans*. *Mol. Microbiol.* 63: 1118-1130.
18. Missall, T.A., M.E. Pusateri, and J.K. Lodge. 2004. Thiol peroxidase is critical for virulence and resistance to nitric oxide and peroxide in the fungal pathogen, *Cryptococcus neoformans*. *Mol. Microbiol.* 51: 1447-1458.
19. Giles, S.S., I. Batinic-Haberle, J.R. Perfect, and G.M. Cox. 2005. *Cryptococcus neoformans* mitochondrial superoxide dismutase: an essential link between antioxidant function and high-temperature growth. *Eukaryot Cell* 4: 46-54.
20. Petzold, E.W., U. Himmelreich, E. Mylonakis, T. Rude, D. Toffaletti, G.M. Cox, J.L. Miller, and J.R. Perfect. 2006. Characterization and regulation of the trehalose synthesis pathway and its importance in the pathogenicity of *Cryptococcus neoformans*. *Infect. Immun.* 74: 5877-5887.
21. Kozel, T.R. 1995. Virulence factors of *Cryptococcus neoformans*. *Trends Microbiol.* 3: 295-299.
22. Nosanchuk, J.D., and A. Casadevall. 1997. Cellular charge of *Cryptococcus neoformans*: contributions from the capsular polysaccharide, melanin, and monoclonal antibody binding. *Infect. Immun.* 65: 1836-1841.

23. Rosas, A.L., and A. Casadevall. 1997. Melanization affects susceptibility of *Cryptococcus neoformans* to heat and cold. *FEMS Microbiol. Lett.* 153: 265-272.
24. Wang, Y., and A. Casadevall. 1994. Decreased susceptibility of melanized *Cryptococcus neoformans* to UV light. *Appl. Environ. Microbiol.* 60: 3864-3866.
25. Garcia-Rivera, J., and A. Casadevall. 2001. Melanization of *Cryptococcus neoformans* reduces its susceptibility to the antimicrobial effects of silver nitrate. *Med. Mycol.* 39: 353-357.
26. Rosas, A. L., and A. Casadevall. 2001. Melanization decreases the susceptibility of *Cryptococcus neoformans* to enzymatic degradation. *Mycopathologia* 151: 53-56
27. Kwon-Chung, K.J., I. Polacheck, and T.J. Popkin. 1982. Melanin-lacking mutants of *Cryptococcus neoformans* and their virulence for mice. *J. Bacteriol.* 150: 1414-1421.
28. Kwon-Chung, K.J., and J.C. Rhodes. 1986. Encapsulation and melanin formation as indicators of virulence in *Cryptococcus neoformans*. *Infect. Immun.* 51: 218-223.
29. Rhodes, J.C., I. Polacheck, and K.J. Kwon-Chung. 1982. Phenoloxidase activity and virulence in isogenic strains of *Cryptococcus neoformans*. *Infect. Immun.* 36: 1175-1184.
30. Wang, Y., P. Aisen, and A. Casadevall. 1995. *Cryptococcus neoformans* melanin and virulence: mechanism of action. *Infect. Immun.* 63: 3131-3136.
31. Jacobson, E.S., and H.S. Emery. 1991. Catecholamine uptake, melanization, and oxygen toxicity in *Cryptococcus neoformans*. *J. Bacteriol.* 173: 401-403.

32. Huffnagle, G.B., G.H. Chen, J.L. Curtis, R.A. McDonald, R.M. Strieter, and G.B. Toews. 1995. Down-regulation of the afferent phase of T cell-mediated pulmonary inflammation and immunity by a high melanin-producing strain of *Cryptococcus neoformans*. *J. Immunol.* 155: 3507-3516.
33. Rosas, A.L., J.D. Nosanchuk, M. Feldmesser, G.M. Cox, H.C. McDade, and A. Casadevall. 2000. Synthesis of polymerized melanin by *Cryptococcus neoformans* in infected rodents. *Infect. Immun.* 68: 2845-2853.
34. Liu, L., K. Wakamatsu, S. Ito, and P.R. Williamson. 1999. Catecholamine oxidative products, but not melanin, are produced by *Cryptococcus neoformans* during neuropathogenesis in mice. *Infect. Immun.* 67: 108-112.
35. Liu, L., R.P. Tewari, and P.R. Williamson. 1999. Laccase protects *Cryptococcus neoformans* from antifungal activity of alveolar macrophages. *Infect. Immun.* 67: 6034-6039.
36. Williamson, P.R. 1994. Biochemical and molecular characterization of the diphenol oxidase of *Cryptococcus neoformans*: identification as a laccase. *J. Bacteriol.* 176: 656-664.
37. Murphy, J.W., and G.C. Cozad. 1972. Immunological unresponsiveness induced by cryptococcal capsular polysaccharide assayed by the hemolytic plaque technique. *Infect. Immun.* 5: 896-901.
38. Feldmesser, M., and A. Casadevall. 1998. Mechanism of action of antibody to capsular polysaccharide in *Cryptococcus neoformans* infection. *Front. Biosci.* 3: d136.

39. Kozel, T.R., and E.C. Gotschlich. 1982. The capsule of *Cryptococcus neoformans* passively inhibits phagocytosis of the yeast by macrophages. *J. Immunol.* 129: 1675-1680.
40. Syme, R.M., T.F. Bruno, T.R. Kozel, and C.H. Mody. 1999. The capsule of *Cryptococcus neoformans* reduces T-lymphocyte proliferation by reducing phagocytosis, which can be restored with anticapsular antibody. *Infect. Immun.* 67: 4620-4627.
41. Retini, C., A. Vecchiarelli, C. Monari, F. Bistoni, and T.R. Kozel. 1998. Encapsulation of *Cryptococcus neoformans* with glucuronoxylomannan inhibits the antigen-presenting capacity of monocytes. *Infect. Immun.* 66: 664-669.
42. Vecchiarelli, A., C. Retini, C. Monari, C. Tascini, F. Bistoni, and T.R. Kozel. 1996. Purified capsular polysaccharide of *Cryptococcus neoformans* induces interleukin-10 secretion by human monocytes. *Infect. Immun.* 64: 2846-2849.
43. Vecchiarelli, A., C. Retini, D. Pietrella, C. Monari, C. Tascini, T. Beccari, and T.R. Kozel. 1995. Downregulation by cryptococcal polysaccharide of tumor necrosis factor alpha and interleukin-1 beta secretion from human monocytes. *Infect. Immun.* 63: 2919-2923.
44. Dong, Z.M., and J.W. Murphy. 1995. Intravascular cryptococcal culture filtrate (CneF) and its major component, glucuronoxylomannan, are potent inhibitors of leukocyte accumulation. *Infect. Immun.* 63: 770-778.
45. Vecchiarelli, A., D. Pietrella, P. Lupo, F. Bistoni, D.C. McFadden, and A. Casadevall. 2003. The polysaccharide capsule of *Cryptococcus neoformans* interferes with human dendritic cell maturation and activation. *J. Leukoc. Biol.* 74: 370-378.

46. Poster, J.B., and N. Dean. 1996. The yeast *VRG4* gene is required for normal Golgi functions and defines a new family of related genes. *J. Biol. Chem.* 271: 3837-3845.
47. Nishikawa, A., B. Mendez, Y. Jigami, and N. Dean. 2002. Identification of a *Candida glabrata* homologue of the *S. cerevisiae VRG4* gene, encoding the Golgi GDP-mannose transporter. *Yeast* 19: 691-698.
48. Nishikawa, A., J.B. Poster, Y. Jigami, and N. Dean. 2002. Molecular and phenotypic analysis of *CaVRG4*, encoding an essential Golgi apparatus GDP-mannose transporter. *J. Bacteriol.* 184: 29-42.
49. Cottrell, T.R., C.L. Griffith, H. Liu, A.A. Nenninger, and T.L. Doering. 2007. The pathogenic fungus *Cryptococcus neoformans* expresses two functional GDP-mannose transporters with distinct expression patterns and roles in capsule synthesis. *Eukaryot Cell* 6: 776-785.
50. Hirschberg, C.B., P.W. Robbins, and C. Abeijon. 1998. Transporters of nucleotide sugars, ATP, and nucleotide sulfate in the endoplasmic reticulum and Golgi apparatus. *Annu. Rev. Biochem.* 67: 49-69.
51. Berninsone, P.M., and C.B. Hirschberg. 2000. Nucleotide sugar transporters of the Golgi apparatus. *Curr. Opin. Struct. Biol.* 10: 542-547.
52. Gerardy-Schahn, R., S. Oelmann, and H. Bakker. 2001. Nucleotide sugar transporters: biological and functional aspects. *Biochimie* 83: 775-782.
53. Maeda, Y., and T. Kinoshita. 2008. Dolichol-phosphate mannosyltransferase: Structure, function and regulation. *Biochim. Biophys. Acta* 1780: 861-868.

54. Qasba, P.K., B. Ramakrishnan, and E. Boeggeman. 2005. Substrate-induced conformational changes in glycosyltransferases. *Trends Biochem. Sci.* 30: 53-62.
55. Coutinho, P.M., E. Deleury, G.J. Davies, and B. Henrissat. 2003. An evolving hierarchical family classification for glycosyltransferases. *J. Mol. Biol.* 328: 307-317.
56. Campbell, J.A., G.J. Davies, V. Bulone, and B. Henrissat. 1997. A classification of nucleotide-diphospho-sugar glycosyltransferases based on amino acid sequence similarities. *Biochem. J.* 326 (Pt 3): 929-939.
57. Hu, Y., and S. Walker. 2002. Remarkable structural similarities between diverse glycosyltransferases. *Chem. Biol.* 9: 1287-1296.
58. Breton, C., L. Snajdrova, C. Jeanneau, J. Koca, and A. Imberty. 2006. Structures and mechanisms of glycosyltransferases. *Glycobiology* 16: 29R-37R.
59. Liu, J., and A. Mushegian. 2003. Three monophyletic superfamilies account for the majority of the known glycosyltransferases. *Protein Sci.* 12: 1418-1431.
60. Kikuchi, N., Y.D. Kwon, M. Gotoh, and H. Narimatsu. 2003. Comparison of glycosyltransferase families using the profile hidden Markov model. *Biochem. Biophys. Res. Commun.* 310: 574-579
61. Weerapana, E., and B. Imperiali. 2006. Asparagine-linked protein glycosylation: from eukaryotic to prokaryotic systems. *Glycobiology* 16: 91R-101R.
62. Bickel, T.,L. Lehle, M. Schwarz, M. Aebi, and C.A. Jakob. 2005. Biosynthesis of lipid-linked oligosaccharides in *Saccharomyces cerevisiae*: Alg13p and Alg14p form a complex required for the formation of GlcNAc(2)-PP-dolichol. *J. Biol. Chem.* 280: 34500-34506.

63. Gao, X.D., H. Tachikawa, T. Sato, Y. Jigami, and N. Dean. 2005. Alg14 recruits Alg13 to the cytoplasmic face of the endoplasmic reticulum to form a novel bipartite UDP-N-acetylglucosamine transferase required for the second step of N-linked glycosylation. *J. Biol. Chem.* 280: 36254-36262.
64. O'Reilly, M.K., G. Zhang, and B. Imperiali. 2006. *In vitro* evidence for the dual function of Alg2 and Alg11: essential mannosyltransferases in N-linked glycoprotein biosynthesis. *Biochemistry (N.Y.)* 45: 9593-9603.
65. Helenius, J., D.T. Ng, C.L. Marolda, P. Walter, M.A. Valvano, and M. Aebi. 2002. Translocation of lipid-linked oligosaccharides across the ER membrane requires Rft1 protein. *Nature* 415: 447-450.
66. Lennarz, W.J. 2007. Studies on oligosaccharyl transferase in yeast. *Acta Biochim. Pol.* 54: 673-677.
67. Herscovics, A. 1999. Processing glycosidases of *Saccharomyces cerevisiae*. *Biochim. Biophys. Acta* 1426: 275-285.
68. Moremen, K.W., and M. Molinari. 2006. N-linked glycan recognition and processing: the molecular basis of endoplasmic reticulum quality control. *Curr. Opin. Struct. Biol.* 16: 592-599.
69. Varki, A. 1999. *Essentials of glycobiology*. Cold Spring Harbor Laboratory Press.
70. Samuelson, J., S. Banerjee, P. Magnelli, J. Cui, D.J. Kelleher, R. Gilmore, and P.W. Robbins. 2005. The diversity of dolichol-linked precursors to Asn-linked glycans likely results from secondary loss of sets of glycosyltransferases. *Proc. Natl. Acad. Sci. U.S.A.* 102: 1548-1553.

71. Nakajima, T., M. Yoshida, N. Hiura, and K. Matsuda. 1984. Oct. Structure of the cell wall proteogalactomannan from *Neurospora crassa*. I. Purification of the proteo-heteroglycan and characterization of alkali-labile oligosaccharides. *J Biochem* 96: 1005-1011.
72. Wallis, G.L., R.L. Easton, K. Jolly, F.W. Hemming, and J.F. Peberdy. 2001. Galactofuranoic-oligomannose *N*-linked glycans of alpha-galactosidase A from *Aspergillus niger*. *Eur. J. Biochem.* 268: 4134-4143.
73. Morelle, W., M. Bernard, J.P. Debeaupuis, M. Buitrago, M. Tabouret, and J.P. Latge. 2005. Galactomannoproteins of *Aspergillus fumigatus*. *Eukaryot Cell* 4: 1308-1316.
74. Willer, T., M.C. Valero, W. Tanner, J. Cruces, and S. Strahl. 2003. *O*-mannosyl glycans: from yeast to novel associations with human disease. *Curr. Opin. Struct. Biol.* 13: 621-630.
75. Goto, M. 2007. Protein *O*-glycosylation in fungi: diverse structures and multiple functions. *Biosci. Biotechnol. Biochem.* 71: 1415-1427.
76. Jigami, Y., and T. Odani. 1999. Mannosylphosphate transfer to yeast mannan. *Biochim. Biophys. Acta* 1426: 335-345.
77. Prill, S.K., B. Klinkert, C. Timpel, C.A. Gale, K. Schroppel, and J.F. Ernst. 2005. PMT family of *Candida albicans*: five protein mannosyltransferase isoforms affect growth, morphogenesis and antifungal resistance. *Mol. Microbiol.* 55: 546-560.

78. Olson, G.M., D.S. Fox, P. Wang, J.A. Alspaugh, and K.L. Buchanan. 2007. Role of protein *O*-mannosyltransferase Pmt4 in the morphogenesis and virulence of *Cryptococcus neoformans*. *Eukaryot. Cell.* 6: 222-234.
79. Willger, S.D., J.F. Ernst, J.A. Alspaugh, and K.B. Lengeler. 2009. Characterization of the PMT gene family in *Cryptococcus neoformans*. *PLoS One* 4: e6321.
80. Gemmill, T.R., and R.B. Trimble. 1999. Overview of *N*- and *O*-linked oligosaccharide structures found in various yeast species. *Biochim. Biophys. Acta* 1426: 227-237.
81. Schutzbach, J., H. Ankel, and I. Brockhausen. 2007. Synthesis of cell envelope glycoproteins of *Cryptococcus laurentii*. *Carbohydr. Res.* 342: 881-893.
82. Orlean, P., and A.K. Menon. 2007. Thematic review series: lipid posttranslational modifications. GPI anchoring of protein in yeast and mammalian cells, or: how we learned to stop worrying and love glycospholipids. *J. Lipid Res.* 48: 993-1011.
83. Reggiori, F., E. Canivenc-Gansel, and A. Conzelmann. 1997. Lipid remodeling leads to the introduction and exchange of defined ceramides on GPI proteins in the ER and Golgi of *Saccharomyces cerevisiae*. *EMBO J.* 16: 3506-3518.
84. Franzot, S.P., and T.L. Doering. 1999. Inositol acylation of glycosylphosphatidylinositols in the pathogenic fungus *Cryptococcus neoformans* and the model yeast *Saccharomyces cerevisiae*. *Biochem. J.* 340 (Pt 1): 25-32.

85. Fontaine, T., T. Magnin, A. Melhert, D. Lamont, J.P. Latge, and M.A. Ferguson. 2003. Structures of the glycosylphosphatidylinositol membrane anchors from *Aspergillus fumigatus* membrane proteins. *Glycobiology* 13: 169-177.
86. Barreto-Bergter, E., M.R. Pinto, and M.L. Rodrigues. 2004. Structure and biological functions of fungal cerebroside. *An. Acad. Bras. Cienc.* 76: 67-84.
87. Dickson, R.C., C. Sumanasekera, and R.L. Lester. 2006. Functions and metabolism of sphingolipids in *Saccharomyces cerevisiae*. *Prog. Lipid Res.* 45: 447-465.
88. Cowart, L.A., and L.M. Obeid. 2007. Yeast sphingolipids: recent developments in understanding biosynthesis, regulation, and function. *Biochim. Biophys. Acta* 1771: 421-431.
89. Toledo, M.S., S.B. Lavery, A.H. Straus, and H.K. Takahashi. 2001. Sphingolipids of the mycopathogen *Sporothrix schenckii*: identification of a glycosylinositol phosphorylceramide with novel core GlcNH(2)alpha1-->2Ins motif. *FEBS Lett.* 493: 50-56.
90. Heise, N., A.L. Gutierrez, K.A. Mattos, C. Jones, R. Wait, J.O. Previato, and L. Mendonca-Previato. 2002. Molecular analysis of a novel family of complex glycoinositolphosphoryl ceramides from *Cryptococcus neoformans*: structural differences between encapsulated and acapsular yeast forms. *Glycobiology* 12: 409-420.
91. Trinel, P.A., E. Maes, J.P. Zanetta, F. Delplace, B. Coddeville, T. Jouault, G. Strecker, and D. Poulain. 2002. *Candida albicans* phospholipomannan, a new member of the fungal mannose inositol phosphoceramide family. *J. Biol. Chem.* 277: 37260-37271.

92. Mille, C., G. Janbon, F. Delplace, S. Ibata-Ombetta, C. Gaillardin, G. Strecker, T. Jouault, P.A. Trinel, and D. Poulain. 2004. Inactivation of *CaMIT1* inhibits *Candida albicans* phospholipomannan beta-mannosylation, reduces virulence, and alters cell wall protein beta-mannosylation. *J. Biol. Chem.* 279: 47952-47960.
93. Warnecke, D., and E. Heinz. 2003. Recently discovered functions of glucosylceramides in plants and fungi. *Cell Mol. Life Sci.* 60: 919-941.
94. Rhome, R., T. McQuiston, T. Kechichian, A. Bielawska, M. Hennig, M. Drago, G. Morace, C. Luberto, and M. Del Poeta. 2007. Biosynthesis and immunogenicity of glucosylceramide in *Cryptococcus neoformans* and other human pathogens. *Eukaryot Cell* 6: 1715-1726.
95. Maciel, D.M., M.L. Rodrigues, R. Wait, M.H. Villas Boas, C.A. Tischer, and E. Barreto-Bergter. 2002. Glycosphingolipids from *Magnaporthe grisea* cells: expression of a ceramide dihexoside presenting phytosphingosine as the long-chain base. *Arch. Biochem. Biophys.* 405: 205-213.
96. Lester, R.L., S.W. Smith, G.B. Wells, D.C. Rees, and W.W. Angus. 1974. The isolation and partial characterization of two novel sphingolipids from *Neurospora crassa*: di(inositolphosphoryl)ceramide and ((gal)₃glu)ceramide. *J. Biol. Chem.* 249: 3388-3394.
97. Leipelt, M., D. Warnecke, U. Zahringer, C. Ott, F. Muller, B. Hube, and E. Heinz. 2001. Sep 7. Glucosylceramide synthases, a gene family responsible for the biosynthesis of glucosphingolipids in animals, plants, and fungi. *J. Biol. Chem.* 276:33621-33629

98. Klis, F.M., A. Boorsma, and P.W. De Groot. 2006. Cell wall construction in *Saccharomyces cerevisiae*. *Yeast* 23: 185-202.
99. Lesage, G., and H. Bussey. 2006. Cell wall assembly in *Saccharomyces cerevisiae*. *Microbiol. Mol. Biol. Rev.* 70: 317-343.
100. Kartsonis, N.A., J. Nielsen, and C.M. Douglas. 2003. Caspofungin: the first in a new class of antifungal agents. *Drug Resist Updat* 6: 197-218.
101. Douglas, C.M. 2001. Fungal beta(1,3)-D-glucan synthesis. *Med. Mycol.* 39 Suppl 1: 55-66.
102. Latge, J. P., I. Mouyna, F. Tekaia, A. Beauvais, J. P. Debeaupuis, and W. Nierman. 2005. May. Specific molecular features in the organization and biosynthesis of the cell wall of *Aspergillus fumigatus*. *Med. Mycol.* 43 Suppl 1:S15-22
103. Shahinian, S., and H. Bussey. 2000. beta-1,6-Glucan synthesis in *Saccharomyces cerevisiae*. *Mol. Microbiol.* 35: 477-489.
104. Humbel, B.M., M. Konomi, T. Takagi, N. Kamasawa, S.A. Ishijima, and M. Osumi. 2001. *In situ* localization of beta-glucans in the cell wall of *Schizosaccharomyces pombe*. *Yeast* 18: 433-444.
105. Vink, E., R.J. Rodriguez-Suarez, M. Gerard-Vincent, J.C. Ribas, H. de Nobel, H. van den Ende, A. Duran, F.M. Klis, and H. Bussey. 2004. An *in vitro* assay for (1->6)-beta-D-glucan synthesis in *Saccharomyces cerevisiae*. *Yeast* 21: 1121-1131.
106. Hochstenbach, F., F.M. Klis, H. van den Ende, E. van Donselaar, P.J. Peters, and R.D. Klausner. 1998. Identification of a putative alpha-glucan synthase essential

- for cell wall construction and morphogenesis in fission yeast. *Proc. Natl. Acad. Sci. U.S.A.* 95: 9161-9166.
107. Garcia, I., V. Tajadura, V. Martin, T. Toda, and Y. Sanchez. 2006. Synthesis of alpha-glucans in fission yeast spores is carried out by three alpha-glucan synthase paralogues, Mok12p, Mok13p and Mok14p. *Mol. Microbiol.* 59: 836-853.
108. Beauvais, A., D. Maubon, S. Park, W. Morelle, M. Tanguy, M. Huerre, D.S. Perlin, and J.P. Latge. 2005. Two alpha(1-3) glucan synthases with different functions in *Aspergillus fumigatus*. *Appl. Environ. Microbiol.* 71: 1531-1538.
109. Rappleye, C.A., J.T. Engle, and W.E. Goldman. 2004. RNA interference in *Histoplasma capsulatum* demonstrates a role for alpha-(1,3)-glucan in virulence. *Mol. Microbiol.* 53: 153-165.
110. Reese, A.J., A. Yoneda, J.A. Breger, A. Beauvais, H. Liu, C.L. Griffith, I. Bose, M.J. Kim, C. Skau, S. Yang, J.A. Sefko, M. Osumi, J.P. Latge, E. Mylonakis, and T.L. Doering. 2007. Loss of cell wall alpha(1-3) glucan affects *Cryptococcus neoformans* from ultrastructure to virulence. *Mol. Microbiol.* 63: 1385-1398.
111. Reese, A.J., and T.L. Doering. 2003. Cell wall alpha-1,3-glucan is required to anchor the *Cryptococcus neoformans* capsule. *Mol. Microbiol.* 50: 1401-1409.
112. Bowman, S.M., and S.J. Free. 2006. The structure and synthesis of the fungal cell wall. *Bioessays* 28:799-808
113. Munro, C.A., and N.A. Gow. 2001. Chitin synthesis in human pathogenic fungi. *Med. Mycol.* 39 Suppl 1: 41-53.

114. Roncero, C. 2002. The genetic complexity of chitin synthesis in fungi. *Curr. Genet.* 41: 367-378.
115. Banks, I.R., C.A. Specht, M.J. Donlin, K.J. Gerik, S.M. Levitz, and J.K. Lodge. 2005. A Chitin Synthase and Its Regulator Protein Are Critical for Chitosan Production and Growth of the Fungal Pathogen *Cryptococcus neoformans*. *Eukaryot Cell* 4: 1902-1912.
116. Mellado, E., G. Dubreucq, P. Mol, J. Sarfati, S. Paris, M. Diaquin, D.W. Holden, J. L. Rodriguez-Tudela, and J.P. Latge. 2003. Cell wall biogenesis in a double chitin synthase mutant (chsG-/chsE-) of *Aspergillus fumigatus*. *Fungal Genet. Biol.* 38: 98-109.
117. Baker, L.G., C.A. Specht, M.J. Donlin, and J.K. Lodge. 2007. Chitosan, the deacetylated form of chitin, is necessary for cell wall integrity in *Cryptococcus neoformans*. *Eukaryot Cell* 6: 855-867.
118. Elbein, A.D., Y.T. Pan, I. Pastuszak, and D. Carroll. 2003. New insights on trehalose: a multifunctional molecule. *Glycobiology* 13: 17R-27R.
119. Francois, J., and J.L. Parrou. 2001. Reserve carbohydrates metabolism in the yeast *Saccharomyces cerevisiae*. *FEMS Microbiol. Rev.* 25: 125-145.
120. Lomako, J., W.M. Lomako, and W.J. Whelan. 2004. Glycogenin: the primer for mammalian and yeast glycogen synthesis. *Biochim. Biophys. Acta* 1673: 45-55.
121. de Paula, R.M., W.A. Wilson, H.F. Terenzi, P.J. Roach, and M.C. Bertolini. 2005. GNN is a self-glucosylating protein involved in the initiation step of glycogen biosynthesis in *Neurospora crassa*. *Arch. Biochem. Biophys.* 435: 112-124.

122. Chayakulkeeree, M., and J. R. Perfect. 2006. Cryptococcosis. *Infect. Dis. Clin. North Am.* 20: 507-44, v-vi.
123. James, P.G., and R. Cherniak. 1992. Galactoxylomannans of *Cryptococcus neoformans*. *Infect. Immun.* 60: 1084-1088.
124. Cherniak, R., H. Valafar, L.C. Morris, and F. Valafar. 1998. *Cryptococcus neoformans* chemotyping by quantitative analysis of ¹H nuclear magnetic resonance spectra of glucuronoxylomannans with a computer-simulated artificial neural network. *Clin. Diagn. Lab. Immunol.* 5: 146-159.
125. Ikeda, R., and T. Maeda. 2004. Structural studies of the capsular polysaccharide of a non-neoformans *Cryptococcus* species identified as *C. laurentii*, which was reclassified as *Cryptococcus flavescens*, from a patient with AIDS. *Carbohydr. Res.* 339: 503-509.
126. Yoneda, A., and T.L. Doering. 2006. A eukaryotic capsular polysaccharide is synthesized intracellularly and secreted via exocytosis. *Mol. Biol. Cell* 17: 5131-5140.
127. Schutzbach, J.S., and H. Ankel. 1971. Multiple mannosyl transferases in *Cryptococcus laurentii*. *J. Biol. Chem.* 246: 2187-2194.
128. Klutts, J.S., S.B. Levery, and T.L. Doering. 2007. A beta-1,2-xylosyltransferase from *Cryptococcus neoformans* defines a new family of glycosyltransferases. *J. Biol. Chem.* 282: 17890-17899.

129. Klutts, J.S., and T.L. Doering. 2008. Cryptococcal xylosyltransferase 1 (Cxt1p) from *Cryptococcus neoformans* plays a direct role in the synthesis of capsule polysaccharides. *J. Biol. Chem.* 283: 14327-14334.
130. Castle, S.A., E.A. Owuor, S.H. Thompson, M.R. Garnsey, J.S. Klutts, T.L. Doering, and S.B. Levery. 2008. Beta1,2-xylosyltransferase Cxt1p is solely responsible for xylose incorporation into *Cryptococcus neoformans* glycosphingolipids. *Eukaryot Cell* 7: 1611-1615.
131. Bar-Peled, M., C.L. Griffith, and T.L. Doering. 2001. Functional cloning and characterization of a UDP- glucuronic acid decarboxylase: the pathogenic fungus *Cryptococcus neoformans* elucidates UDP-xylose synthesis. *Proc. Natl. Acad. Sci. U.S.A.* 98: 12003-12008.
132. Bar-Peled, M., C.L. Griffith, J.J. Ory, and T.L. Doering. 2004. Biosynthesis of UDP-GlcA, a key metabolite for capsular polysaccharide synthesis in the pathogenic fungus *Cryptococcus neoformans*. *Biochem. J.* 381: 131-136.
133. Griffith, C.L., J.S. Klutts, L. Zhang, S.B. Levery, and T.L. Doering. 2004. UDP-glucose dehydrogenase plays multiple roles in the biology of the pathogenic fungus *Cryptococcus neoformans*. *J. Biol. Chem.* 279: 51669-51676.
134. Doering, T.L. 1999. A unique alpha-1,3 mannosyltransferase of the pathogenic fungus *Cryptococcus neoformans*. *J. Bacteriol.* 181:5482-5488.
135. Sommer, U., H. Liu, and T.L. Doering. 2003. An alpha-1,3-mannosyltransferase of *Cryptococcus neoformans*. *J. Biol. Chem.* 278: 47724-47730.

136. Faltynek, C.R., J.E. Silbert, and L. Hof. 1982. Xylosylphosphoryldolichol synthesized by chick embryo epiphyses. Not an intermediate in proteoglycan biosynthesis. *J. Biol. Chem.* 257: 5490-5495.
137. Vaishnav, V.V., B.E. Bacon, M. O'Neill, and R. Cherniak. 1998. Structural characterization of the galactoxylomannan of *Cryptococcus neoformans* Cap67. *Carbohydr. Res.* 306: 315-330.
138. Moyrand, F., B. Klaproth, U. Himmelreich, F. Dromer, and G. Janbon. 2002. Isolation and characterization of capsule structure mutant strains of *Cryptococcus neoformans*. *Mol. Microbiol.* 45: 837-849.
139. Kozel, T.R., S.M. Levitz, F. Dromer, M.A. Gates, P. Thorkildson, and G. Janbon. 2003. Antigenic and biological characteristics of mutant strains of *Cryptococcus neoformans* lacking capsular O acetylation or xylosyl side chains. *Infect. Immun.* 71: 2868-2875.
140. Sahu, A., T.R. Kozel, and M.K. Pangburn. 1994. Specificity of the thioester-containing reactive site of human C3 and its significance to complement activation. *Biochem. J.* 302 (Pt 2): 429-436.
141. Moyrand, F., T. Fontaine, and G. Janbon. 2007. Systematic capsule gene disruption reveals the central role of galactose metabolism on *Cryptococcus neoformans* virulence. *Mol. Microbiol.* 64: 771-781.
142. Bose, I., A.J. Reese, J.J. Ory, G. Janbon, and T.L. Doering. 2003. A yeast under cover: the capsule of *Cryptococcus neoformans*. *Eukaryot Cell* 2: 655-663.

CHAPTER II

A NOVEL XYLOSYLPHOSPHOTRANSFERASE ACTIVITY DISCOVERED IN *CRYPTOCOCCUS NEOFORMANS*^{*}

**Morgann C. Reilly[‡], Steven B. Levery[§], Sherry A. Castle[¶], J. Stacey Klutts^{‡,||},
and Tamara L. Doering[‡]**

From the [‡]Department of Molecular Microbiology, Washington University School of Medicine, St. Louis, MO 63110, USA; the [§]Department of Cellular and Molecular Medicine, University of Copenhagen, 2200 Copenhagen N, Denmark; the [¶]Department of Chemistry, University of New Hampshire, Durham, NH 03824, USA; and the ^{||}Department of Pathology, University of Iowa Carver College of Medicine and Pathology and Laboratory Medicine, Veteran's Affairs Medical Center, Iowa City, IA 52246, USA.

** Previously published; reprinted with permission:*

Reilly M.C., Kazuhiro A., Tiemeyer M., Levery S.B., and Doering T.L. 2009. A novel xylosylphosphotransferase activity discovered in *Cryptococcus neoformans*. *Journal of Biological Chemistry*: Oct 28 [epub ahead of print].

ABSTRACT

Cryptococcus neoformans is a fungal pathogen that causes serious disease in immunocompromised individuals. The organism produces a distinctive polysaccharide capsule that is necessary for its virulence, a predominantly polysaccharide cell wall, and a variety of protein- and lipid-linked glycans. The glycan synthetic pathways of this pathogen are of great interest. Here we report the detection of a novel glycosylphosphotransferase activity in *C. neoformans*, identification of the corresponding gene, and characterization of the encoded protein. The observed activity is specific for UDP-xylose as a donor and for mannose acceptors, and forms a xylose- α -1-phosphate-6-mannose linkage. This is the first report of a xylosylphosphotransferase activity in any system.

INTRODUCTION

Fungi generate a wide variety of glycans, many of which differ from those of higher eukaryotes. In pathogenic fungal species, these unique structures and their synthetic pathways represent possible drug targets. One example of these distinctive cellular glycans is the extensive polysaccharide capsule of the basidiomycete, *Cryptococcus neoformans*. An environmental yeast, *C. neoformans* can be isolated from soil, avian excreta, and certain trees, but is also capable of causing disease in mammals following the inhalation of spores or small yeast cells (1). *C. neoformans* is typically neutralized within the lung by the immune system without any symptomatic evidence of infection. Under conditions of compromised host immunity, however, the organism may disseminate from its primary site of infection in the lungs to more distal sites in the body, demonstrating a particular tropism for the central nervous system. If *C. neoformans* reaches the brain, it can form lesions called cryptococcomas and cause a meningoencephalitis that is fatal if not treated.

Although other yeasts bear polysaccharide capsules, members of the *C. neoformans* species complex are the only known pathogenic fungi with this feature. The capsule, which is required for virulence (2), is primarily composed of two polysaccharides: glucuronoxylomannan and glucuronoxylomannogalactan (GXM (3) and GXMGal (4, 5), respectively). In addition to this distinguishing structure, *C. neoformans* synthesizes a diverse array of glycans, which differ from those of its mammalian host as well as the ‘model’ yeast *Saccharomyces cerevisiae*. For example, the core oligosaccharide of *N*-glycans is truncated in *C. neoformans* such that it lacks the three terminal glucose (Glc)

residues present on the same structure in most eukaryotes, including *S. cerevisiae* and mammals (6). Cryptococcal *O*-glycans also differ from the oligomannose structures found in *S. cerevisiae* (7): studies in the environmental yeast *Cryptococcus laurentii* have identified *O*-glycans that are branched and contain galactose (Gal), xylose (Xyl), and mannose (Man) residues (8). These oligosaccharides are thus more like mammalian *O*-glycans in complexity, although the array of components is quite distinct (9). In addition, some glycan structures found in fungi do not have an equivalent in mammalian cells, such as the lipid-linked glycosylinositol phosphorylceramides (GIPCs). In *S. cerevisiae*, GIPCs contain only a single Man residue while cryptococcal GIPCs contain residues of Man, Xyl, Gal, and glucosamine (10). Despite the obvious significance of glycan biosynthetic pathways as potential drug targets among pathogenic fungi, however, few have been studied in detail.

In order to investigate glycan biosynthesis, our laboratory studies the central enzymes in these pathways, known as glycosyltransferases. These enzymes generally catalyze the transfer of a monosaccharide moiety from an activated sugar donor to a specific acceptor molecule, forming a particular linkage. Donors of sugar molecules can include nucleotide mono- and diphosphosugars, sugar phosphates, and dolichol-linked sugars; proteins, lipids, and other saccharides can all serve as acceptors in transferase reactions. Glycosyltransferases are divided into families based on their tertiary structure and catalytic mechanism, including their requirements for metal ion cofactors (11). Conservation in sequence at the amino acid level occurs only between some closely related glycosyltransferases.

We are particularly interested in the addition of Xyl residues to the cellular glycans of *C. neoformans*. This stems from a series of studies on the synthesis of UDP-xylose (UDP-Xyl), the Xyl donor in eukaryotic cells, which is formed upon the decarboxylation of UDP-glucuronic acid (UDP-GlcA) by Uxs1p. The cryptococcal gene encoding Uxs1p was identified in our laboratory (12). Deletion of *UXS1* in *C. neoformans* yields a strain that generated no UDP-Xyl (13); as a consequence, isolated GXM contains no detectable Xyl (14), capsule fibers appear short and thickened when viewed by electron microscopy (13), and cellular GIPCs lack Xyl and are truncated (15, 16). Importantly, *uxs1*Δ strains are avirulent in a murine model of cryptococcal infection (14), indicating that the incorporation of Xyl residues into cellular glycans is required for *C. neoformans* to cause disease. This compelling result led us to investigate xylosyltransferases in *C. neoformans*.

In this report, we document the discovery of a novel xylosyltransferase activity in *C. neoformans* that generates a highly unusual product, xylosylphosphomannose. Below, we describe the initial identification of this activity, our determination of the corresponding gene, and our characterization of this unique and intriguing enzyme.

EXPERIMENTAL PROCEDURES

Materials. DNA polymerases (*Taq* and AccuPrime™ *Pfx*) and oligos used for PCR (Supplemental Table 1) were from Invitrogen; DNA purification kits were from Qiagen. GDP-[2-³H(N)]mannose (22.2 Ci/mmol), UDP-[1-³H(N)]glucuronic acid (10.2 Ci/mmol), and UDP-[¹⁴C(U)]xylose (151 mCi/mmol) were from PerkinElmer; UDP-[6-³H(N)]galactose (60 Ci/mmol), UDP-[1-³H(N)]glucose (15 Ci/mmol), and UDP-[6-³H(N)]N-acetylglucosamine (34.8 Ci/mmol) were from American Radiolabeled

Supplemental Table 1. Primers used in these studies.

Name	Sequence (5' to 3')^{a,b}
CNJ001	<u>GGACTAGTCCCCAGCGAGCAAACGAGCTGGTCCACTCG</u>
CNJ002	<u>GGACTAGTCCCCTTCTTCTTCCACTCATTTC</u>
MCR035	<u>GGACTAGTCCTCACGCCGACATGGCATGAAGCC</u>
MCR036	<u>GGACTAGTCCGGATCCCAATCTCTTTCCCATACCG</u>
MCR063	CGAATCAAAGGCAAGTGTTTGATCC
MCR101	CATGGTCATAGCTGTTTCTGAGAAGATGCAAAGAGGATG GACG
MCR068	CGACTACATCGATTTGTTCAATCAATACG
MCR104	CACTGGCCGTCGTTTTACAACAAAGGTTGATAAACCGAATG CATG
MCR102	CCATCCTCTTTTGCATCTTCTCAGGAAACAGCTATGACCATG
MCR103	GCATTCGGTTTATCAACCTTTGTTGTAAAACGACGGCCAGTG
MCR069	GGATAACTGACAATTATTATATCAGTGC
MCR070	CTGTTGTCCATTGATTATGATTTCG
MCR127	CCTTAATTAAGGCCTCACAACTATCCAACGACATGG
MCR120	<u>TTAAGCGTAGTCTGGGACGTCGTATGGGTAATCATTATACCT</u> ATCTTTTACAGGATCCC
MCR121	<u>TACCATACGACGTCCCAGACTACGCTTAAACATAGAACGT</u> AGAAGGAGATGGAGG
MCR149	CCATCGGTTCTTACAACGGCTGG

^a Underlined sequences indicate SpeI restriction sites

^b Bold-underlined sequences encode HA epitope tag

Chemicals. α -1,2-D-mannobiose and α -1,6-D-mannobiose were from Sigma Aldrich; α -1,3-D-mannobiose was from Carbohydrate Synthesis (Oxford, United Kingdom); α -1,4-D-mannobiose was from V-Labs. Restriction enzymes were from New England BioLabs. Unless specified, all other chemicals or reagents were obtained from Sigma Aldrich.

Strains and cell growth. *C. neoformans* strains (Table 1) were grown in liquid culture at 30°C in YPD medium (1% w/v yeast extract, 2% w/v peptone, 2% w/v dextrose) with shaking (230 rpm) or at 30°C on YPD agar plates (YPD medium with 2% w/v agar). As appropriate, media included 100 μ g/ml nourseothricin (NAT; from Werner Bio-Agents) or Geneticin[®] (G418; from Invitrogen). For RNA interference (RNAi) studies, strains were cultured at 30°C in a Gal-5FOA Minimal Medium (1.34% w/v yeast nitro-

Table 1. *C. neoformans* strains used in these studies.

Name ^{a,b}	Origin
CAP67	Jacobson <i>et al.</i> 1982 (26)
CAP67 <i>cxt1</i> Δ	Klutts <i>et al.</i> 2007 (17)
CAP67 <i>cxt2</i> Δ	J.S. Klutts and T.L. Doering, manuscript in preparation
CAP67 <i>cxt1</i> Δ <i>cxt2</i> Δ	J.S. Klutts and T.L. Doering, manuscript in preparation
CAP67 <i>cxt1</i> Δ pIBP103	This study
CAP67 <i>cxt1</i> Δ p <i>XPTI</i> i	This study
JEC21	Kwon-Chung <i>et al.</i> 1992 (43)
KN99 α	Nielsen <i>et al.</i> 2003 (44)
KN99a	Nielsen <i>et al.</i> 2003 (44)
KN99 α <i>cxt1</i> Δ <i>cxt2</i> Δ	J.S. Klutts and T.L. Doering, manuscript in preparation
KN99 α <i>xpt1</i> Δ	This study
KN99 α <i>xpt1</i> Δ p <i>XTP1</i>	This study
KN99 α <i>xpt1</i> Δ p <i>XTP1-HA</i>	This study

^a All strains are MAT α , except for KN99a is MATa

^b All KN99 strains are serotype A; all other strains are serotype D

gen base without amino acids, 2% w/v galactose, 0.087% w/v complete dropout mix without uracil, 1.2% w/v uracil, 1 mg/ml 5-fluoroorotic acid (5-FOA), 1 mM NaOH) or at 30°C on Gal-5FOA agar plates (Gal-5FOA Minimal Media with 2.5% w/v agar). Genetic crosses were performed at room temperature on V8 agar plates (5% v/v V8 juice, 0.05% KH₂PO₄ pH 7.0, 4% w/v agar).

Escherichia coli strains were grown in liquid culture at 37°C in LB medium (1% w/v tryptone, 0.5% w/v yeast extract, 1% w/v NaCl) with shaking (250 rpm) or at 37°C on LB agar plates (LB medium with 2% w/v agar). As appropriate, media included 100 µg/ml ampicillin or 60 µg/ml kanamycin.

Total membrane preparation and detergent extraction. For membrane preparation and detergent extraction all steps were performed at 4°C. *C. neoformans* was cultured overnight in 50 ml YPD to late log phase ($\sim 1 \times 10^8$ cells/ml), harvested by centrifugation (3,000 × g; 10 min), and washed in 40 ml Tris-EDTA Buffer (100 mM Tris-HCl pH 8.0, 0.1 mM EDTA). The washed cell pellet was resuspended in an equal volume of Tris-EDTA Buffer and 800 µl aliquots were transferred to 2-ml screw-cap microcentrifuge tubes. Samples were bead-beaten with 800-µl 0.5-mm glass beads (BioSpec Products) in 1 min bursts on a Mini-Bead Beater (BioSpec Products), alternating with 2 min on ice. Once ~75% of the cells were disrupted (as assessed by microscopy), the lysate was transferred to a 15-ml conical tube and the glass beads rinsed with 800 µl Tris-EDTA Buffer; this buffer and three more rinses were pooled with the lysate. The pooled material was subjected to a clearing centrifugation step (1,000 × g; 20 min) and the resulting supernatant fraction transferred to an ultracentrifuge tube. Total membranes were isolated by

ultracentrifugation (60,000 × g; 45 min), resuspended in 50-200 µl Tris Buffer (100 mM Tris-HCl pH 8.0), and stored at 4°C. Protein concentrations of the total membrane samples were determined using the Bio-Rad Protein Assay (Bio-Rad Laboratories).

For detergent extraction, Triton X-100 was added to the membranes to a final concentration of 1% and the sample was incubated on ice for 30 min with vortex mixing every 5 min. Particulate material was removed by ultracentrifugation (75,000 × g; 30 min) and the supernatant stored at 4°C. Protein concentrations of the detergent-extracted cellular membrane samples were determined using the Bio-Rad Detergent-Compatible Protein Assay (Bio-Rad Laboratories).

For substrate titration studies, Triton X-100-extracts were prepared in bulk to minimize any variability in manganese-dependent xylosyltransferase activity levels between membrane preparations. Detergent extracts were prepared as above from a 1-L culture of KN99α *cxt1*Δ *cxt2*Δ; glycerol was added to a final concentration of 15% and the material was stored in aliquots at -80°C. For xylosyltransferase reactions, an aliquot of this extract was thawed at 37°C and immediately placed on ice. Glycerol was removed by subjecting the sample to two rounds of 10-fold dilution with Tris Buffer and concentration using an Amicon® Ultra-15 Centrifugal Filter Device (30,000 MWCO; from Millipore), and protein concentration was determined using the Bio-Rad Detergent-Compatible Protein Assay.

Xylosyltransferase activity assays. Enzyme activity was assayed by monitoring the transfer of [¹⁴C]Xyl from a UDP-[¹⁴C]Xyl donor to an α-1,3-D-mannobiose acceptor (α-1,3-Man₂). Standard reactions included 625 µg protein (from total membranes or Tri-

ton X-100-extracts), 1 μM UDP- ^{14}C Xyl, 8.8 mM α -1,3-Man₂, and 7.5 mM MnCl₂ in 100 mM Tris-HCl pH 6.5 and were incubated at 20°C for either 4 hrs (for substrate titration) or overnight (for other studies). The reaction products were isolated and visualized as described in (17). Briefly, unincorporated UDP- ^{14}C Xyl was removed by passing the sample over an 800- μl column of AG[®] 2-X8 resin (Bio-Rad) with water elution. The product was resolved by thin layer chromatography (TLC) using Silica Gel 60 plates (EM Sciences) and developed in a solvent system of 5:4:1 1-propanol:acetone:water; plates were sprayed with En³Hance[®] Spray (PerkinElmer) and radiolabeled products visualized by autoradiography.

Isolation of the manganese-dependent reaction product. Xylosyltransferase reactions using Triton X-100-extracts of CAP67 *xtlA* membranes were performed with 0.5 μM UDP- ^{14}C Xyl plus 14.7 mM non-radioactive UDP-Xyl and incubated at 20°C for 36 hrs. Samples were processed and resolved by TLC as above and the product of interest localized using a System 200A Imaging Scanner (Bioscan Inc). The appropriate region of silica was scraped from the plate, and the product eluted from the silica with water and purified using an Envi-Carb solid phase extraction column (Supelco) as in (17).

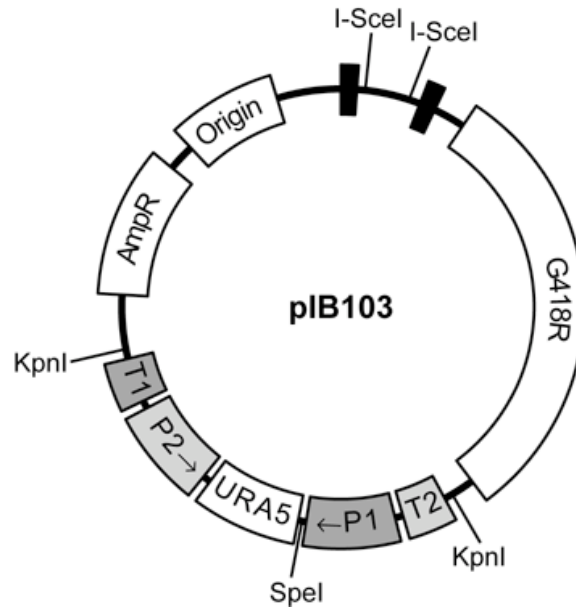
Additional product analysis. For some studies, the products of standard xylosyltransferase reactions were treated with or without acetic acid (final concentration of 1%) at 100°C for 1 hr. For others, samples were incubated at 25°C overnight with or without Jack Bean mannosidase (final concentration of 21 $\mu\text{g}/\text{ml}$ in 150 mM citric acid pH 5.0). Treated samples were resolved by TLC and visualized by autoradiography as above.

One-dimensional ^1H and two-dimensional ^1H - ^1H nuclear magnetic resonance spectroscopy. The product of the manganese-dependent xylosyltransferase reaction (~0.5 mg) was deuterium-exchanged by repeated lyophilization from D_2O , and then dissolved in 0.5 ml D_2O for NMR analysis. One-dimensional ^1H -NMR, two-dimensional ^1H - ^1H -gCOSY, and two-dimensional ^1H - ^1H -TOCSY spectra were acquired at 25°C on a Varian Unity Inova 500-MHz spectrometer (Varian Inc), using standard acquisition software available in the Varian VNMR software package. Proton chemical shifts were referenced to internal acetone ($\delta = 2.225$ ppm).

Electrospray-ionization mass spectrometry. Mass spectrometry was performed in both positive and negative ion modes on a linear ion trap (LTQ; from Thermo Fisher Scientific), with sample introduction via direct infusion in 50% methanol in water (for the native manganese-dependent xylosyltransferase reaction product) or 100% methanol (for the permethylated manganese-dependent xylosyltransferase reaction product), and sample concentration of ~100 ng/ μl .

RNAi targeting. The construct for RNAi in *C. neoformans*, pIB103, is diagrammed in Supplemental Figure 1; its construction is described elsewhere.¹ The plasmid contains two opposing pairs of promoters and terminators cloned from the *GAL7* locus (NCBI accession number U16994) flanking a ~250 bp fragment of the *URA5* gene (NCBI accession number AF140188). Bidirectional transcription across this segment produces double-stranded RNA that effectively silences *URA5*, allowing cell growth in the pres-

¹ I. Bose and T.L. Doering manuscript in preparation



Supplemental Figure 1. Plasmid for RNA interference in *C. neoformans*. P1 and P2, *GAL7* promoter; T1 and T2, *GAL7* terminator; URA5, *URA5* fragment (see text); G418R, G418 resistance cassette; AmpR, ampicillin resistance cassette; Origin, bacterial plasmid origin of replication; black wedges, telomeric sequences. The P1 and T1 sequences are in the same orientation (indicated by the arrow on P1); the P2 and T2 sequences are both in the opposite orientation. Restriction enzyme sites mentioned in the text are indicated. Not drawn to scale.

ence of 5-FOA. I-SceI digestion linearizes the plasmid while exposing telomeric sequences (18).

To isolate total RNA, an overnight culture of the *C. neoformans* strain JEC21 was harvested by centrifugation (3,000 × g; 10 min) and washed with 50 ml diethylpyrocarbonate-treated water; the pellet was frozen in a dry ice / methanol bath and lyophilized

overnight. Four milliliters of 0.5-mm glass beads were added to the dried pellet and the sample was beaten to a fine powder using a vortex mixer, mixed with 4 ml TRIzol[®] (Invitrogen), and incubated at room temperature for 5 min. Next, the sample was mixed with 800 μ l chloroform, incubated at room temperature for 3 min, and centrifuged at 3,000 \times g for 30 min. The upper aqueous phase was mixed with an equal volume of 70% ethanol and applied to an RNeasy[®] maxi column (RNeasy[®] Maxi Kit; from Qiagen). Total RNA was isolated according to the manufacturer's protocol and used to generate cDNA using the Superscript[™] First-Strand Synthesis System for RT-PCR (Invitrogen).

Two regions of *XPT1* (nucleotides 724-1267 and 2551-2966) were targeted for RNAi. Each was PCR-amplified from JEC21 cDNA using primer pairs that introduced SpeI restriction sites at both ends (CNJ001/CNJ002 and MCR035/MCR036). When the CNJ001/CNJ002 amplicon was cloned into the pCR[®]2.1-TOPO[®] vector (TOPO TA Cloning[®] Kit; from Invitrogen) it formed the plasmid TOPO *XPT1* RNAi, which was then transformed into TOP10 *E. coli* cells. The pTOPO *XPT1* RNAi and pIB103 plasmids were isolated and digested with SpeI; the latter was also treated with Calf Intestinal Alkaline Phosphatase (CIAP; from Fisher). The RNAi target insert and the linearized vector were purified, and the fragments ligated with T4 DNA Ligase (Roche) to form the *XPT1* RNAi construct p*XPT1i*, which was then transformed into DH5 α *E. coli* cells (Invitrogen).

Purified p*XPT1i* was linearized with I-SceI and transformed into the *C. neoformans* strain CAP67 *ctx1* Δ by electroporation (19). Colonies were selected on YPD G418 agar and then screened for growth on Gal 5-FOA agar.

Confirmation of the XPT1 transcript. The coding sequence of *XPT1* was PCR-amplified in overlapping fragments using primers directed against predicted exon sequences (*C. neoformans* var. *grubii* H99 Database maintained by the Broad Institute) and cDNA generated as above but from strain KN99 α . The resulting DNA segments were cloned into the pCR[®]2.1-TOPO[®] vector and sequenced. The 5' and 3' untranslated regions (UTRs) of the *XPT1* transcript were verified using the GeneRacer[™] Kit (Invitrogen). The *XPT1* transcript sequence has been submitted to the NCBI database (accession number GQ403790).

XPT1 deletion strain and complementation. Regions of ~1 kb immediately 5' to the start codon of *XPT1* (5'UTR) and immediately 3' to the stop codon of *XPT1* (3'UTR) were PCR-amplified from KN99 α genomic DNA prepared as in (20) using the primer pairs MCR063/MCR101 and MCR104/MCR068, respectively. The NAT resistance cassette (NAT^R) was amplified from the plasmid pGMC200-MCS (13) by PCR using primers MCR102 and MCR103. To form the *XPT1* deletion (*xpt1* Δ) construct, the purified 5'UTR, NAT^R, and 3'UTR amplicons were assembled into a single sequence by overlap-PCR (21) using primers MCR069 and MCR070.

The *xpt1* Δ construct was biolistically transformed into KN99 α cells (22). Genomic DNA was prepared from NAT-resistant transformants and screened by PCR for loss of the native *XPT1* locus and presence of the *xpt1* Δ construct. Finally, candidate deletion strains were confirmed by Southern blot analysis (23). Verified KN99 α *xpt1* Δ strains were crossed to KN99 α on V8 agar as described in (24) and the resulting spores plated on YPD NAT plates; a NAT^R *MATa* progeny strain was then back-crossed to

KN99 α . This crossing procedure (switching mating type) was repeated three times with spore selection on YPD NAT plates. The progeny of two independent KN99 α *xpt1* Δ strains were confirmed to lack Xpt1p activity and used for further study.

For plasmid-based complementation of the *xpt1* Δ strain, *XPT1* with ~1 kb of flanking sequence on either side was PCR-amplified using primers MCR063 and MCR068 from KN99 α genomic DNA prepared as above. The amplicon was cloned into the PCR[®]-XL-TOPO[®] vector (TOPO[®] XL PCR Cloning Kit; from Invitrogen) to form the plasmid pXL-TOPO *XPT1*, which was then transformed into TOP10 *E. coli* cells, purified, and sequenced to ensure that no errors were introduced during PCR. Confirmed *XPT1* was released from pXL-TOPO *XPT1* by digestion with SpeI and XbaI, blunted with T4 DNA Polymerase (from New England Biolabs), and cloned into KpnI-digested and CIAP-treated pIB103; the resulting p*XPT1* plasmid was then transformed into DH5 α *E. coli* cells. p*XPT1* was isolated, linearized with I-SceI, and transformed into the *C. neoformans* strain KN99 α *xpt1* Δ by electroporation (25). Genomic DNA prepared from G418-resistant transformants was screened by PCR and candidate KN99 α *xpt1* Δ p*XPT1* clones were assayed for recovery of xylosyltransferase activity as above.

Generation of epitope-tagged XPT1 strains. Xpt1p was epitope-tagged by replacing a region extending from the middle of the gene through the 3'UTR with the same sequences modified to incorporate hemagglutinin (HA) at the C-terminus. The replacement cassette was created by overlap-PCR (21), which combined two PCR products: a ~1.5 kb region immediately 5' to the stop codon of *XPT1* (PCR-amplified from the plasmid pXL-TOPO *XPT1* using the primer pair MRC127 and MCR120) and a ~650 bp region includ-

ing and immediately 3' to the stop codon of *XPT1* (PCR-amplified from pXL-TOPO *XPT1* using the primer pair MCR121 and MCR149). Primers MCR120 and MCR121 each introduced sequence encoding the HA epitope, enabling fragment joining by overlap-PCR using primers MCR127 and MCR149. The resulting product and pXL-TOPO *XPT1* were both digested with SacII and NheI; the insert and the linearized vector were purified and the fragments ligated with T4 DNA Ligase to form pXL-TOPO *XPT1-HA*, containing the complete and tagged sequence. This was transformed into DH5 α *E. coli* cells and confirmed by sequencing.

To express *XPT1-HA* in *C. neoformans*, the complete tagged sequence was released from pXL-TOPO *XPT1-HA* by digestion with SpeI and XbaI, blunted with T4 DNA Polymerase, and cloned into KpnI-digested and CIAP-treated pIB103. The resulting p*XPT1-HA* plasmid was linearized with I-SceI and transformed into the *C. neoformans* strain KN99 α *xpt1* Δ by electroporation (25). G418-resistant transformants were screened by PCR and candidate KN99 α *xpt1* Δ p*XPT1-HA* clones were assayed for recovery of xylosyltransferase activity as above.

Immunoprecipitation studies. Detergent-extracts of total membranes from KN99 α *xpt1* Δ p*XPT1* and KN99 α *xpt1* Δ p*XPT1-HA* were prepared as above. Total protein (5 mg) was rotated at 4°C for 1 hr with 50 μ l Anti-HA MicroBeads from the μ MACS™ HA Epitope Tag Protein Isolation Kit (Miltenyi Biotec) in a total of 500 μ l Tris-EDTA Buffer. The samples were then applied to μ Columns placed in the magnetic field of a μ MACS Separator and the columns washed with 200 μ l Tris Buffer five times. The μ Columns were removed from the magnetic field of the μ MACS Separator and 100 μ l Tris Buffer

applied to each column to elute the Anti-HA MicroBeads and associated material. The eluates were assayed for xylosyltransferase activity as above.

RESULTS

Xylosyltransferase activities in C. neoformans. We are interested in identifying and characterizing glycosyltransferases that synthesize the unique glycan structures of *C. neoformans* in order to better understand these fungal-specific processes. We have focused in particular on the transfer of Xyl residues because of the requirement for this moiety in virulence (14). In one assay of Xyl modification, we monitored the transfer of [¹⁴C]Xyl from UDP-[¹⁴C]Xyl to an α -1,3-Man₂ acceptor. As shown in track 1 of Figure 1, this assay yielded two distinct products (indicated by the arrowheads), as well as a small amount of free Xyl near the solvent front, presumably formed by degradation of the radiolabeled precursor. The generation of both products depended on the presence of α -1,3-Man₂ (Figure 1, compare tracks 1 and 3); the slower migrating product (filled arrowhead) additionally required MnCl₂ for its formation (Figure 1, compare tracks 1 and 2). CAP67, an acapsular strain mutated in the *CAP59* gene (26), was used here because these cells are more readily lysed than wild-type. Deletion of *CAP59* or several other genes (*CAP10*, 60, and 64 (27-29)) that are required for capsule synthesis and suggested to be glycosyltransferases (30) did not affect the formation of either product (data not shown).

In previous work, we identified a protein responsible for the formation of the majority of the manganese-independent product (Figure 1, open arrowhead) as Cxt1p (17). Deletion of the corresponding gene (*CXT1*) significantly reduced this signal (Figure 2, compare tracks 2 and 4). The small amount of similarly migrating product seen in a *cxt1* Δ strain is generated by a related enzyme, Cxt2p,² and disappeared in a *cxt2* Δ strain

² J.S. Klutts and T.L. Doering, manuscript in preparation.

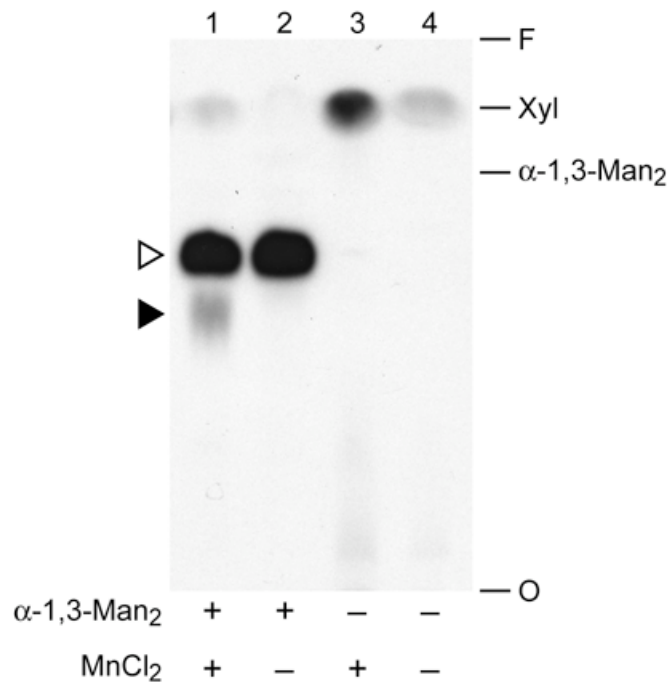
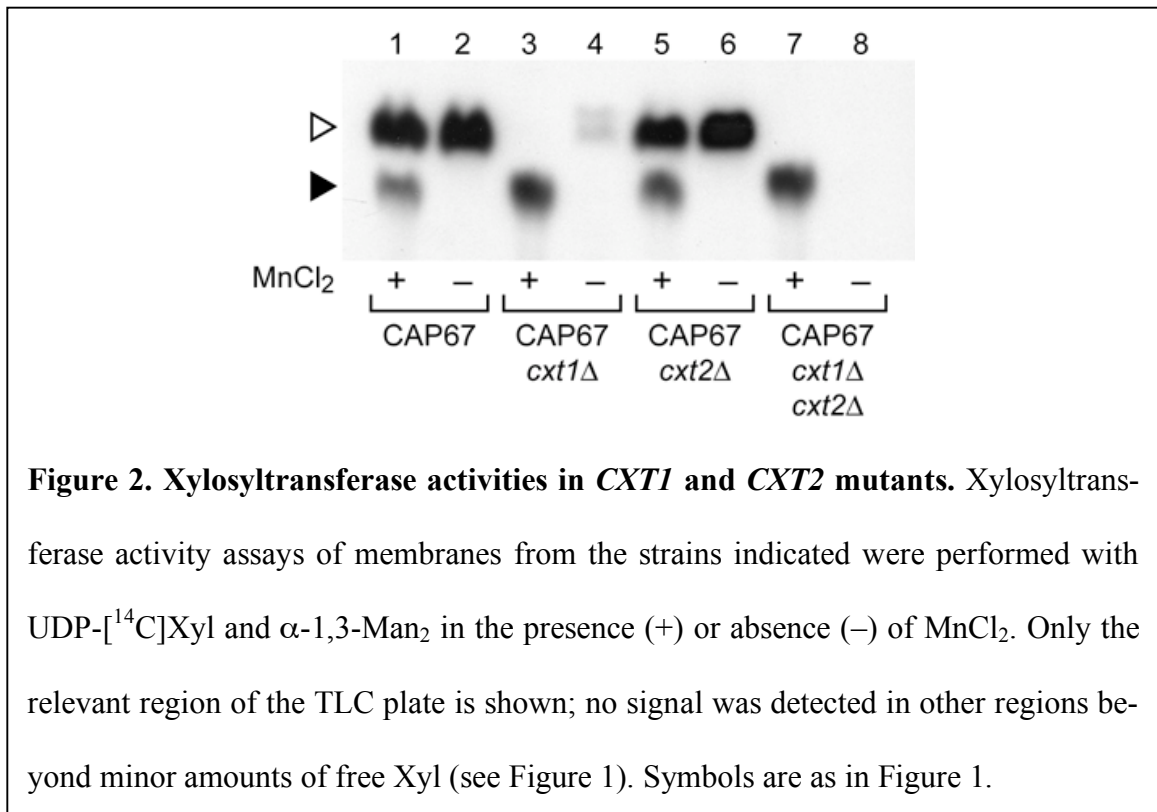


Figure 1. Xylosyltransferase activities of *C. neoformans*. Total membranes prepared from CAP67 cells were assayed as described in the Experimental Procedures with UDP-[¹⁴C]Xyl in the presence (+) or absence (-) of the α -1,3-Man₂ acceptor and MnCl₂ cofactor as indicated. An autoradiograph of the products resolved by TLC is shown, with the migration positions of free Xyl and α -1,3-Man₂ standards indicated at the right. O, origin; F, solvent front. In this and subsequent figures, the filled arrowhead indicates the product of the manganese-dependent xylosyltransferase activity and the open arrowhead indicates the products of unrelated xylosyltransferase activities (refer to Results).

(Figure 2, compare tracks 4 and 8). In this investigation, we focused on the activity responsible for forming the manganese-dependent assay product (Figure 2, filled arrowhead). The migration of this product in our TLC system differed significantly from that of the Cxt1p/Cxt2p product (open arrowhead), indicating that the carbohydrate structure is not the same. Further, the manganese requirement for its formation suggested that it is made by a distinct enzymatic activity. To confirm this hypothesis, we assessed formation of the lower mobility material in strains deleted for *CXT1* and *CXT2*. As shown in Figure 2 (compare tracks 1 and 7), these deletions did not compromise formation of the manganese-dependent product, but rather enhanced it, presumably by eliminating competition for the reaction donor or substrate. Targeting other members of the Cxt1p enzyme family

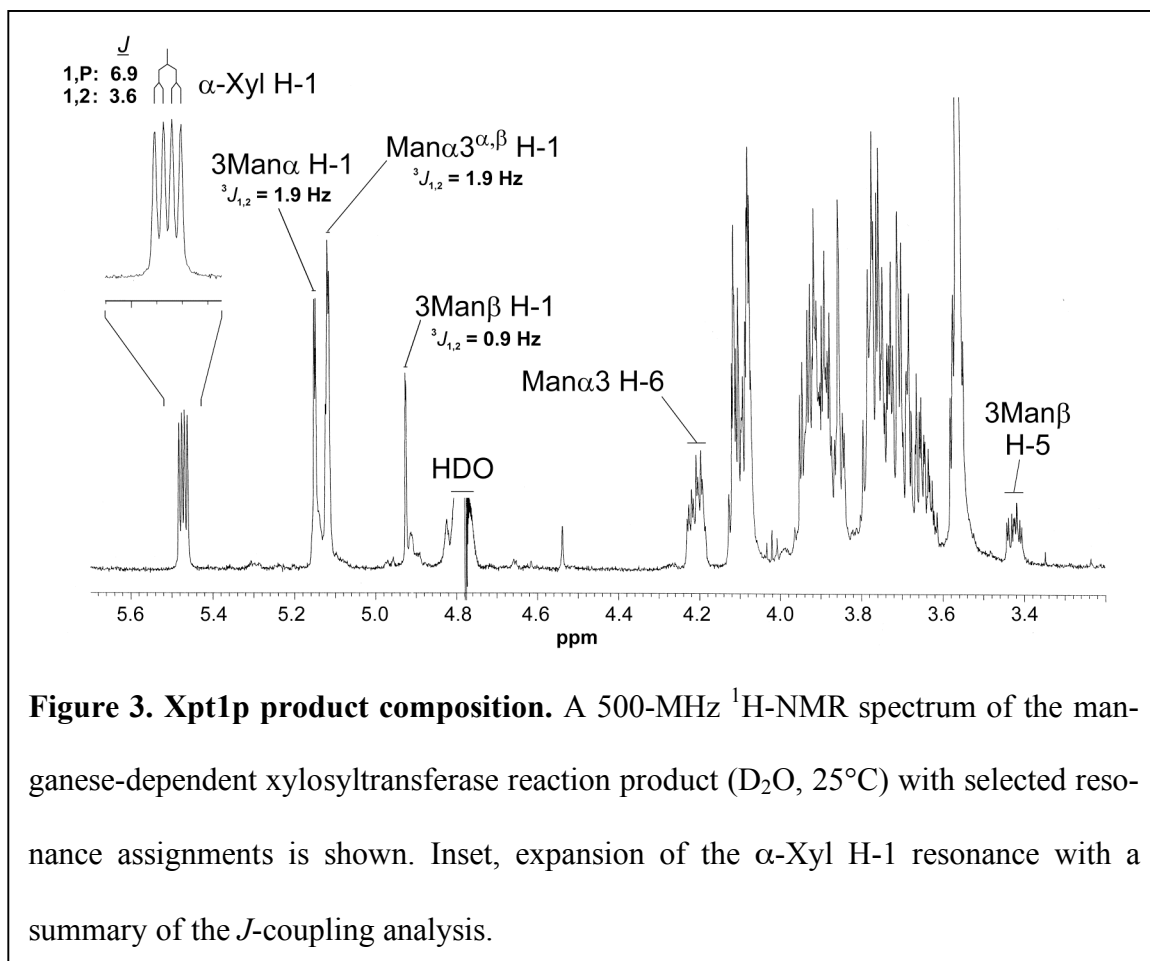


(31) by RNA interference (RNAi) also failed to alter production of the Xpt1p product (data not shown). These studies confirmed the novelty of the activity under investigation. The increased formation of the manganese-dependent product by *cxt1* Δ membranes also suggested that these cells would be useful in additional studies; this strain is used in several experiments below.

The manganese-dependent xylosyltransferase product is formed over a broad pH range (4-7) and at temperatures of 4-30°C (data not shown). For our assays we generally used pH 6.5, since that also allowed for efficient formation of the Cxt1p/Cxt2p product as a convenient internal control for membrane activity. Standard assays were performed overnight at 20°C to maximize product yield.

Manganese-dependent xylosyltransferase product analysis. In our standard assay, the Cxt1p and Cxt2p activities generated a trisaccharide product of Xyl linked β -1,2 to the reducing Man of the α -1,3-Man₂ (17).² The manganese-dependent xylosyltransferase product migrated nearer to the TLC plate origin than the Cxt1p/Cxt2p trisaccharide in our solvent system (Figure 1, track 1). This behavior suggested the manganese-dependent product was more polar, but was also potentially consistent with products that differ only with respect to the linkage of the Xyl residue to α -1,3-Man₂. To determine the structure of the manganese-dependent product, the reaction was scaled up and the product was recovered from the TLC plate as described in the Experimental Procedures. Glycosyl composition analysis by GC/MS was consistent with material containing Man and Xyl in a 2:1 ratio (data not shown), as would be expected for the addition of a single Xyl residue to the α -1,3-Man₂ acceptor substrate. Surprisingly, the ¹H NMR spectrum of the product

(Figure 3) did not exhibit a simple doublet resonance corresponding to H-1 of an added β -Xyl residue anywhere near the chemical shift (4.3-4.6 ppm) expected for this scenario. Instead, in addition to the expected resonances for the dimannosyl substrate, a doublet of doublets (dd) resonance was detected far downfield at 5.471 ppm ($J = 3.6, 6.9$ Hz). A possible explanation was suggested by comparison to our published spectrum of UDP-Xyl (12), which showed a similar dd signal for H-1 of the α -Xyl-1-O-phosphate residue at 5.517 ppm (${}^3J_{1,2} = 3.5$ Hz and ${}^3J_{1,P} = 7.0$ Hz). The nearly identical splitting pattern in



the manganese-dependent xylosyltransferase product indicated that it included an α -Xyl-1-O-phosphate, presumably derived from UDP-Xyl, linked to the dimannose substrate.

The presence of phosphate in the manganese-dependent xylosyltransferase product was confirmed by positive-mode electrospray ionization mass spectrometry in a linear ion trap ($^+$ ESI-LIT-MS): an abundant ion was observed in MS¹ at m/z 599, consistent with a molecular salt/adduct ion $[M(\text{Na}) + \text{Na}]^+$ corresponding to $\text{Man}_2\text{Xyl} + \text{P}$ (where P represents phosphate ester; data not shown). Furthermore, in the negative mode ($^-$ ESI-QIT-MS) analysis, a deprotonated molecular ion $[M - \text{H}]^-$ was observed abundantly at m/z 553 (Figure 4, Panel A), consistent with a molecular mass of 554 units for the product; this is 98 units more than that expected for the trisaccharide alone, again consistent with the presence of phosphate. In the MS² spectrum of m/z 553 (Figure 4, Panel B), the major product ion was observed at m/z 391, consistent with a loss of one Man residue, leaving Xyl-P-Man. Structurally significant product ions were observed in pairs at m/z 259/241 and m/z 229/211; the same products were observed in an MS³ spectrum acquired by isolation and activation of the m/z 391 fragment generated in MS² (Figure 4, Panel C). These product ions correspond to $[\text{Man-P}]^-/[\text{Man-P} - \text{H}_2\text{O}]^-$ and $[\text{Xyl-P}]^-/[\text{Xyl} - \text{H}_2\text{O}]^-$ product pairs, respectively, which can only be generated if the Man and Xyl residues share the same phosphate residue via a phosphodiester linkage. Consistent with this assignment, treatment of the manganese-dependent xylosyltransferase product with mild acid resulted in the release of free [¹⁴C]Xyl due to hydrolysis of the phosphate bond (data not shown).

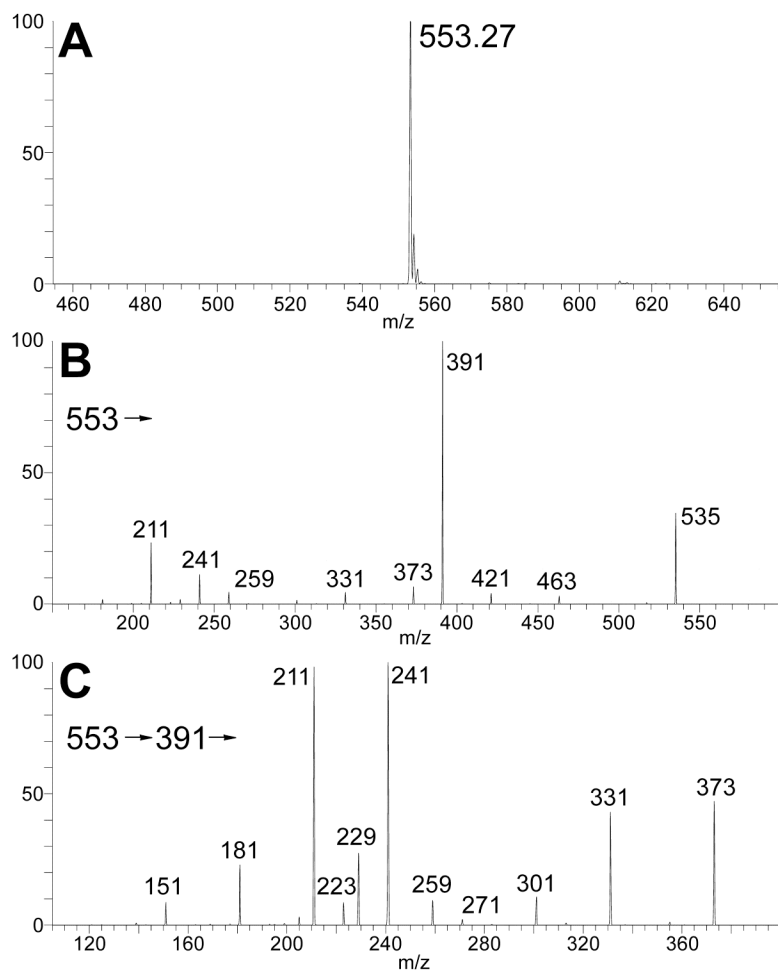


Figure 4. Xpt1p product structure. Negative ion mode ESI-QIT-MSⁿ analysis of the manganese-dependent xylosyltransferase reaction product is shown. Panel A, MS¹ molecular ion profile showing [M-H]⁻ at *m/z* 553; Panel B, MS² product spectrum of precursor ion *m/z* 553; Panel C, MS³ product spectrum of intermediate precursor ion *m/z* 391 (*m/z* 553→391→).

Neither positive nor negative mode ion mass spectra yielded information regarding the specific hydroxyl of either Man residue to which the Xyl-P is linked. However, analysis of two dimensional ^1H - ^1H -NMR spectra (gCOSY and TOCSY; data not shown) supported linkage of the phosphate to the 6-hydroxyl of the non-reducing Man residue. First, long range TOCSY cross-peaks showed the complex resonance observed at 4.211 ppm (Figure 3) to be in the same spin system as the H-1 centered at 5.116 ppm; this was observed as a pair of closely overlapping doublets, which clearly belong to the non-reducing terminal Man, slightly perturbed by the equilibrium exchange between the α - and β -anomers of the reducing terminal Man (β -anomer H-1 at 4.925 ppm, $^3J_{1,2} = 0.9$ Hz; α -anomer H-1 at 5.149 ppm, $^3J_{1,2} = 1.9$ Hz). Second, connectivity analysis of this resonance showed it to be one of the exocyclic H-6 resonances of the Man residue in question. Third, analysis of the splitting pattern of this resonance showed one more coupling than expected for a Man H-6 resonance; in other words, like the α -Xyl H-1, it exhibits an additional coupling with the phosphate atom ($^3J_{6,P} = 5.8$ Hz, while $^3J_{5,6} = 2.0$ Hz and $^2J_{6,6} = 11.3$ Hz). Finally, along with the additional coupling, the far downfield shift of this resonance compared with its position in the spectrum of the unmodified dimannose substrate (e.g. Figure 3, Panel A of (31)) was consistent with O-6 of the corresponding Man residue as the linkage point for the Xyl-P moiety.

We also treated the manganese-dependent xylosyltransferase product with a mannosidase isolated from Jack Bean known to release non-reducing terminal Man residues from α -1,2, α -1,3 or α -1,6 linkages (32). This treatment did not affect the manganese-dependent xylosyltransferase product, although it did cleave the α -1,3-Man₂ substrate

when it was modified on the reducing mannose (as in the Cxt1p activity product; data not shown). This further supported the linkage of the Xyl-P to the non-reducing mannose of the α -1,3-Man₂ substrate. In sum, our results indicated that the product of the manganese-dependent xylosyltransferase activity is Xyl- α -1-phosphate-6-Man- α -1,3-Man, and the enzyme responsible was a xylosylphosphotransferase (Xpt1p).

Identification of XPT1. To determine the enzyme responsible for the manganese-dependent xylosylphosphotransferase activity, we looked to potentially related enzyme sequences for clues. We first reviewed the literature for reports of glycosylphosphotransferases from other organisms and then compared the sequences of these enzymes to the

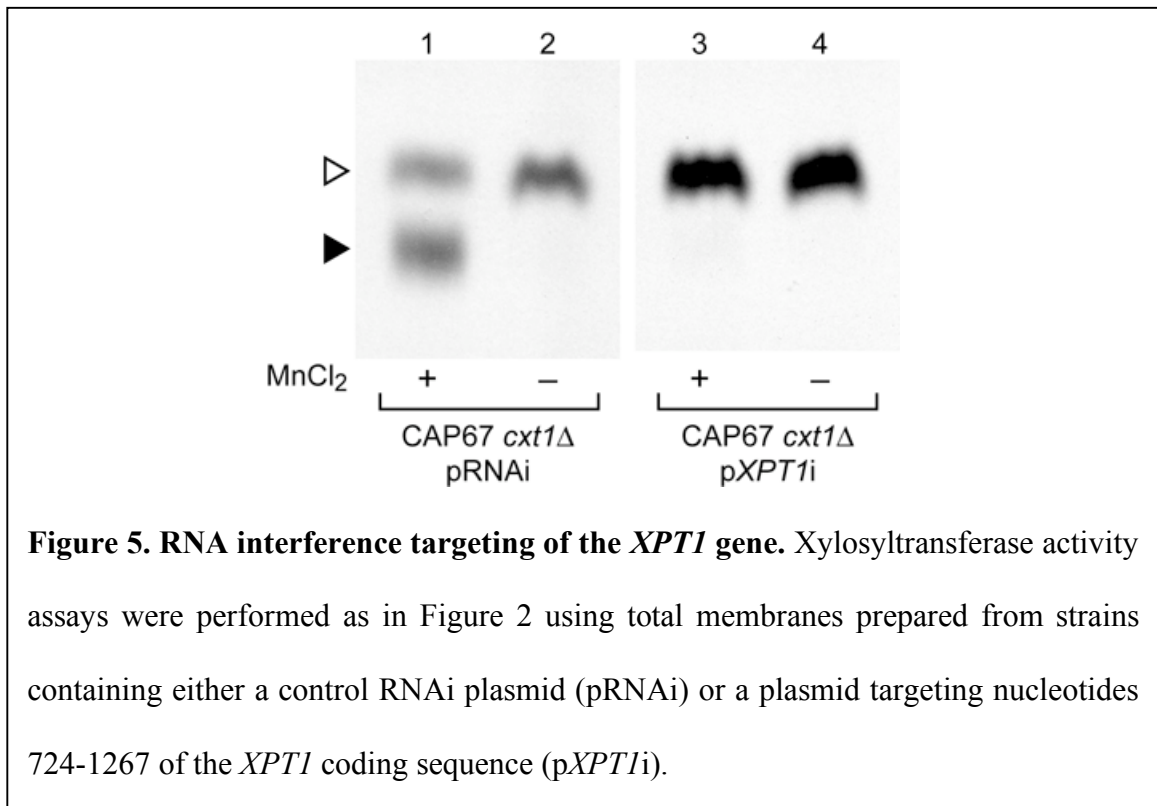
Table 2. Known glycosylphosphotransferases from other organisms.

<u>Glycosylphosphotransferases</u>	<u>Nearest cryptococcal homologs</u>		
	Protein	NCBI locus identifier	NCBI locus identifier E-value ^a
<i>S. cerevisiae</i> mannosylphosphate transferase (Ktr1p/Mnn6p)	NP_015272	XP_568891	4e-58
<i>H. sapiens</i> UDP-GlcNAc-1-phosphotransferase alpha/beta subunits	NP_077288	XP_567514	0.04 ^b
		XP_567569	0.21 ^b
<i>H. sapiens</i> UDP-GlcNAc-1-phosphotransferase gamma subunit	NP_115909	XP_566800	2e-09
<i>H. sapiens</i> UDP-GlcNAc:dolichyl-phosphate N-acetylglucosaminophosphotransferase	NP_001373	XP_567597	2e-81

^a Results indicated are from searches run with NCBI Blastp version 2.2.20 on July 17, 2009 using the entire protein sequence of the indicated known enzymes against all cryptococcal sequences in the NCBI database.

^b Not significant; see Discussion.

genome of *C. neoformans* (*C. neoformans* var. *neoformans* JEC21 Database, maintained by TIGR). As shown in Table 2, the four probe sequences identified five candidate loci with widely varying degrees of homology. Each of the candidate sequences was targeted by RNAi in CAP67 *cxt1*Δ, a strain with both the manganese-dependent Xpt1p activity and the Cxt2p activity. In the presence of an empty RNAi vector containing no target gene sequence (pRNAi), products of both enzymes were detected in standard assays (Figure 5, tracks 1 and 2). Excitingly, RNAi targeting sequence from one candidate locus (XP_567569), a weak homolog of the α/β subunit of the human N-acetylglucosamine (GlcNAc)-1-phosphate transferase, eliminated all detectable Xpt1p product (Figure 5, track 3) whereas the Cxt2p product was unaffected. A second RNAi construct directed



against an independent region of the same target locus caused a similarly striking reduction in the manganese-dependent xylosyltransferase activity (data not shown); this demonstrated that the decrease in Xpt1p activity was due to reduced transcription of the targeted gene and was not the result of off-target interference. Targeting the other four candidate loci, including one encoding a predicted protein with 32% homology to Xpt1p (XP_567514), did not alter the generation of either the Xpt1p or Cxt2p products (data not shown). We concluded that the XP_567569 candidate locus likely encodes the Xpt1p activity and termed it *XPT1*.

The *XPT1* locus was annotated as a hypothetical predicted protein in both the TIGR database of the JEC21 genome and the Broad Institute database of the H99 genome. Several expressed sequence tag sequences corresponding to this locus had been reported, indicating that it was transcribed, but these did not represent the entire predicted transcript. To confirm the *XPT1* transcript and the predicted Xpt1p sequence, we generated cDNA for sequencing and 5' rapid amplification of cDNA ends (RACE) and 3'RACE of the *XPT1* transcript. The encoded 864 amino acid Xpt1 protein sequence contains a single predicted transmembrane domain and demonstrated no significant homology to any known proteins or recognized protein domains.

Deletion of XPT1 and episomal complementation of the xpt1Δ strain. To confirm the association between *XPT1* and the manganese-dependent xylosyltransferase activity, we replaced the *XPT1* locus in the wild-type strain KN99α with a drug resistance cassette (see Experimental Procedures). Consistent with our RNAi studies, deletion of *XPT1* yielded a corresponding loss of the manganese-dependent xylosyltransferase product

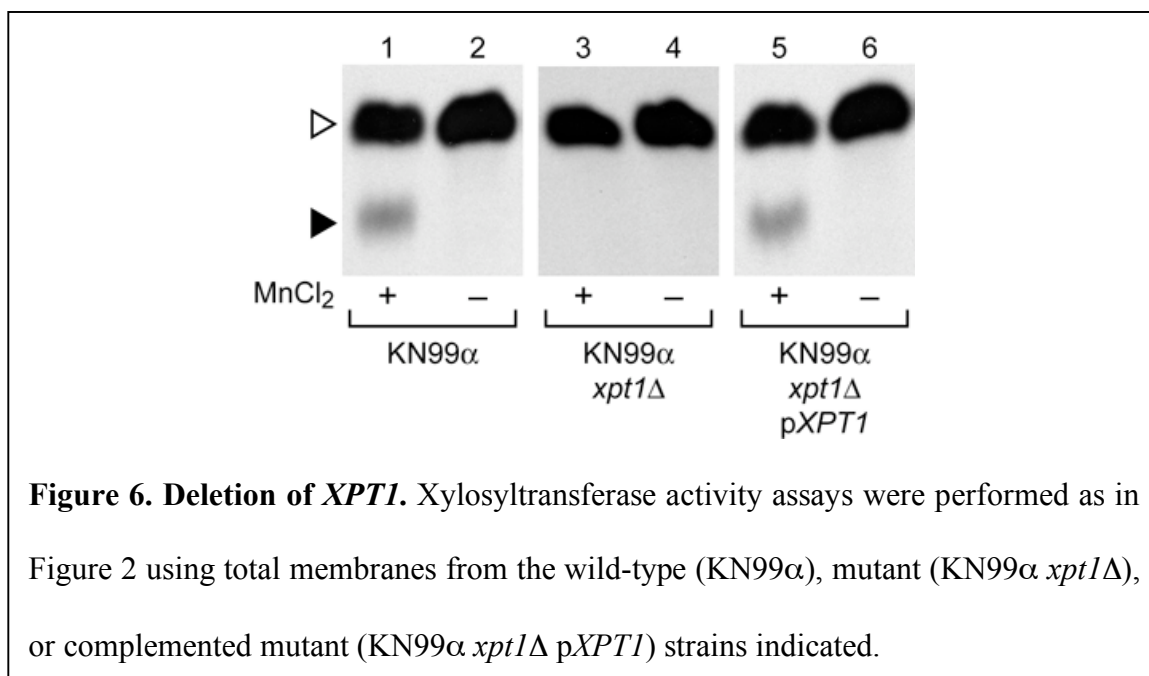
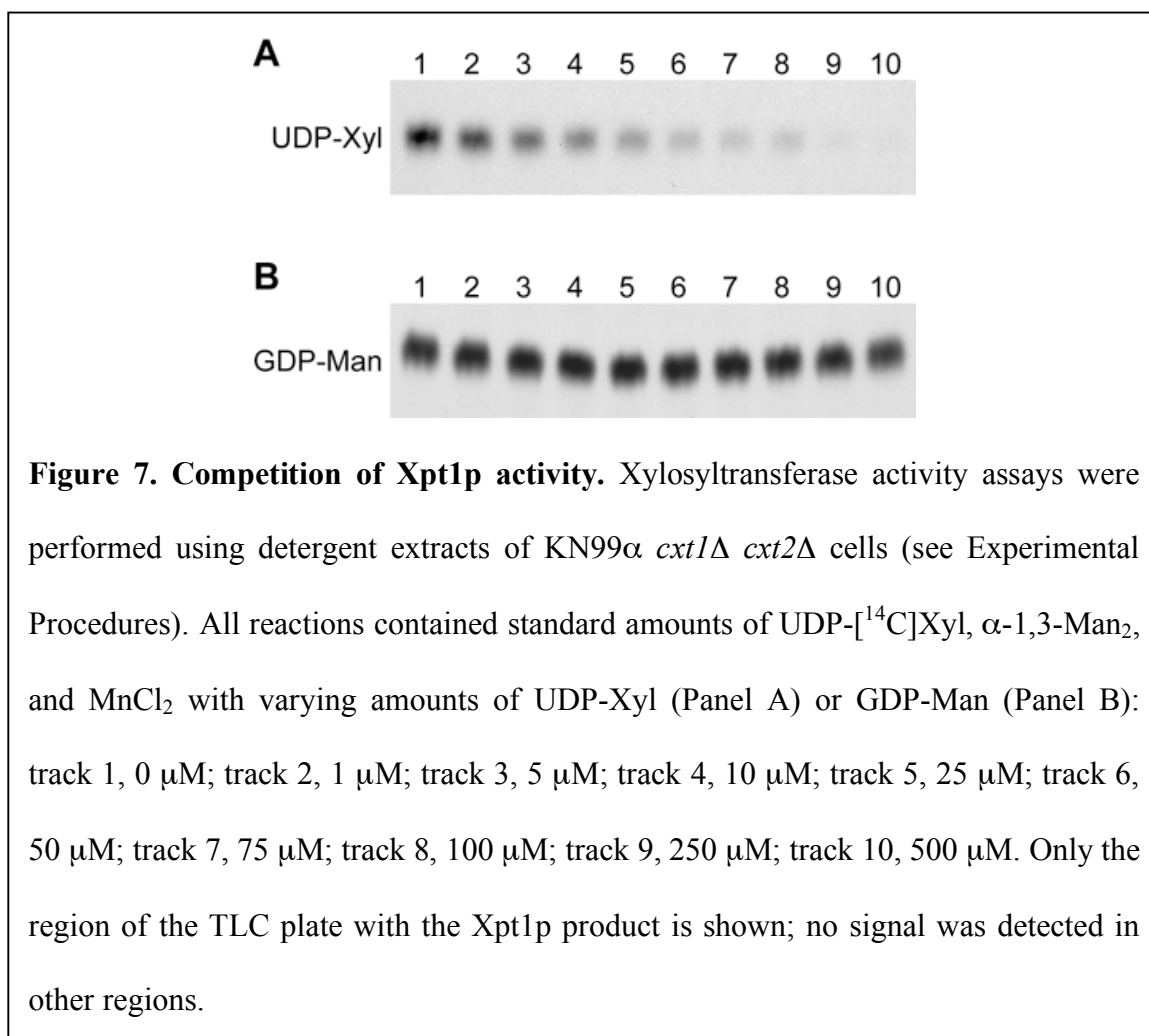


(Figure 6, compare tracks 1 and 3). This loss of activity was observed in two independent deletion strains and was maintained through a series of back-crosses (data not shown), indicating that the change correlated with the deletion of *XPT1* and was not due to unrelated alterations in the genome potentially generated during the transformation process (33). Complementation of the KN99α *xpt1*Δ strain by episomal expression of *XPT1* under control of its native promoter (*pXPT1*) restored the manganese-dependent xylosyltransferase activity to wild-type levels (Figure 6, track 5).

Xpt1p reaction components. Several glycosylphosphotransferases have been described (34, 35) but we are aware of no other reports of a xylosylphosphotransferase activity. For this reason we investigated the specificity of the novel Xpt1p activity. Our standard Xpt1p reaction utilizes a UDP-[¹⁴C]Xyl donor, α-1,3-Man₂ acceptor, and MnCl₂

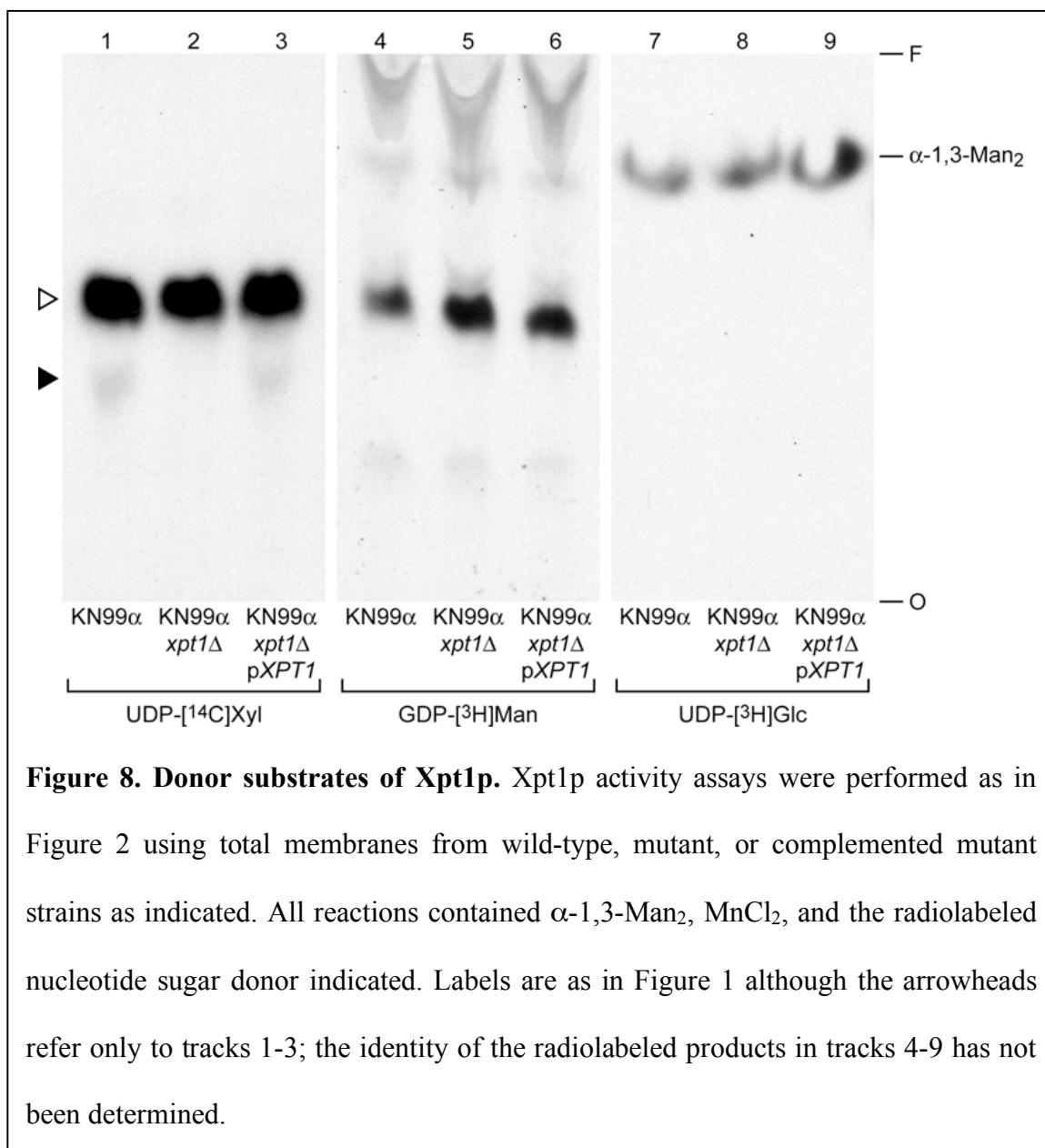
cofactor. The preference of the Xpt1p activity for each of these reaction components was assessed.

To explore the specificity of the Xpt1p activity for UDP-Xyl as the donor, we first performed standard xylosyltransferase reactions in the presence of non-radiolabeled nucleotide sugars or their components; membrane proteins were prepared from KN99 α *cxt1* Δ *cxt2* Δ to prevent any competition from Cxt1p or Cxt2p activities. We were particularly interested in whether Xpt1p could use GDP-Man as a donor molecule given that



transfer of sugar phosphate from this nucleotide sugar has been reported in *S. cerevisiae* (34). As expected, the addition of increasing concentrations of unlabeled UDP-Xyl reduced formation of the radiolabeled Xpt1p product (Figure 7, Panel A). In contrast, no inhibition of the [¹⁴C]Xyl product was seen in the presence of GDP-Man (Figure 7, Panel B), suggesting that Xpt1p does not utilize that donor. Inhibition of radiolabeled product formation was observed in the presence of UDP-Gal, UDP-Glc, UDP-GlcA, and UDP-GlcNAc, but the pattern of inhibition in each case was similar to that induced by UDP alone (data not shown). GDP alone did not inhibit Xpt1p activity and neither did monosaccharide Xyl (data not shown).

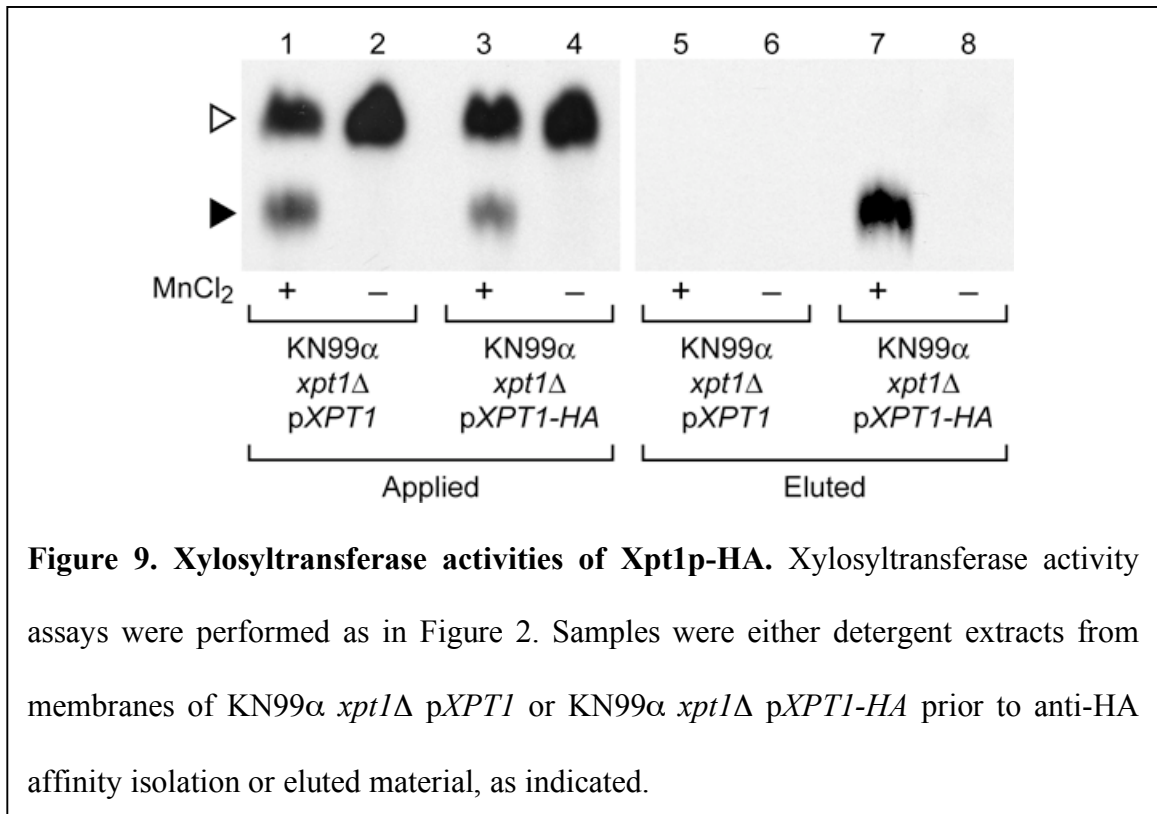
Although our competition studies indicated that Xpt1p does not utilize GDP-Man, we were unable to distinguish between the various UDP-sugars as potential donors because all were inhibitory (likely due to the shared UDP moiety). To further examine Xpt1p donor substrate specificity, we analyzed the products of transferase reactions in which UDP-[¹⁴C]Xyl was replaced with other radiolabeled nucleotide sugars. To assess Xpt1p-dependent reaction products, we compared products from assays of membranes from *XPT1* wild-type, mutant, or complemented mutant strains (KN99 α , KN99 α *xpt1* Δ , or KN99 α *xpt1* Δ p*XPT1*, respectively). Only those reactions in which UDP-[¹⁴C]Xyl was supplied as a donor demonstrated any Xpt1p-dependent variation in the pattern of radiolabeled products (Figure 8, tracks 1-3, filled arrowhead). In contrast, no radiolabeled products generated by reactions containing GDP-[³H]Man, UDP-[³H]Glc, UDP-[³H]Gal, UDP-[³H]GlcA, or UDP-[³H]GlcNAc (Figure 8 and data not shown) were dependent on



the presence of Xpt1p. Together, these studies suggested specificity for UDP-Xyl as the reaction donor for Xpt1p.

Having identified UDP-Xyl as the preferred xylose donor in Xpt1p-mediated reactions, we considered the source of the phosphate moiety in the Xpt1p product. With

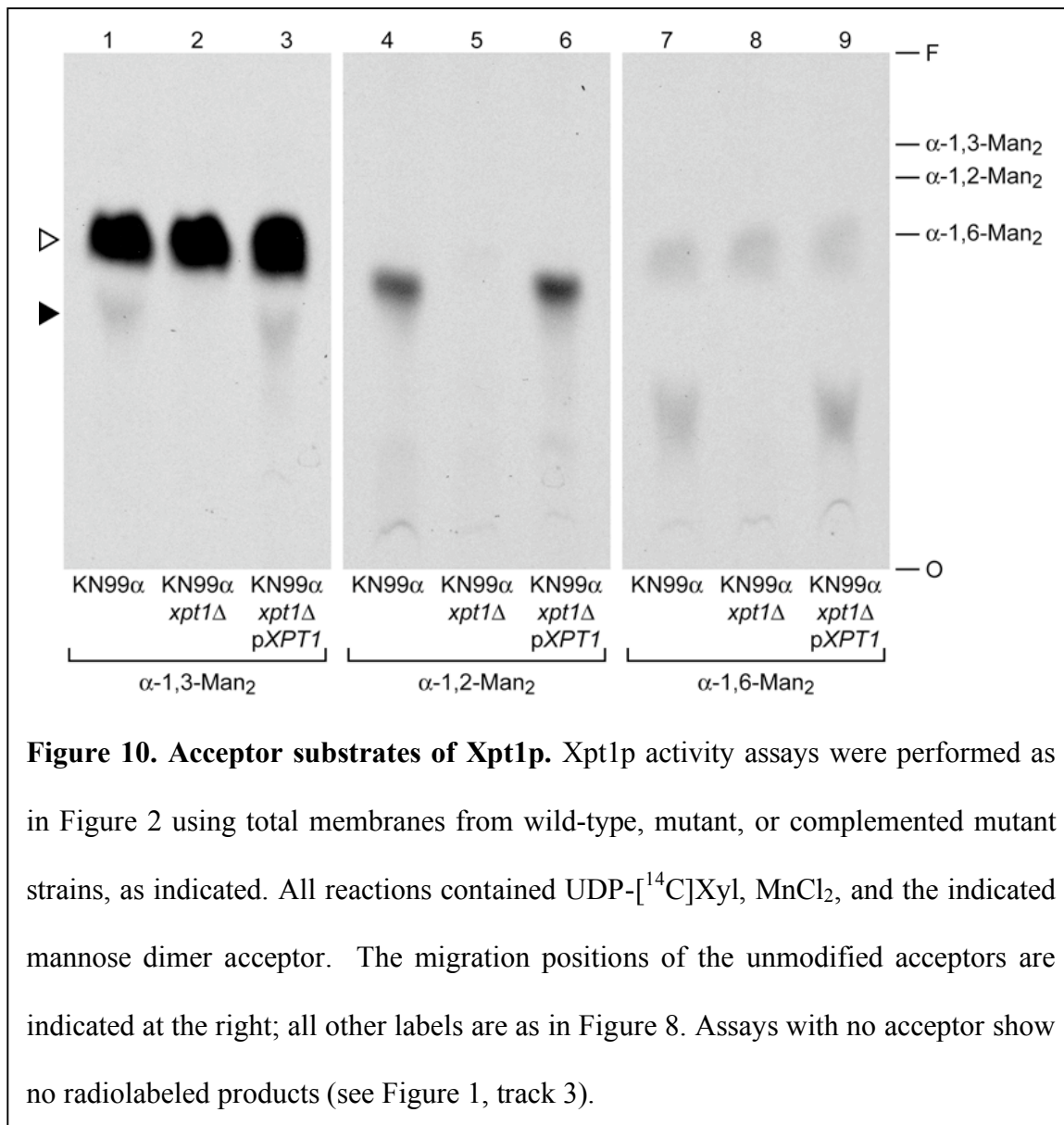
other known glycosylphosphotransferases, the phosphate is derived from the nucleotide sugar donor (36). It is possible, however, that the phosphate in the Xpt1p product is independently derived, in a step preceding xylose transfer, from some other compound present in the assayed membranes or extracts. To generate more pure material to test in our transferase assays, we added sequence encoding a C-terminal HA epitope tag to *pXPT1* and isolated the tagged protein by magnetic immunoprecipitation methods (see Experimental Procedures). The addition of the HA epitope did not alter the overall activity of Xpt1p (Figure 9, compare tracks 1 and 3, and data not shown) and did mediate specific isolation of the manganese-dependent activity (Figure 9, compare tracks 5 and 7). This demonstration of [¹⁴C]Xyl-P transfer mediated by affinity-purified protein strongly sug-



gests that the phosphate moiety found in the Xpt1p product is derived from the UDP-¹⁴C]Xyl donor.

We next used a series of dimannose molecules to examine the acceptor preferences of Xpt1p. As with the donor specificity experiments above, xylosyltransferase reactions were prepared using membranes from KN99 α , KN99 α *xpt1* Δ , or KN99 α *xpt1* Δ p*XPT1*; the standard α -1,3-Man₂ reaction substrate was replaced with various potential acceptors. We observed Xpt1p-dependent modification of the dimannose compounds α -1,2-Man₂, α -1,4-Man₂, and α -1,6-Man₂ in addition to the α -1,3-Man₂ acceptor used in our earlier experiments (Figure 10 and data not shown). Similar studies demonstrated Xpt1p utilization of D-Man as an acceptor molecule, but not of D-Gal, D-Glc, D-GlcNAc, or D-Xyl (data not shown). It appeared that Xpt1p was specific for Man as an acceptor, but was flexible as to the structural context of the Man residue.

Finally, we tested product formation in xylosyltransferase assays containing a panel of chloride salts in place of the MnCl₂ cofactor using membranes prepared from KN99 α *cxt1* Δ *cxt2* Δ . Although the most robust Xpt1p activity was seen in the presence of MnCl₂, some similarly migrating product was detected in the presence of both CoCl₂ and MgCl₂ (~5% and ~15% of the MnCl₂ product, respectively; data not shown). Assays using other cations (CaCl₂, CuCl₂, Fe(II)Cl₂, NiCl₂, and ZnCl₂) did not yield any detectable product and including EDTA in the reactions resulted in the absence of any detectable product regardless of which cation was present (data not shown). MnCl₂ was therefore the preferred metal ion cofactor of Xpt1p.



DISCUSSION

We have discovered a unique xylosylphosphotransferase activity in *C. neoformans* and the gene encoding it, which we named *XPT1* (for *xylosylphosphotransferase 1*). This activity appears to be specific for UDP-Xyl, making it distinct from previously reported mannosylphosphotransferases and N-acetylglucosaminylphosphotransferases (34, 35). The modification of Man with Xyl-P is novel: to our knowledge this structure has not been reported in any biological system nor have activities similar to those of Xpt1p been previously observed.

Our studies indicate that the Xpt1p is specific for UDP-Xyl. However, we cannot exclude the possibility that this enzyme can also utilize some uncommon UDP-sugar donor that we did not include in our test panel. Although there are no data to indicate *C. neoformans* synthesizes any such donor, comprehensive studies have not been performed in this system. Additionally, our studies with affinity-purified protein suggest that the only reaction components needed for Xpt1p-dependent Xyl-P transfer are UDP-Xyl, a Man-containing substrate molecule, and MnCl₂. This suggests that UDP-Xyl serves as the source for both the phosphate and the sugar moiety, as with the GlcNAc-1-phosphate transferase (36).

The predicted 100 kDa protein encoded by *XPT1* does not resemble other known xylosyltransferases and has no conserved domains as identified by either NCBI or other publicly available search engines. A cluster of hydrophobic amino acids at residues 83-103 of Xpt1p may comprise a transmembrane domain, consistent with the observed enrichment of the manganese-dependent xylosyltransferase activity in detergent extracts of

cryptococcal membranes (data not shown). The Xpt1p sequence contains several possible DXD motifs, sites of metal ion binding commonly found in glycosyltransferases (37). There are also potential *N*- and *O*-linked glycosylation sites present within the protein sequence (38). Interestingly, Xpt1p demonstrates strong homology to hypothetical proteins found in the basidiomycetous fungi *Postia placenta* (brown wood rot; 28% identity overall) and *Ustilago maydis* (corn smut; 27% identity overall). Although no biological role or biochemical activity has been attributed to these two proteins, it is possible that they perform similar catalytic functions to Xpt1p.

Overall, Xpt1p has extremely limited homology to proteins of known function. We identified its sequence based on a 43 amino acid stretch (residues 407-449 of Xpt1p) that is 38% identical to a region in the α/β subunit of UDP-GlcNAc phosphotransferase. The UDP-GlcNAc phosphotransferase, which has an $\alpha_2\beta_2\gamma_2$ subunit structure, catalyzes the initial step in the mannose-6-phosphate modification of lysosomal hydrolases that is necessary for targeting these proteins to the lysosome. The α and β subunits are encoded by a single gene and are thought to contain the catalytic portion of the protein (39), while the γ subunit is encoded by a separate gene and is thought to be a regulatory element (40, 41). Based on our studies, Xpt1p cannot utilize UDP-GlcNAc as a donor. We propose that the region of homology between the α/β subunit of UDP-GlcNAc phosphotransferase and Xpt1p may be involved in sugar-phosphate transfer from a nucleotide sugar donor.

Kudo and colleagues first speculated that a region of the α/β subunit of UDP-GlcNAc phosphotransferase (residues 321-432) “might be involved in the binding of nu-

cleotide sugar or transfer of sugar phosphate” (39) because of its similarity to sequence elements found in bacterial capsule polymerases. This possibility was revisited in a broad *in silico* analysis of predicted glycosyltransferases in pathogen genomes (42). Several proteins identified by Sperisen and colleagues in that study were previously implicated in the biosynthesis of exopolysaccharide phosphoglycans, although the functions of these proteins were indicated only by indirect association with a given phenotype rather than by functional assays. Among the identified hypothetical loci were two from *C. neoformans*, including *XPT1*. The region of homology between the α/β subunit of UDP-GlcNAc phosphotransferase and Xpt1p was included both within the potential domain described by Kudo (39) and the conserved regions identified by Sperisen (42).

A key question for the future is the biological role of Xpt1p. As mentioned earlier, the cryptococcal cell contains a variety of glycan structures, several of which are unique to this pathogen. The best-studied of these is the cryptococcal capsule, but analyses of the polysaccharide components of this structure have not indicated the presence of xylophosphomannose linkages (3-5). Preliminary studies suggest that Xpt1p acts in the modification of cryptococcal proteins (not shown), but further work will be required to elucidate the cellular function of this novel and intriguing enzyme.

ACKNOWLEDGEMENTS

Studies of cryptococcal glycan synthesis in the Doering laboratory are supported by NIH Grant RO1 GM071007. S.B.L. is supported by the Danish Medical Research Council for Technology and Innovation, the Stjerne Program of Excellence, and the Copenhagen Center for Glycomics. Use of the 500-MHz NMR facility of the Department of Chemistry, University of New Hampshire, as well as the mass spectrometry facilities of the University of New Hampshire Glycomics Center (Vernon N. Reinhold, principal investigator), are gratefully acknowledged. The authors thank David Haslam, Igor Almeida, and Andrew Lovering for helpful insights on this project; Matthew Williams and Elizabeth Held for technical assistance; and Aki Yoneda for comments on the manuscript.

ABBREVIATIONS USED

dd, double of doublets; ESI-LIT-MS, electrospray ionization linear ion trap mass spectroscopy; ESI-QIT-MS, electrospray ionization quadrupole ion trap mass spectroscopy; Gal, galactose; gCOSY, gradient-selected correlation spectroscopy; GIPC, glycosylinositol phosphorylceramide; Glc, glucose; GlcA, glucuronic acid; GlcNAc, N-acetylglucosamine; GXM, glucuronoxylomannan; GXMGal, glucuronoxylomannogalactan; G418, geneticin; HA, hemagglutinin; Man, mannose; NAT, nourseothricin; P, phosphate ester; RACE, rapid amplification of cDNA ends; RNAi, RNA interference; TLC, thin layer chromatography; TOCSY, total correlation spectroscopy; UTR, untranslated region; Xyl, xylose; 5-FOA, 5-fluoroorotic acid.

REFERENCES

1. Casadevall, A., and J. Perfect. 1998. *Cryptococcus neoformans*. American Society for Microbiology, Washington DC.
2. Fromtling, R.A., H.J. Shadomy, and E.S. Jacobson. 1982. Decreased virulence in stable, acapsular mutants of *Cryptococcus neoformans*. *Mycopathologia* 79: 23-29.
3. Cherniak, R., E.B. O'Neill, and S. Sheng. 1998. Assimilation of xylose, mannose, and mannitol for synthesis of glucuronoxylomannan of *Cryptococcus neoformans* determined by ¹³C nuclear magnetic resonance spectroscopy. *Infect. Immun.* 66: 2996-2998.
4. Vaishnav, V.V., B. E. Bacon, M. O'Neill, and R. Cherniak. 1998. Structural characterization of the galactoxylomannan of *Cryptococcus neoformans* Cap67. *Carbohydr. Res.* 306: 315-330.
5. Heiss, C., J.S. Klutts, Z. Wang, T.L. Doering, and P. Azadi. 2009. The structure of *cryptococcus neoformans* galactoxylomannan contains beta-D-glucuronic acid. *Carbohydr. Res.* 344: 915-920.
6. Samuelson, J., S. Banerjee, P. Magnelli, J. Cui, D.J. Kelleher, R. Gilmore, and P. W. Robbins. 2005. The diversity of dolichol-linked precursors to asn-linked glycans likely results from secondary loss of sets of glycosyltransferases. *Proc. Natl. Acad. Sci. U.S.A.* 102: 1548-1553.
7. Goto, M. 2007. Protein O-glycosylation in fungi: Diverse structures and multiple functions. *Biosci. Biotechnol. Biochem.* 71: 1415-1427.
8. Schutzbach, J., H. Ankel, and I. Brockhausen. 2007. Synthesis of cell envelope glycoproteins of *Cryptococcus laurentii*. *Carbohydr. Res.* 342: 881-893.

- proteins of *Cryptococcus laurentii*. *Carbohydr. Res.* 342: 881-893.
9. Wopereis, S., D.J. Lefeber, E. Morava, and R.A. Wevers. 2006. Mechanisms in protein *O*-glycan biosynthesis and clinical and molecular aspects of protein *O*-glycan biosynthesis defects: A review. *Clin. Chem.* 52: 574-600.
 10. Heise, N., A.L. Gutierrez, K.A. Mattos, C. Jones, R. Wait, J.O. Previato, and L. Mendonca-Previato. 2002. Molecular analysis of a novel family of complex glycosyltolphosphoryl ceramides from *Cryptococcus neoformans*: Structural differences between encapsulated and acapsular yeast forms. *Glycobiology* 12: 409-420.
 11. Lairson, L.L., B. Henrissat, G.J. Davies, and S.G. Withers. 2008. Glycosyltransferases: Structures, functions, and mechanisms. *Annu. Rev. Biochem.* 77: 521-555.
 12. Bar-Peled, M., C.L. Griffith, and T.L. Doering. 2001. Functional cloning and characterization of a UDP-glucuronic acid decarboxylase: The pathogenic fungus *Cryptococcus neoformans* elucidates UDP-xylose synthesis. *Proc. Natl. Acad. Sci. U.S.A.* 98: 12003-12008.
 13. Griffith, C.L., J.S. Klutts, L. Zhang, S.B. Levery, and T.L. Doering. 2004. UDP-glucose dehydrogenase plays multiple roles in the biology of the pathogenic fungus *Cryptococcus neoformans*. *J. Biol. Chem.* 279: 51669-51676.
 14. Moyrand, F., B. Klaproth, U. Himmelreich, F. Dromer, and G. Janbon. 2002. Isolation and characterization of capsule structure mutant strains of *Cryptococcus neoformans*. *Mol. Microbiol.* 45: 837-849.
 15. Gutierrez, A.L., L. Farage, M.N. Melo, R.S. Mohana-Borges, Y. Guerardel, B. Coddeville, J.M. Wieruszeski, L. Mendonca-Previato, and J.O. Previato. 2007. Char-

- acterization of glycoinositolphosphoryl ceramide structure mutant strains of *Cryptococcus neoformans*. *Glycobiology* 17: 1-11C.
16. Castle, S.A., E.A. Owuor, S.H. Thompson, M.R. Garnsey, J.S. Klutts, T.L. Doering, and S.B. Levery. 2008. Beta1,2-xylosyltransferase Cxt1p is solely responsible for xylose incorporation into *Cryptococcus neoformans* glycosphingolipids. *Eukaryot Cell* 7: 1611-1615.
 17. Klutts, J.S., S.B. Levery, and T.L. Doering. 2007. A beta-1,2-xylosyltransferase from *Cryptococcus neoformans* defines a new family of glycosyltransferases. *J. Biol. Chem.* 282: 17890-17899.
 18. Liu, X., G. Hu, J. Panepinto, and P.R. Williamson. 2006. Role of a *VPS41* homologue in starvation response, intracellular survival and virulence of *Cryptococcus neoformans*. *Mol. Microbiol.* 61: 1132-1146.
 19. Wickes, B.L., T.D. Moore, and K.J. Kwon-Chung. 1994. Comparison of the electrophoretic karyotypes and chromosomal location of ten genes in the two varieties of *Cryptococcus neoformans*. *Microbiology* 140 (Pt 3): 543-550.
 20. Nelson, R.T., J. Hua, B. Pryor, and J.K. Lodge. 2001. Identification of virulence mutants of the fungal pathogen *Cryptococcus neoformans* using signature-tagged mutagenesis. *Genetics* 157: 935-947.
 21. Davidson, R.C., J.R. Blankenship, P.R. Kraus, M. deJesus Berrios, C.M. Hull, C. D'Souza, P. Wang, and J. Heitman. 2002. A PCR-based strategy to generate integrative targeting alleles with large regions of homology. *Microbiology* 148: 2607-2615.

22. Toffaletti, D.L., T.H. Rude, S.A. Johnston, D.T. Durack, and J. R. Perfect. 1993. Gene transfer in *Cryptococcus neoformans* by use of biolistic delivery of DNA. *J. Bacteriol.* 175: 1405-1411.
23. Brown, T. 2004. Southern Blotting, p. 2.9.1-2.9.20. *In* Current Protocols in Molecular Biology.
24. Yan, Z., X. Li, and J. Xu. 2002. Geographic distribution of mating type alleles of *Cryptococcus neoformans* in four areas of the United States. *J. Clin. Microbiol.* 40: 965-972.
25. Edman, J.C., and K.J. Kwon-Chung. 1990. Isolation of the URA5 gene from *Cryptococcus neoformans* var. *neoformans* and its use as a selective marker for transformation. *Mol. Cell. Biol.* 10: 4538-4544.
26. Jacobson, E.S., D.J. Ayers, A.C. Harrell, and C.C. Nicholas. 1982. Genetic and phenotypic characterization of capsule mutants of *Cryptococcus neoformans*. *J. Bacteriol.* 150: 1292-1296.
27. Chang, Y.C., and K.J. Kwon-Chung. 1999. Isolation, characterization, and localization of a capsule-associated gene, *CAP10*, of *Cryptococcus neoformans*. *J. Bacteriol.* 181: 5636-5643.
28. Chang, Y.C., and K.J. Kwon-Chung. 1998. Isolation of the third capsule-associated gene, *CAP60*, required for virulence in *Cryptococcus neoformans*. *Infect. Immun.* 66: 2230-2236.
29. Chang, Y.C., L.A. Penoyer, and K.J. Kwon-Chung. 1996. The second capsule gene of *Cryptococcus neoformans*, *CAP64*, is essential for virulence. *Infect. Immun.* 64:

1977-1983.

30. Doering, T.L. 2009. How sweet it is! Cell wall biogenesis and polysaccharide capsule formation in *Cryptococcus neoformans*. *Annu. Rev. Microbiol.* 63: 223-247
31. Klutts, J.S., and T.L. Doering. 2008. Cryptococcal xylosyltransferase 1 (Cxt1p) from *Cryptococcus neoformans* plays a direct role in the synthesis of capsule polysaccharides. *J. Biol. Chem.* 283: 14327-14334.
32. Li, Y.T. 1967. Studies on the glycosidases in jack bean meal. I. Isolation and properties of alpha-mannosidase. *J. Biol. Chem.* 242: 5474-5480.
33. Kwon-Chung, K.J., W.E. Goldman, B. Klein, and P.J. Szanislo. 1998. Fate of transforming DNA in pathogenic fungi. *Med. Mycol.* 36 Suppl 1: 38-44.
34. Jigami, Y., and T. Odani. 1999. Mannosylphosphate transfer to yeast mannan. *Biochim. Biophys. Acta* 1426: 335-345.
35. Braulke, T., S. Pohl, and S. Storch. 2008. Molecular analysis of the GlcNac-1-phosphotransferase. *J. Inherit. Metab. Dis.* Epub Apr. 15.
36. Bao, M., B.J. Elmendorf, J.L. Booth, R.R. Drake, and W. M. Canfield. 1996. Bovine UDP-N-acetylglucosamine:Lysosomal-enzyme N-acetylglucosamine-1-phosphotransferase. II. Enzymatic characterization and identification of the catalytic subunit. *J. Biol. Chem.* 271: 31446-31451.
37. Wiggins, C.A., and S. Munro. 1998. Activity of the yeast *MNN1* alpha-1,3-mannosyltransferase requires a motif conserved in many other families of glycosyltransferases. *Proc. Natl. Acad. Sci. U.S.A.* 95: 7945-7950.
38. Gemmill, T.R., and Trimble, R.B. 1999. Overview of N- and O-linked oligosaccha-

- ride structures found in various yeast species. *Biochim. Biophys. Acta* 1426: 227-237
39. Kudo, M., M. Bao, A. D'Souza, F. Ying, H. Pan, B. A. Roe, and W. M. Canfield. 2005. The alpha- and beta-subunits of the human UDP-N-acetyl-glucosamine: Lysosomal enzyme N-acetylglucosamine-1-phosphotransferase are encoded by a single cDNA. *J. Biol. Chem.* 280: 36141-36149.
40. Raas-Rothschild, A., V. Cormier-Daire, M. Bao, E. Genin, R. Salomon, K. Brewer, M. Zeigler, H. Mandel, S. Toth, B. Roe, A. Munnich, and W. M. Canfield. 2000. Molecular basis of variant pseudo-hurler polydystrophy (mucopolidosis IIIC). *J. Clin. Invest.* 105: 673-681.
41. Pohl, S., S. Tiede, M. Castrichini, M. Cantz, V. Gieselmann, and T. Bräulke. 2009. Compensatory expression of human N-acetylglucosaminyl-1-phosphotransferase subunits in mucopolidosis type III gamma. *Biochim. Biophys. Acta* 1792: 221-225.
42. Sperisen, P., C.D. Schmid, P. Bucher, and O. Zilian. 2005. Stealth proteins: *In silico* identification of a novel protein family rendering bacterial pathogens invisible to host immune defense. *PLoS Comput. Biol.* 1: e63.
43. Kwon-Chung, K.J., Wickes, B.L., Stockman, L., Roberts, G.D., Ellis, D., and Howard, D.H. 1992. Genetic association of mating types and virulence in *Cryptococcus neoformans*. *Infect. Immun.* 60: 1869-1874.
44. Nielsen, K., Cox, G.M., Wang, P., Toffaletti, D.L., Perfect, J.R., and Heitman, J. 2003. Sexual cycle of *Cryptococcus neoformans* var. *grubii* and virulence of congeneric alpha and alpha isolates. *Infect. Immun.* 71: 4831-4841.

CHAPTER III

A XYLOSYLPHOSPHOTRANSFERASE OF *CRYPTOCOCCUS NEOFORMANS* FUNCTIONS IN PROTEIN GLYCOSYLATION

**Morgann C. Reilly[‡], Kazuhiro Aoki[§], Michael L. Skowrya[‡], Matthew Williams[‡],
Michael Tiemeyer[§], and Tamara L. Doering[‡]**

From the [‡]Department of Molecular Microbiology, Washington University School of
Medicine, St. Louis, MO 63110, USA; and the [§]Complex Carbohydrate Research Center
and Department of Biochemistry and Molecular Biology, University of Georgia,
Athens, GA 30602, USA.

ABSTRACT

Cryptococcal meningoencephalitis is an AIDS-defining illness caused by the opportunistic pathogen *Cryptococcus neoformans*. The organism possesses an elaborate polysaccharide capsule that is unique among pathogenic fungi; as such, the glycobiology of *C. neoformans* has been a focus of research in the field. The structure of the capsule as well as other glycans and glycoconjugates within the cell have been described, but the machinery responsible for their synthesis remains largely unexplored. We recently identified Xpt1p, the first described xylosyltransferase capable of generating a Xyl-P-Man linkage, and are interested in determining the function of this novel enzyme within the cryptococcal cell. In studies presented here, we demonstrate that the Xpt1p activity is capable of modifying protein-linked glycans. Specifically, we show that Xpt1p influences the synthesis of *O*-linked glycans.

INTRODUCTION

Members of the *Cryptococcus neoformans* species complex are the only organisms in the cryptococcal genus that are commonly associated with human disease. Historically categorized into four serotypes (A-D), these yeasts have more recently been classified into separate species and varieties: *C. neoformans* var. *grubii* (serotype A), *C. neoformans* var. *neoformans* (serotype D), and *Cryptococcus gattii* (serotypes B and C) (1). All four serotypes have been isolated from the environment, with serotypes A and D most commonly found in association with avian excreta and soil, and serotypes B and C in association with certain tree species. Humans are infected via the inhalation of small yeast cells or basidiospores, which are typically neutralized within the lungs by the immune system without any symptomatic evidence of infection (2). The organism can, however, disseminate from the lungs to other organs; if it reaches the brain, *C. neoformans* causes a fatal meningoencephalitis. Serotypes A and D are responsible for most infections and are generally associated with disease in immunocompromised individuals, while serotypes B and C characteristically infect immunocompetent populations.

The capsule is the most distinctive structure of *C. neoformans* and, because it is known to be required for virulence, has been intensively studied. This extensive structure is primarily composed of two polysaccharides, glucuronoxylomannan (GXM) (3) and glucuronoxylomannogalactan (GXMGal) (4, 5). The capsule surrounds a cell wall composed of cross-linked polymers of glucose (glucans), mannose (mannans), and N-acetylglucosamine (chitin or, upon deacetylation, chitosan). The wall also contains proteins that bear elaborate mannose modifications, referred to as mannoproteins. Members of the

Cryptococcus genus are known to synthesize proteins with glycosylphosphatidylinositol (GPI) anchors (6-8) as well as both *N*- and *O*-linked modifications (9-12). The organism also synthesizes lipids modified with mannose, xylose, and galactose (13, 14). *C. neoformans* synthesizes a diverse array of cellular glycans and glycoconjugates, the structures of which are only partially characterized.

Our laboratory is interested in glycosyltransferases, those enzymes that catalyze the transfer of sugar moieties from nucleotide sugar donors to cellular acceptors (proteins, lipids, or other sugars) in the synthesis of cellular glycans. Previous studies of nucleotide sugar synthesis pathways in *C. neoformans* found that cells unable to produce UDP-xylose (UDP-Xyl) had no detectable Xyl residues in capsule polysaccharides, displayed shortened and deformed capsule fibers, and were avirulent in animal models of infection (15, 16). This physiological relevance of Xyl, together with its frequent occurrence in cryptococcal glycoconjugates, stimulated our interest in Xyl transfer activities. Using a radiolabeled UDP-Xyl molecule (UDP-[¹⁴C]Xyl) as a donor and an α -1,3-linked dimannose molecule (α -1,3-Man₂) as an acceptor in an *in vitro* assay of glycosyltransferase activities, we have characterized several xylosyltransferase reactions in *C. neoformans*. One is the transfer of Xyl from UDP-Xyl to the reducing Man of the disaccharide substrate, forming a β -1,2-linkage (17)¹. This is mediated by either of two proteins: Cxt1p and Cxt2p. Cxt1p acts in the synthesis of both cellular glycolipids (18, 19) and the two capsule polysaccharides (GXM and GXMGal); less is known regarding the function of the closely related Cxt2p.

¹ J.S. Klutts and T.L. Doering, in preparation

In addition to the straightforward addition of Xyl that is mediated by the Cxt proteins, we have also discovered a completely distinct and novel activity of *C. neoformans* that adds xylose-phosphate (Xyl-P) to Man-containing substrates (20). The resulting Xyl-P-Man linkage has not been previously observed in the glycan structures of *C. neoformans* or any other organism, nor has an enzyme with xylosylphosphotransferase activity been described. We have identified and characterized the *C. neoformans* protein responsible for this activity, xylosylphosphotransferase 1 (Xpt1p; (20)). This protein is specific for UDP-Xyl as the reaction donor, but readily modifies a variety of Man-containing substrates. A significant gap in our knowledge is the biological function of Xpt1p; the moiety it forms has not been detected in glycolipid or capsule polysaccharides structures so far examined in *C. neoformans*, but many glycan elements of the cell remain uncharacterized. Below, we describe our investigation into the function of Xpt1p and present evidence that this enzyme plays a role in the *O*-linked glycosylation of proteins.

EXPERIMENTAL PROCEDURES

Materials. UDP-[¹⁴C(U)]xylose (UDP-[¹⁴C]Xyl; 151 mCi/mmol) was from PerkinElmer and α -1,3-D-mannobiose (α -1,3-Man₂) was from Carbohydrate Synthesis (Oxford, United Kingdom). The murine monoclonal anti-GXM antibodies used were 3C2 and 339 (21); F12D2 (22); 1255 (23); and 1326 (24). Unless specified, all other chemicals or reagents were obtained from Sigma Aldrich.

Strains and cell growth. *C. neoformans* strains (Table 1) were grown in liquid culture at 30°C in YPD medium (1% w/v yeast extract, 2% w/v peptone, 2% w/v dextrose) with shaking (230 rpm) or at 30°C on YPD agar plates (YPD medium with 2% w/v agar). As appropriate, media included 100 μ g/ml nourseothricin (NAT; from Werner Bio-Agents) and/or Geneticin[®] (G418; from Invitrogen). For immunofluorescence localization, strains were cultured at 30°C in Minimal Medium (0.17% yeast nitrogen base without amino acids, 2% w/v dextrose).

Table 1. *C. neoformans* strains used in these studies.

Name ^a	Serotype	Origin
KN99 α	A	Nielsen <i>et al.</i> 2003 (41)
KN99 α <i>xpt1</i> Δ	A	Reilly <i>et al.</i> 2009 (20)
KN99 α <i>xpt1</i> Δ p <i>XPT1</i>	A	Reilly <i>et al.</i> 2009 (20)
KN99 α <i>xpt1</i> Δ p <i>XPT1-HA</i>	A	Reilly <i>et al.</i> 2009 (20)
KN99 α <i>cap59</i> Δ	A	Baker <i>et al.</i> 2007 (42)
WM276	B	Warren <i>et al.</i> 2005 (43)
MMRL2651	C	Fraser <i>et al.</i> 2005 (44)
JEC21	D	Kwon-Chung <i>et al.</i> 1992 (45)

^a All strains are MAT α .

To test *C. neoformans* viability under various growth conditions, cells from an overnight culture were washed in water and adjusted to 2×10^6 cells/ml; 5 μ l (1×10^4 cells) of this suspension and of four ten-fold serial dilutions were spotted on YPD agar or YPD stressor plates (YPD agar with 0.5 mg/ml caffeine, 0.05% sodium dodecyl sulfate (SDS), 1 mM sodium nitrite, or 0.5 mM hydrogen peroxide) and then incubated at 30°C or 37°C.

Total membrane preparation and detergent extraction. *C. neoformans* membranes and their detergent extracts were prepared as in (20). Briefly, cells from an overnight culture were washed in Tris-EDTA Buffer (100 mM Tris-HCl pH 8.0, 0.1 mM EDTA), broken with glass beads, and the resulting lysate subjected to a clearing centrifugation step. Total membranes were isolated from the resulting supernatant fraction by ultracentrifugation, resuspended in Tris Buffer (100 mM Tris-HCl pH 8.0), and stored at 4°C. Protein concentration of the total membrane sample was determined using the Bio-Rad Protein Assay (Bio-Rad Laboratories). For some studies, membranes were extracted with 1% Triton X-100, subjected to a second round of ultracentrifugation, and the resulting supernatant fraction stored at 4°C. Protein concentration of the Triton X-100-extract sample was determined using the Bio-Rad Detergent Compatible Protein Assay (Bio-Rad Laboratories).

Xylosyltransferase activity assays. Enzyme activity was assayed by monitoring the transfer of [14 C]Xyl from a UDP-[14 C]Xyl donor to an α -1,3-Man₂ acceptor as in (20). Briefly, reactions containing 625 μ g protein (from *C. neoformans* total membranes or Triton X-100-extracts), 1 μ M UDP-[14 C]Xyl, 8.8 mM α -1,3-Man₂, and 7.5 mM MnCl₂ in 100 mM Tris-HCl pH 6.5 were incubated overnight at 20°C. The reaction products

were isolated using an anion exchange resin, resolved by thin layer chromatography (TLC), and visualized by autoradiography.

Growth in mice. For each strain tested, eight 4-6 week-old female C57Bl/6 mice (Jackson Laboratories) were anesthetized with a combination of ketaset-HCl and xylazine, and inoculated intranasally with 50 μ l of a 2.5×10^5 cells/ml suspension in phosphate-buffered saline pH 7.4 (PBS). Three animals from each cohort were sacrificed at 1 hr post-inoculation; the remaining five were sacrificed at 7 days post-inoculation. Following sacrifice, lungs were harvested, homogenized in PBS, and serial dilutions of the homogenate were plated on YPD agar for determination of colony-forming units (CFUs). Initial inocula were also plated to confirm CFUs.

Capsule staining. Cells from an overnight culture of *C. neoformans* were washed twice with PBS, resuspended at 1×10^7 cells/ml in PBS containing 1% bovine serum albumin (PBS + 1% BSA), and rotated for 1 hr at room temperature with a final concentration of 8 μ g/ml murine anti-capsular antibody. Cells were washed twice with PBS and then incubated for 1 hr at room temperature with rotation in PBS + 1% BSA containing 3.2 μ g/ml Alexa Fluor[®] 546 goat anti-mouse IgG (Invitrogen). Cells were again washed twice with PBS and suspended in PBS for visualization. Bright field and fluorescence images were acquired simultaneously on a Zeiss Axioskop 2 MOT Plus wide-field fluorescence microscope; all samples were imaged with identical acquisition settings.

Capsule induction. Cells from an overnight culture of *C. neoformans* were resuspended at 1×10^5 cells/ml in 50 ml YPD media plus appropriate antibiotics and again cultured overnight. The sub-cultured cells were resuspended at 1×10^7 cells/ml in 10 ml Dul-

becco's Modified Eagle's Medium, transferred to a 25 cm² tissue culture flask, and incubated at 37°C with 5% CO₂ for 20 hrs. One milliliter of cells was harvested, washed once with water, and resuspended in 100 µl India Ink for visualization. Bright field images were acquired on a Zeiss Axioskop 2 MOT Plus wide-field fluorescence microscope as above.

Lipid glycosylation. Reactions of 625 µg total membrane protein, 1 µM UDP-[¹⁴C]Xyl, and 7.5 mM MnCl₂ in 100 mM Tris-HCl pH 6.5 were incubated overnight at 20°C. Chloroform and methanol were added for a final ratio of 10:10:3 (chloroform:methanol:buffer); the sample was incubated for 30 min at room temperature with occasional vortex mixing and then centrifuged to remove particulate material (16,000 × g; 2 min). The supernatant fraction was transferred to a fresh tube and dried under a stream of nitrogen gas. The sample was then resuspended in *n*-butanol, vortexed with an equal volume of water, centrifuged as before, and the resulting organic phase transferred to a fresh tube. The remaining aqueous phase was again extracted with an equal volume of *n*-butanol and this organic phase pooled with the previous. The pooled organic phases were washed with an equal volume of water and the final organic phase transferred to a fresh tube and dried as before. The sample was resuspended in 1:1 methanol:water, applied to a Silica Gel 60 plate (EM Sciences), and resolved by TLC in a solvent system of 10:10:3 chloroform:methanol:water. The dried plate was sprayed with En³Hance[®] Spray (PerkinElmer) and radiolabeled products were visualized by autoradiography.

Protein glycosylation. Xylosyltransferase reactions were performed as in the previous section. Following overnight incubation, some reactions were treated with Protease

Type XIV (from *Streptomyces griseus*) or a buffer control (0.01 M sodium acetate, 0.005 M calcium acetate, and 0.01 M CaCl₂) for 24 hr at 37°C. All samples were mixed with sample buffer, heated for 15 min at 100°C, and resolved by SDS-PAGE on a 10% gel according to standard methods (25). The gel was fixed for 1 hr in 5:4:1 methanol:water:acetic acid, incubated in Enlightning Rapid Autoradiography Enhancer (PerkinElmer) for 30 min, dried onto 3MM chromatography paper (Whatman), and visualized by autoradiography.

Preparation of protein-linked glycans for analysis. A 50-ml overnight culture of *C. neoformans* was sub-cultured into 1 L YPD, grown overnight, harvested by centrifugation, and washed with Tris-EDTA Buffer. Cells ($\sim 1 \times 10^7$ cells/ml) were resuspended in 10 ml of the same buffer, disrupted with glass beads, and the resulting lysate subjected to a clearing centrifugation step as above. The supernatant fraction was then extracted with 1% CHAPS and subjected to ultracentrifugation. The detergent-soluble material was transferred to cellulose dialysis tubing (8,000 MWCO; from Fisher Scientific) and dialyzed against 2 L 50 mM ammonium bicarbonate buffer at 4°C; the buffer was changed every 12 hrs for a total of 8 L over 60 hrs. The dialyzed sample was transferred to a 50-ml conical tube, frozen at -80°C, and lyophilized. Lyophilized protein powder was further washed with 80% acetone to remove residual detergent and then dried under a stream of nitrogen gas.

Oligosaccharides were released from the *C. neoformans* samples by reductive and β -elimination as detailed in (26) and summarized here. The lyophilized *C. neoformans* material (2.5 mg) was resuspended in a solution of 100 mM sodium hydroxide and 1 M

sodium borohydride, and incubated for 18 hrs at 45°C in a glass tube sealed with a Teflon-lined screw top. The tube was transferred on ice and the reaction mixture was neutralized with 10% acetic acid. The sample was then loaded onto a column of AG 50W-X8 cation exchange resin (Bio-Rad) to desalt. Released oligosaccharide were eluted from the resin with three bed-volumes 5% acetic acid and lyophilized to dryness. To remove borate from the sample, a solution of 10% acetic acid in methanol was added and the sample then dried under a stream of nitrogen gas at 37°; this was repeated for a total of five times. The sample was then resuspended in 5% acetic acid and loaded onto a C18 cartridge column (J.T. Baker Co.) that was previously washed with acetonitrile and pre-equilibrated with 5% acetic acid. Run-through from the column was collected after loading; the column was then washed a total of five times with 5% acetic acid. The run-through and washes were combined and evaporated to dryness.

Analysis of glycans by nanospray ionization mass spectrometry (NIS-MS). Samples were analyzed as in (26). Briefly, the released oligosaccharide sample was permethylated (27), dissolved in 1 mM sodium hydroxide in 50% methanol, and infused into a linear ion trap mass spectrometer (LTQ; Thermo Finnigan) equipped with an orbitrap. MS analysis was performed in positive ion mode. The total ion mapping (TIM) function of the Xcalibur software package was utilized to detect and quantify the prevalence of individual glycans in the total glycan profile; peaks were quantified if they were two-fold or greater above background.

Protein localization. Cells were cultured overnight in Minimal Medium (final density $\sim 5 \times 10^7$ cells/ml), mixed with Formalin (10% final), and incubated for 30 min at

30°C with shaking. All subsequent steps were performed at room temperature. Cells (5×10^8) were harvested by centrifugation ($1,000 \times g$; 5 min), washed once with water, resuspended in 2 ml of a fresh solution of 4% formaldehyde in PBS, and incubated for 30 min with rotation. The sample was then washed three times with PBS, resuspended in 4 ml Lysis Buffer (50 mM sodium citrate pH 6.0, 1 M D-sorbitol, 2 mM DTT) plus 25 mg/ml Lysing Enzymes (from *Trichoderma harzianum*), and incubated for 2 hr with occasional inversion. Following digestion, the cells were washed three times with HS Buffer (100 mM HEPES pH 7.5, 1 M D-sorbitol), resuspended in HS Buffer containing 1% Triton X-100, and incubated for 10 min. Finally, cells were washed three times with HS Buffer and resuspended in 1 ml HS Buffer.

The washed cell suspension was spotted in 20 μ l aliquots on a glass microscope slide coated with 0.1% poly-L-lysine, incubated for 20 min at room temperature, and the buffer removed by aspiration. All subsequent treatments and washes were performed by the application of 20 μ l volumes, incubation at room temperature, and aspiration. The slides were treated with Blocking Buffer (5% goat serum, 0.05% Triton X-100 in PBS) for 1 hr followed by either a high-affinity rat anti-HA monoclonal antibody (20 ng/ml in Blocking Buffer; from Roche) or Blocking Buffer alone overnight in a moist chamber. Samples were then washed six times with Blocking Buffer and stained with Alexa Fluor[®] 594 goat anti-rat IgG (1 μ g/ml in Blocking Buffer; from Invitrogen) for 1 hr in the dark; next, slides were washed three times with Blocking Buffer and stained with DAPI (4 μ g/ml in PBS) for 15 min in the dark. Finally, samples were washed twice with Blocking Buffer, then twice with PBS, and allowed to air-dry. Prolong Gold was applied to

each sample, followed by a glass coverslip, and the slide was incubated for 30 min at -20°C in the dark. Bright field and fluorescence images were acquired as for the capsule staining assays above using the Zeiss Axioskop 2 MOT Plus wide-field fluorescence microscope.

RESULTS

Xylosyltransferases in C. neoformans. We have identified several xylosyltransferase activities in *C. neoformans* by assaying the transfer of radiolabeled Xyl from the nucleotide sugar donor UDP-[¹⁴C]Xyl to an α -1,3-Man₂ oligosaccharide acceptor (see Experimental Procedures). When membranes prepared from the wild-type strain KN99 α were used as the source of enzyme activity in this assay, two distinct products were observed (Figure 1, track 1). A combination of nuclear magnetic resonance spectroscopy and mass spectrometry analyses were employed to determine the structures of these two oligosaccharides. The upper product (Figure 1, track 1, open arrowhead) is Xyl linked β -1,2 to the reducing Man of the α -1,3-Man₂ substrate (17); this is synthesized primarily by Cxt1p, which generates a Man- α (1 \rightarrow 3)[Xyl- β (1 \rightarrow 2)]-Man motif present in cryptococcal glycosylinositol phosphorylceramide (GIPCs), GXM, and GXMGal (18, 19). The lower product (Figure 1, track 1, closed arrowhead) is Xyl-P linked to the non-reducing Man of α -1,3-Man₂ and is generated by Xpt1p (20). The Xyl-P-Man modification has never been observed in *C. neoformans* or any other organism. Our current investigation focuses on identifying a biological function for Xpt1p, the enzyme responsible for generating this novel linkage.

As mentioned above, members of the *C. neoformans* species complex differ in terms of ecological niche, host preference, and disease outcome (1). We began our investigation into the function of Xpt1p by exploring its conservation among these closely related species. To do this, we performed xylosyltransferase activity assays on membranes prepared from cryptococcal strains representing the four major historically defined

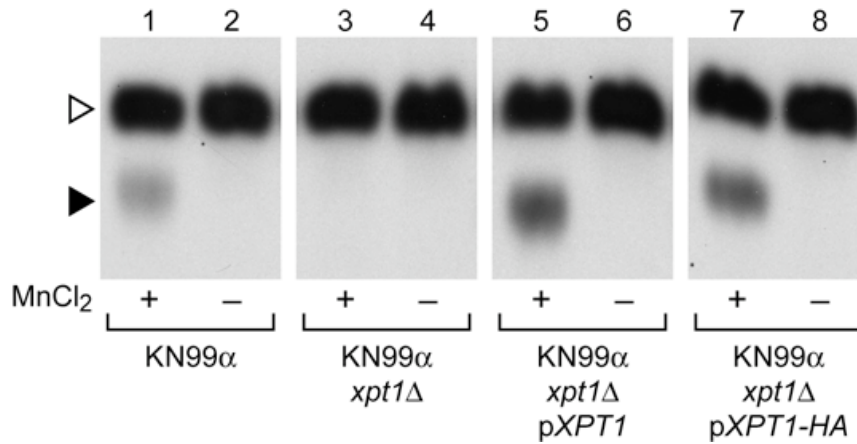
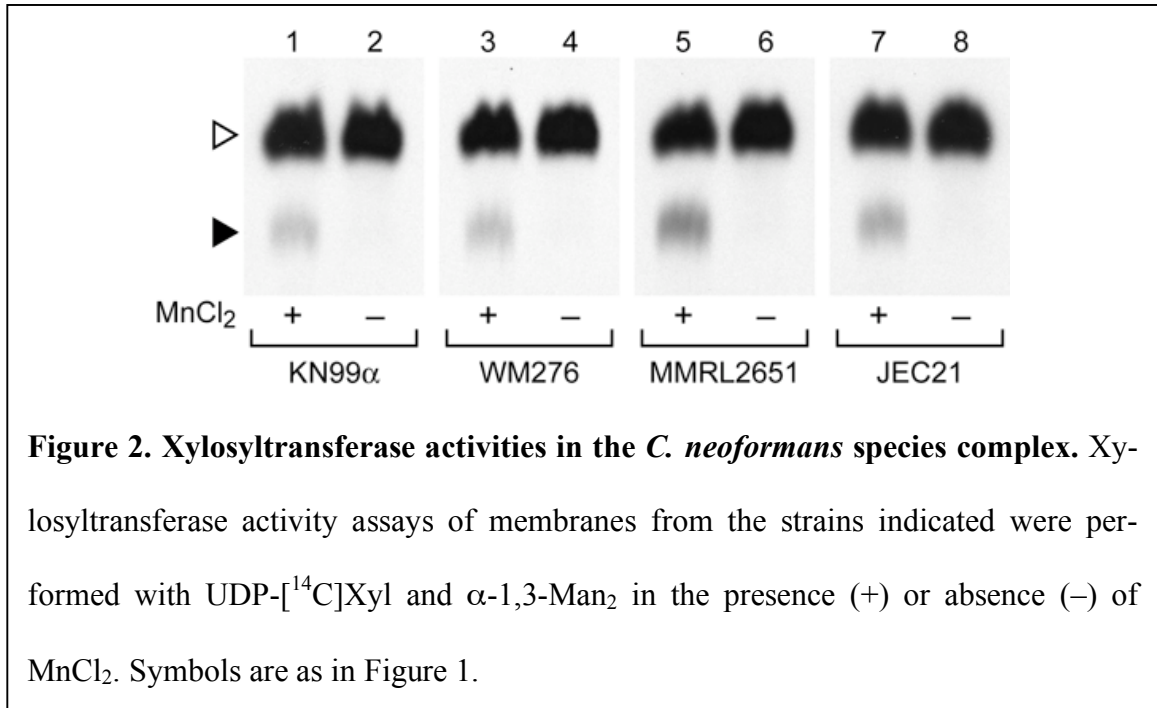


Figure 1. Xylosyltransferase activities in *C. neoformans*. Total membranes prepared from wild-type (KN99α), mutant (KN99α *xpt1*Δ), or complemented mutant (KN99α *xpt1*Δ *pXPT1* and KN99α *xpt1*Δ *pXPT1-HA*) strains were assayed as described in the Experimental Procedures with UDP-[¹⁴C]Xyl and α-1,3-Man₂ in the presence (+) or absence (-) of the MnCl₂ cofactor as indicated. An autoradiograph of the products resolved by TLC is shown; no signal was detected in other regions of the plate beyond minor amounts of free Xyl. The filled triangle indicates the product of the manganese-dependent xylosyltransferase activity and the open triangle indicates the products of unrelated xylosyltransferase activities (refer to Results). Note that no signal was detected in the absence of the α-1,3-Man₂ acceptor.

serotypes: serotype A (KN99α, H99), serotype B (WM276, R265), serotype C (NIH312, MMRL2751), and serotype D (JEC21, KN355α, KN433α). In each of the strains examined, a xylosylated product was observed that migrated in parallel with that of the Xpt1p activity of KN99α and was also manganese-dependent (Figure 2, closed arrowhead, and



data not shown). These results were consistent with our identification of sequences homologous to the serotype A *XPT1* (locus *CNAG_04860*; from the *C. neoformans* var. *grubii* H99 database maintained by the Broad Institute) in the genomes of serotypes B (locus *CNBG_5687*; from the *C. gattii* R265 Database maintained by the Broad Institute) and D (locus *CNJ02890*; from the *C. neoformans* var. *neoformans* JEC21 Database maintained by TIGR)². The presence of an Xpt1p-like activity in each of the strains tested confirmed that not only was the *XPT1* sequence conserved, but that the encoded protein was expressed and active in growing cultures of these cells.

Growth of xpt1Δ strains. To begin defining the biological function of Xpt1p, we examined the basic growth characteristics of cells deleted for *XPT1* (*xpt1Δ*) compared to wild-type. Cultures of KN99α and KN99α *xpt1Δ* grew comparably in liquid rich medium

² A representative genome of serotype C has not been sequenced.

and on solid rich medium; this held true at both 30°C (the optimal growth temperature for *C. neoformans*) and 37°C (internal body temperature of cryptococcal human hosts; data not shown). Similar results were obtained when the plate medium was supplemented with caffeine, SDS, sodium nitrate, or hydrogen peroxide, which act as cell wall, cell membrane, nitrosative, and oxidative stressors, respectively (data not shown). We also assessed the relative growth of KN99 α and KN99 α *xpt1* Δ in a mouse model of cryptococcal infection. The levels of CFUs recovered from the lungs of mice following intranasal inoculation were the same for both the wild-type and deletion strains (data not shown). Collectively, these studies indicated that the loss of Xpt1p did not influence growth or viability under the conditions tested, but they gave no information as to the cellular function of Xpt1p.

Potential roles of Xpt1p. We examined the potential role of Xpt1p in capsule formation by comparing the capsule morphologies of KN99 α , KN99 α *xpt1* Δ , and KN99 α *xpt1* Δ *pXPT1* cells. To do this, we used immunofluorescence microscopy to assess the binding of monoclonal anti-GXM antibodies to the cell surface. Each of the antibodies tested (see Experimental Procedures) demonstrated uniform staining around the cell periphery (shown for antibody F12D2 in Figure 3, panel A), indicating no obvious difference in the mutant strain from wild-type at the level of light microscopy. We also assessed the ability of mutant and wild-type strains to increase the radius of their capsule in response to ‘inducing’ growth conditions (28). Again, both the KN99 α and KN99 α *xpt1* Δ strains enlarged capsule to a comparable extent (Figure 3, panel B). This lack of change in the capsule was consistent with prior studies of capsule polysaccharides that detected

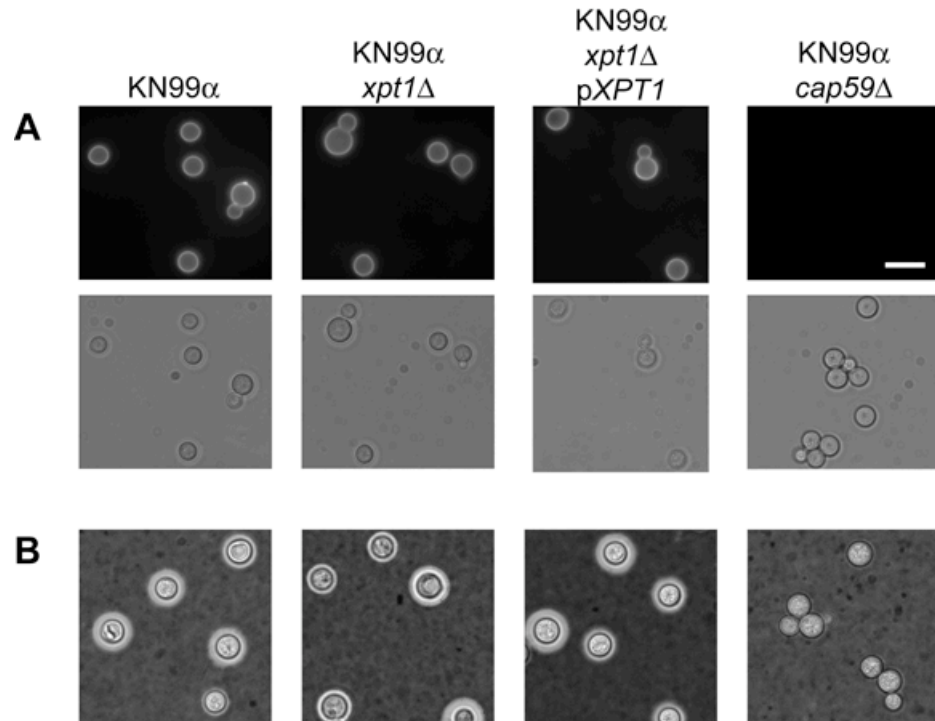


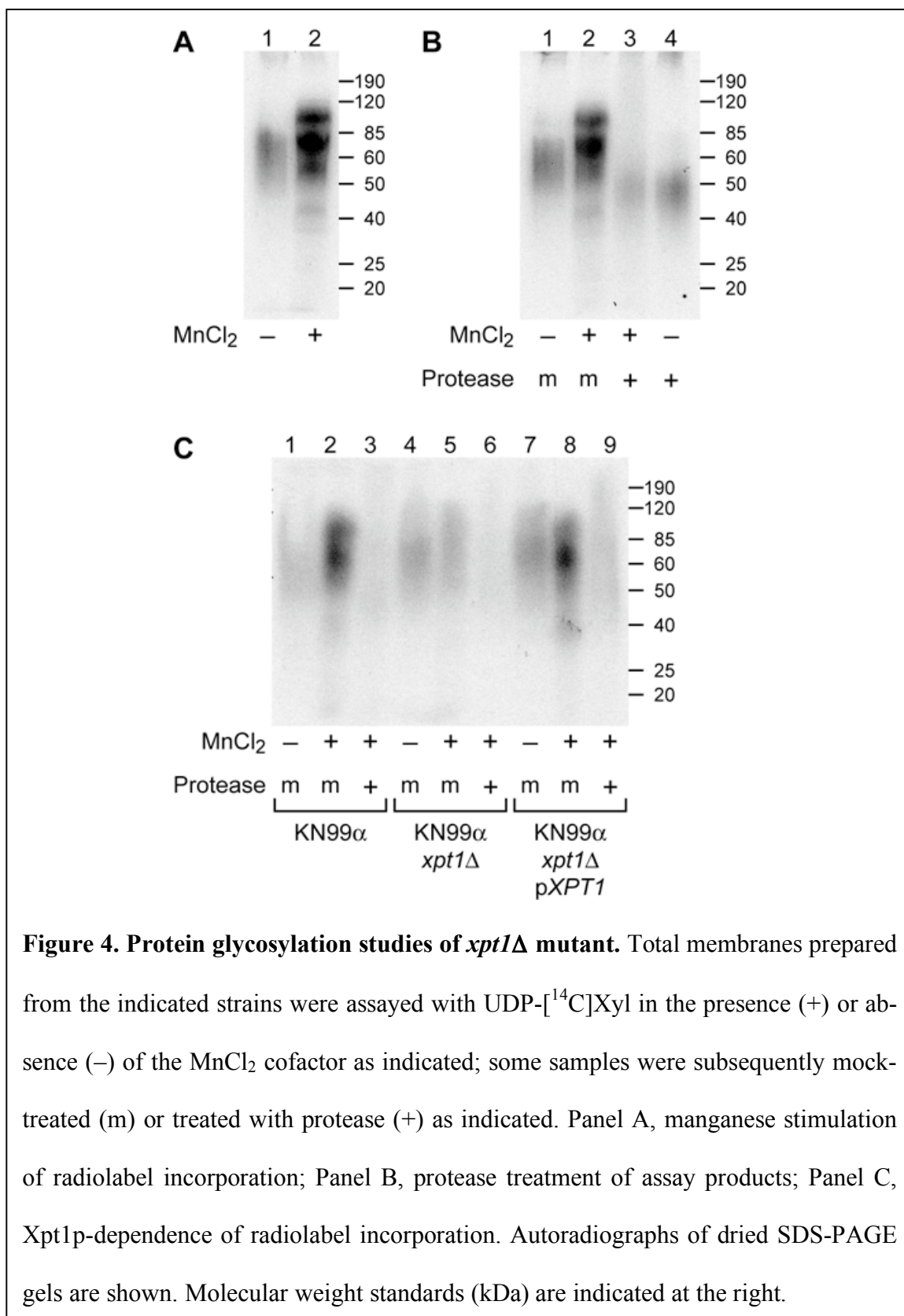
Figure 3. Capsule morphology in wild-type and *xpt1Δ* mutant cells. Panel A, immunofluorescence microscopy of the indicated strains labeled with monoclonal antibody F12D2 followed by Alexa Fluor[®] 546 (Experimental Procedures). Bright field (upper) and fluorescent (lower) images are shown. Panel B, bright field image of the indicated strains grown under capsule-inducing conditions (Experimental Procedures) and then mixed with India Ink. Bar, 10 μ M.

no Xyl-P in GXM or GXMGal (3-5). To confirm this finding, ³¹P NMR analysis was performed on GXM prepared from KN99 α ; we were unable to detect any phosphate signal in the sample (data not shown).³ Therefore we did not pursue additional analysis of the capsule polysaccharides in the *xpt1Δ* deletion mutant.

³ C. Heiss, personal communication

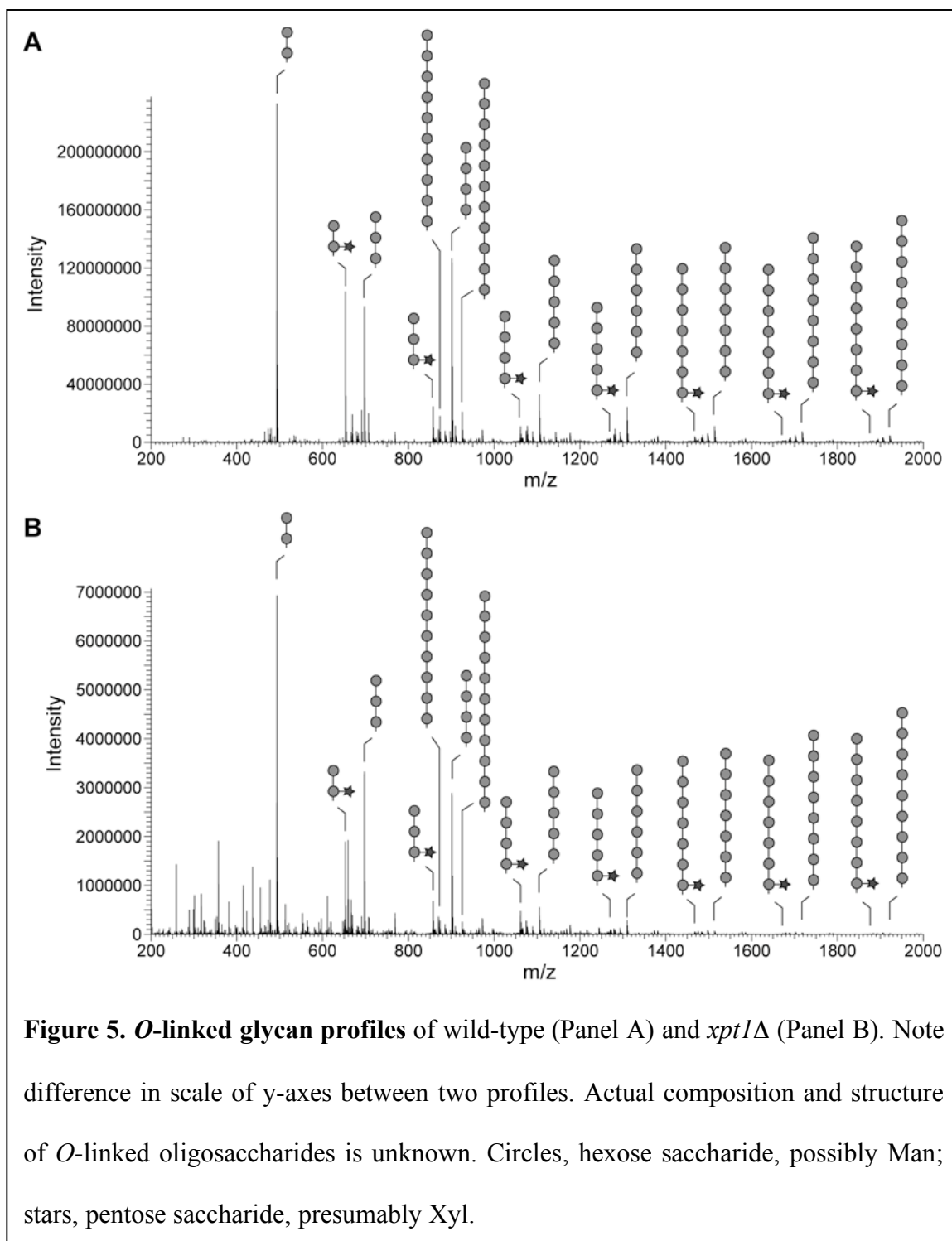
We next assessed the participation of Xpt1p in the xylosylation of cryptococcal glycolipids. We examined the utilization of UDP-[¹⁴C]Xyl by cryptococcal membrane proteins prepared from wild-type, mutant, and control strains (KN99 α , KN99 α *xpt1* Δ , and KN99 α *xpt1* Δ *pXPT1*, respectively) in reactions similar to our standard xylosyltransferase assay but lacking the α -1,3-Man₂ substrate such that only endogenous compounds were available as acceptor molecules. Following incubation, lipids were extracted from the radiolabeled samples for analysis by TLC. Although we detected the incorporation of [¹⁴C]Xyl into several lipid species, this activity was not dependent on the presence of Xpt1p (data not shown). These data indicated that Xpt1p does not act in glycolipid synthesis.

We next assessed the involvement of Xpt1p in protein glycosylation. Similar to the lipid experiment outlined above, we incubated cryptococcal membranes with UDP-[¹⁴C]Xyl (but not α -1,3-Man₂), and then analyzed the samples by SDS-PAGE. As seen in Panel A of Figure 4, KN99 α membranes assayed in this manner incorporated significant amounts of radiolabel into material that migrated between 50 kDa and 100 kDa. Notably, the incorporation of [¹⁴C]Xyl increased with the addition of MnCl₂ to the reactions, indicating that some of the xylosylation was due to a manganese-dependent enzymatic activity (Figure 4, Panel A, compare lanes 1 and 2). The subsequent addition of protease to these reactions significantly reduced the [¹⁴C]Xyl signal relative to mock-treated controls, demonstrating that the radiolabel was in fact associated with a polypeptide species (Figure 4, Panel B).

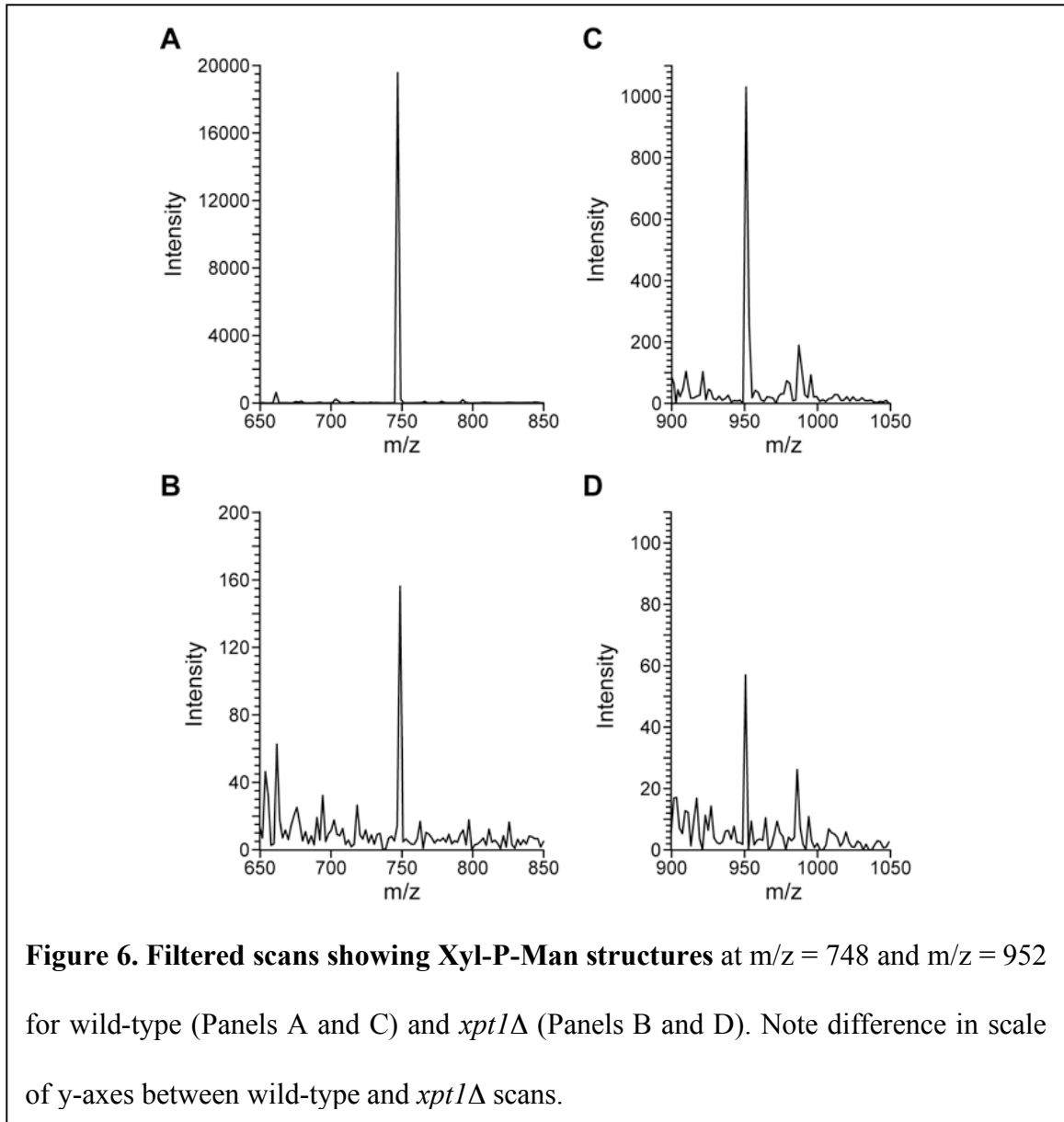


Although [^{14}C]Xyl-labeling of protein in KN99 α membranes was clearly stimulated by the addition of MnCl_2 , this could have been due to any of a number of synthesis activities that are native to *C. neoformans*. To test whether the manganese-dependent labeling correlated with the presence of Xpt1p, we performed similar experiments with membrane preparations from KN99 α , KN99 α *xpt1* Δ , and KN99 α *xpt1* Δ p*XPT1* cells. The intensity and pattern of radiolabel incorporation was comparable for both the wild-type and complemented strains (Figure 4, Panel C, lanes 1-3 and lanes 6-9): in both strains the inclusion of MnCl_2 increased [^{14}C]Xyl incorporation while protease treatment of reaction products significantly reduced [^{14}C]Xyl-labeling. In contrast, membranes from the KN99 α *xpt1* Δ strain showed no increase in protein radiolabeling upon addition of MnCl_2 (Figure 4, Panel C, lanes 4-6). These studies strongly implicated Xpt1p in protein glycosylation.

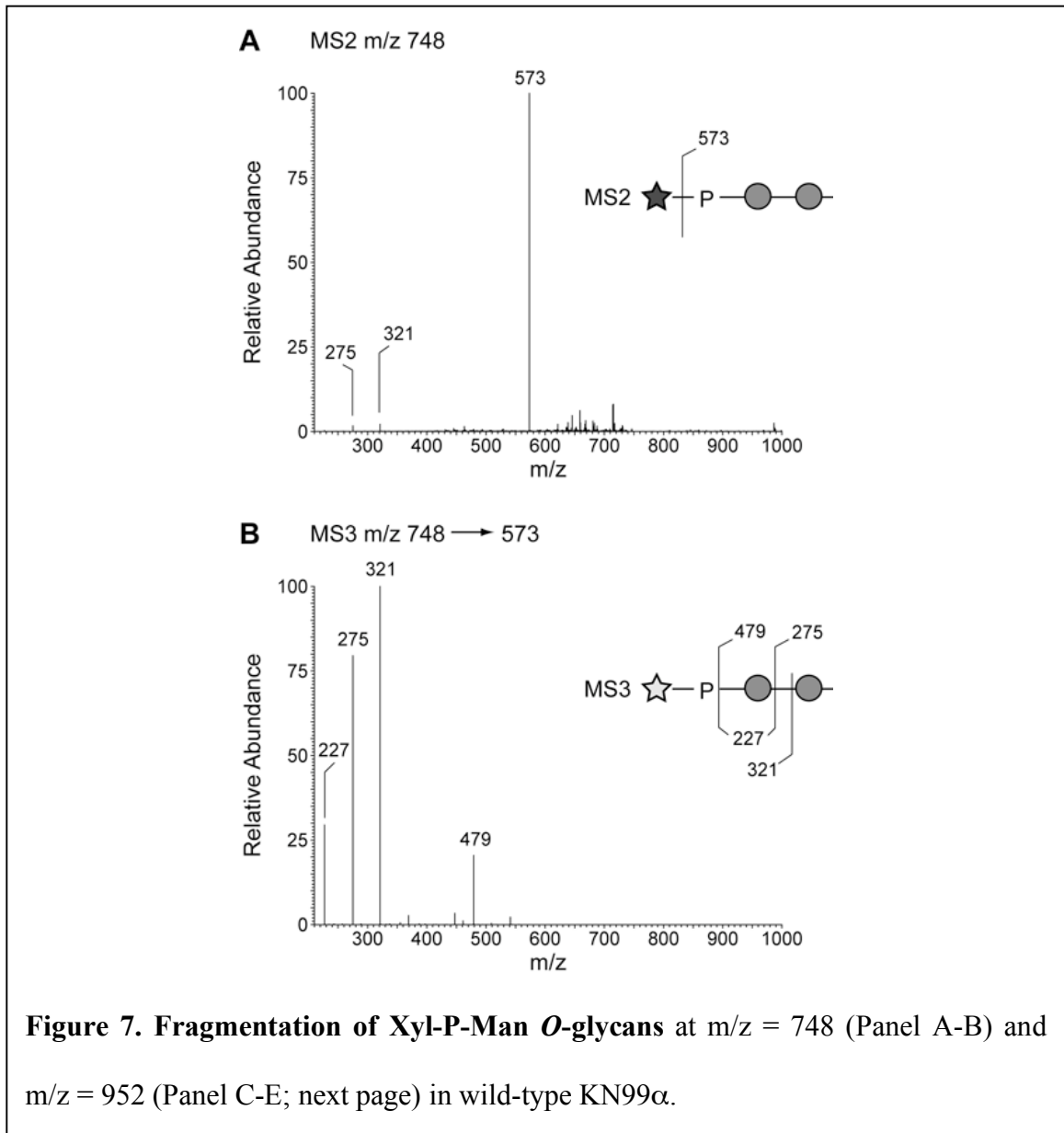
Analysis of O-linked glycans. In order to examine the protein-linked structures formed by Xpt1p, we turned to glycan analysis. Total cell lysates were prepared from KN99 α and KN99 α *xpt1* Δ strains and extracted with 1% CHAPS. *O*-glycans were released from the detergent-soluble material by β -elimination, permethylated, and analyzed by NSI-MS (see Experimental Procedures). The major species of *O*-linked glycans in both the wild-type and *xpt1* Δ samples were consistent with structures of Man_2 , Man_3 , Man_4 , and Xyl- Man_2 (Figure 5). There was, however, a significantly lower (~25-fold) level of *O*-glycans expressed by the mutant strain compared to wild-type.

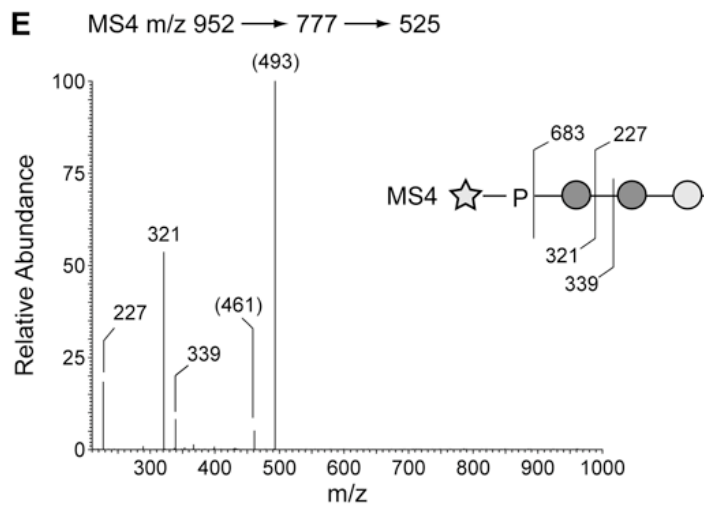
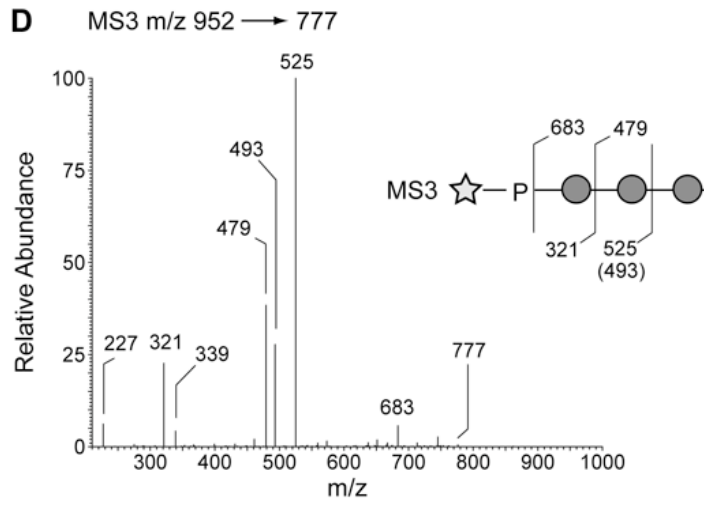
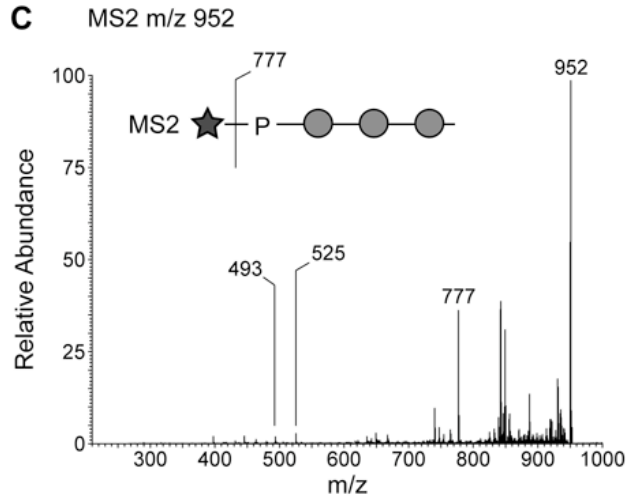


TIM data filtered by the loss of terminal Xyl (Δ mass, 175) and Xyl-1-P (Δ mass, 285) revealed the presence of minor *O*-glycan components of masses consistent with Xyl-1-P-substituted O-Man-type glycans. These included mass consistent with compositions of Xyl-P-Man₂ ($m/z = 748$), Xyl-P-Man₃ ($m/z = 952$), and Xyl-P-Man₄ ($m/z = 1156$) in

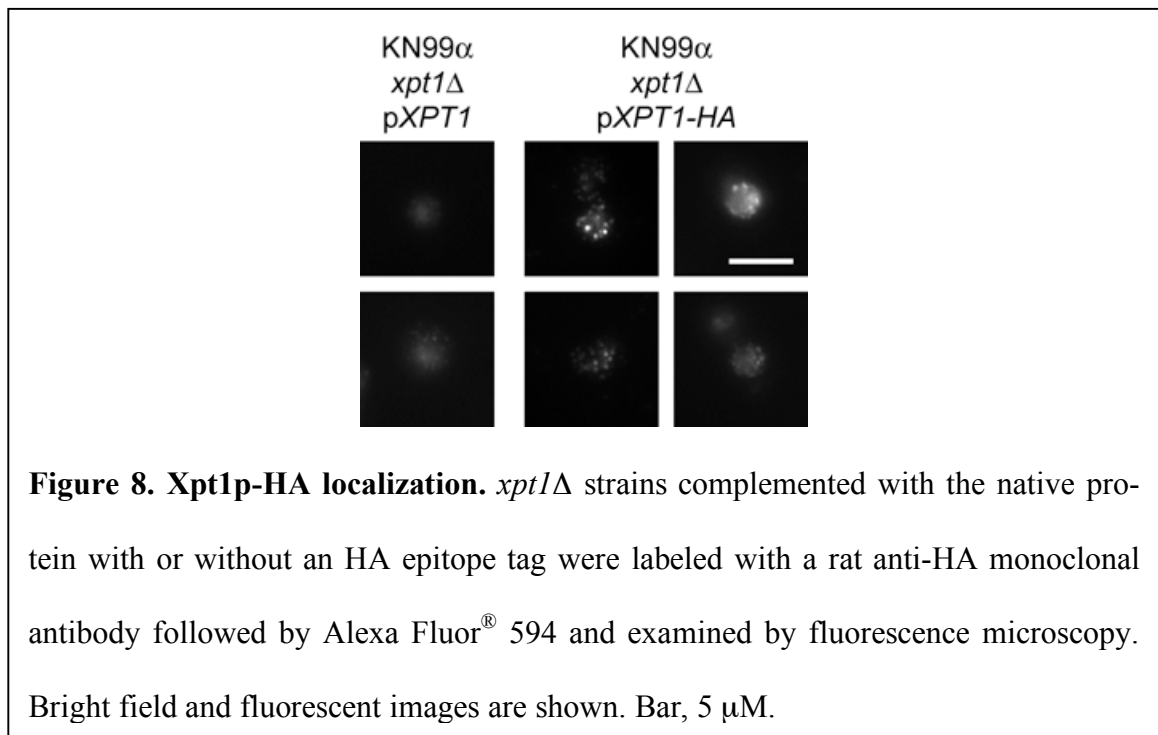


the wild-type KN99 α sample (Figure 6, Panels A and C; and data not shown). Fragmentation analysis (Figure 7) supported these structural assignments. Species of $m/z = 748$ and $m/z = 952$ were also detected in the KN99 α *xpt1* Δ sample (Figure 6, Panels B and D), although quantities were insufficient for fragmentation.





Localization studies. Although most *O*-glycosylation of proteins occurs in the endoplasmic reticulum (ER) and Golgi (29) there are also important examples of cytosolic *O*-glycosylation (30). To localize Xpt1p, we used an *xpt1Δ* strain expressing an HA-tagged form of the protein; as a control strain we used the same deletion background expressing wild-type protein. Both p*XPT1* and p*XPT1-HA* were regulated by the native *XPT1* promoter and the xylosyltransferase activity levels of both strains were comparable to that of wild-type (Figure 1, tracks 5-8). Immunofluorescence microscopy of cells probed with an anti-HA antibody (refer to Experimental Procedures) allowed visualization of Xpt1p-HA in a punctate pattern within the cell (Figure 8), clearly distinct from the nucleus and the plasma membrane. This staining did not coincide with staining of an ER marker, BiP (data not shown; (31)) and is consistent with staining of Golgi structures in other budding yeast such as *Saccharomyces cerevisiae* (32).



DISCUSSION

We previously identified Xpt1p as a novel glycosyltransferase of *C. neoformans* that generates a Xyl-P modification of Man (20). In the current study, we focused on determining the role of this unusual enzyme within the cryptococcal cell. Based on its biochemical function, we expect Xpt1p to participate in glycan synthesis. While the capsule polysaccharides, GIPCs, and *O*-linked glycans of *C. neoformans* are all known to include Xyl residues (3, 4, 11, 13), none have been previously reported to contain a Xyl-P modification. However, the possibility that this unusual structure may have been overlooked in the previous analyses, together with the lack of definitive structures for many cellular glycans, left open many potential roles for Xpt1p.

We detected structures consistent with the Xyl-P modification in the *O*-glycans of cryptococcal proteins isolated from a wild-type strain, which led us to perform similar analyses in the *xpt1Δ* mutant strain. Notably, the *xpt1Δ* strain synthesizes dramatically fewer *O*-glycans overall (~25-fold reduction). The putative Xyl-P-containing structures were further reduced (~2-fold for the Xyl-P-Man₂ species and ~12-fold for the Xyl-P-Man₃ species), but not eliminated, in the mutant. This suggests that other enzymes participate in the synthesis of these species. However, these results also implicate Xpt1p, or the structure it generates, in *O*-glycan synthesis. Future work will be needed in order to elucidate the role of Xpt1p in the generation of *O*-linked glycans.

The detection of structures consistent with Xyl-Man and Xyl-P-Man among the *O*-linked glycans of *C. neoformans* differentiates the *O*-glycans of this pathogen from those of the model yeast *S. cerevisiae*, which are composed only of Man residues (33).

Also, although phosphate moieties have been previously observed in the *O*-linked modifications of *S. cerevisiae* and *Pichia pastoris*, in these examples the phosphate was always present at the glycan terminus (34, 35). The product of the cryptococcal Xpt1p activity is, to our knowledge, the first example of phosphate acting as a bridge between two sugar residues in *O*-glycans.

Further studies are also needed to address a possible role for Xpt1p in generating modifications within *N*-linked glycans. The Man-P modifications found in some of the highly mannosylated *N*-linked glycan structures of *S. cerevisiae* provides some precedence for the presence of a phosphate moiety in these structures (36). However, outside of the plant kingdom, Xyl has only been detected in the *N*-glycans of mollusks (37, 38) and the pathogenic fungus *Pneumocystis jiroveci* (39).

We found no difference between the ability of wild-type and *xpt1Δ* cells to colonize mice or to grow under stress conditions. Nonetheless, both the *XPT1* gene and enzyme activity are conserved among members of the *C. neoformans* species complex (Figure 2). Serotypes A and D (*C. neoformans*) are estimated to have split from serotypes B and C (*C. gattii*) over 37 million years ago (40). The maintenance of Xpt1p through the evolution of these species suggests that Xpt1p performs a necessary function for the cell, possibly under conditions we have not yet tested.

It may be informative to identify those proteins that are modified by the activities of Xpt1p. As seen in Figure 4, the diffuse Xpt1p-dependent [¹⁴C]Xyl labeling that appears between 50 kDa and 100 kDa sometimes resolves into more focused bands (Figure 4, Panel A). Isolating these few highly radiolabeled polypeptides from the rest of

the proteinaceous material present in the total membrane sample preparations will likely prove difficult. In addition, the radioabeling of membrane proteins in our *in vitro* assay may not accurately represent the native targets of the Xpt1p activity in terms of cellular protein modification. In the future, it may be possible to develop an antibody specific for the Xyl-P-Man motif, which could then be used in the purification and identification of the Xpt1p protein substrates.

The data presented in Figure 5, Panel A represents our first insights into the structures of *O*-linked glycans in *C. neoformans*. Further studies are required to fully define the protein-linked glycan structures of this pathogenic fungus. Such investigations will help to catalogue the unusual glycans of *C. neoformans* as well as suggest the underlying biosynthetic pathways required for their generation. Significant differences in either glycan structure or assembly between this organism and its occasional human host represent possible drug targets in a cryptococcal infection.

ACKNOWLEDGEMENTS

Studies of glycan synthesis in the Doering laboratory are supported by NIH Grant RO1 GM071007. The authors thank David Haslam and Jacques Baenziger for helpful insights on this project; Robert Cherniak and Christian Heiss for discussion regarding the structures of GXM and GXMGal; and Thomas Kozel for providing anti-GXM antibodies.

ABBREVIATIONS USED

BSA, bovine serum albumin; CFU, colony-forming unit; GPI, glycosylphosphatidylinositol; GXM, glucuronoxylomannan; GXMGal, glucuronoxylomannogalactan; G418, geneticin; Man, mannose; NAT, nourseothricin; NSI-MS, nanospray mass spectrometry; PBS, phosphate-buffered saline; SDS, sodium dodecyl sulfate; TIM, total ion mapping; TLC, thin layer chromatography; Xyl, xylose; Xyl-P, xylose-phosphate.

REFERENCES

1. Lin, X., and J. Heitman. 2006. The biology of the *Cryptococcus neoformans* species complex. *Annu. Rev. Microbiol.* 60: 69-105.
2. Casadevall, A., and J. Perfect. 1998. *Cryptococcus neoformans*. American Society for Microbiology.
3. Cherniak, R., H. Valafar, L.C. Morris, and F. Valafar. 1998. *Cryptococcus neoformans* chemotyping by quantitative analysis of ¹H nuclear magnetic resonance spectra of glucuronoxylomannans with a computer-simulated artificial neural network. *Clin. Diagn. Lab. Immunol.* 5: 146-159.
4. Vaishnav, V.V., B.E. Bacon, M. O'Neill, and R. Cherniak. 1998. Structural characterization of the galactoxylomannan of *Cryptococcus neoformans* Cap67. *Carbohydr. Res.* 306: 315-330.
5. Heiss, C., J.S. Klutts, Z. Wang, T.L. Doering, and P. Azadi. 2009. The structure of *Cryptococcus neoformans* galactoxylomannan contains beta-D-glucuronic acid. *Carbohydr. Res.* 344: 915-920.
6. Franzot, S.P., and T.L. Doering. 1999. Inositol acylation of glycosylphosphatidylinositols in the pathogenic fungus *Cryptococcus neoformans* and the model yeast *Saccharomyces cerevisiae*. *Biochem. J.* 340 (Pt 1): 25-32.
7. Djordjevic, J.T., M. Del Poeta, T.C. Sorrell, K.M. Turner, and L.C. Wright. 2005. Secretion of cryptococcal phospholipase B1 (PLB1) is regulated by a glycosylphosphatidylinositol (GPI) anchor. *Biochem. J.* 389: 803-812.

8. Eigenheer, R. A., Y. Jin Lee, E. Blumwald, B.S. Phinney, and A. Gelli. 2007. Extracellular glycosylphosphatidylinositol-anchored mannoproteins and proteases of *Cryptococcus neoformans*. *FEMS Yeast Res.* 7: 499-510.
9. Samuelson, J., S. Banerjee, P. Magnelli, J. Cui, D.J. Kelleher, R. Gilmore, and P.W. Robbins. 2005. The diversity of dolichol-linked precursors to Asn-linked glycans likely results from secondary loss of sets of glycosyltransferases. *Proc. Natl. Acad. Sci. U.S.A.* 102: 1548-1553.
10. Olson, G.M., D.S. Fox, P. Wang, J.A. Alspaugh, and K.L. Buchanan. 2007. Role of protein *O*-mannosyltransferase Pmt4 in the morphogenesis and virulence of *Cryptococcus neoformans*. *Eukaryot. Cell.* 6: 222-234.
11. Schutzbach, J., H. Ankel, and I. Brockhausen. 2007. Synthesis of cell envelope glycoproteins of *Cryptococcus laurentii*. *Carbohydr. Res.* 342: 881-893.
12. Willger, S.D., J.F. Ernst, J.A. Alspaugh, and K.B. Lengeler. 2009. Characterization of the *PMT* gene family in *Cryptococcus neoformans*. *PLoS One* 4: e6321.
13. Heise, N., A.L. Gutierrez, K.A. Mattos, C. Jones, R. Wait, J.O. Previato, and L. Mendonca-Previato. 2002. Molecular analysis of a novel family of complex glycosylphosphoryl ceramides from *Cryptococcus neoformans*: structural differences between encapsulated and acapsular yeast forms. *Glycobiology* 12: 409-420.
14. Rhome, R., T. McQuiston, T. Kechichian, A. Bielawska, M. Hennig, M. Drago, G. Morace, C. Luberto, and M. Del Poeta. 2007. Biosynthesis and immunogenicity of glucosylceramide in *Cryptococcus neoformans* and other human pathogens. *Eukaryot Cell* 6: 1715-1726.

15. Moyrand, F., B. Klaproth, U. Himmelreich, F. Dromer, and G. Janbon. 2002. Isolation and characterization of capsule structure mutant strains of *Cryptococcus neoformans*. *Mol. Microbiol.* 45: 837-849.
16. Griffith, C.L., J.S. Klutts, L. Zhang, S.B. Lavery, and T.L. Doering. 2004. UDP-glucose dehydrogenase plays multiple roles in the biology of the pathogenic fungus *Cryptococcus neoformans*. *J. Biol. Chem.* 279: 51669-51676.
17. Klutts, J.S., S.B. Lavery, and T.L. Doering. 2007. A beta-1,2-xylosyltransferase from *Cryptococcus neoformans* defines a new family of glycosyltransferases. *J. Biol. Chem.* 282: 17890-17899.
18. Klutts, J.S., and T.L. Doering. 2008. Cryptococcal xylosyltransferase 1 (Cxt1p) from *Cryptococcus neoformans* plays a direct role in the synthesis of capsule polysaccharides. *J. Biol. Chem.* 283: 14327-14334.
19. Castle, S.A., E.A. Owuor, S.H. Thompson, M.R. Garnsey, J.S. Klutts, T.L. Doering, and S.B. Lavery. 2008. Beta1,2-xylosyltransferase Cxt1p is solely responsible for xylose incorporation into *Cryptococcus neoformans* glycosphingolipids. *Eukaryot Cell* 7: 1611-1615.
20. Reilly, M.C., S.B. Lavery, S.A. Castle, J.S. Klutts, and T.L. Doering. 2009. A novel xylosylphosphotransferase activity discovered in *Cryptococcus neoformans*. *J. Biol. Chem.* [online].
21. Spiropulu, C., R.A. Eppard, E. Otteson, and T.R. Kozel. 1989. Antigenic variation within serotypes of *Cryptococcus neoformans* detected by monoclonal antibodies specific for the capsular polysaccharide. *Infect. Immun.* 57: 3240-3242.

22. Kozel, T.R., S.M. Levitz, F. Dromer, M.A. Gates, P. Thorkildson, and G. Janbon. 2003. Antigenic and biological characteristics of mutant strains of *Cryptococcus neoformans* lacking capsular O acetylation or xylosyl side chains. *Infect. Immun.* 71: 2868-2875.
23. Eckert, T.F., and T.R. Kozel. 1987. Production and characterization of monoclonal antibodies specific for *Cryptococcus neoformans* capsular polysaccharide. *Infect. Immun.* 55: 1895-1899.
24. Netski, D., and T.R. Kozel. 2002. Fc-dependent and Fc-independent opsonization of *Cryptococcus neoformans* by anticapsular monoclonal antibodies: importance of epitope specificity. *Infect. Immun.* 70: 2812-2819.
25. Gallagher, S.R. 2006. One-dimensional SDS gel electrophoresis of proteins. *Curr. Protoc. Mol. Biol.* Chapter 10:Unit 10.2A.
26. Aoki, K., M. Porterfield, S.S. Lee, B. Dong, K. Nguyen, K.H. McGlamry, and M. Tiemeyer. 2008. The diversity of O-linked glycans expressed during *Drosophila melanogaster* development reflects stage- and tissue-specific requirements for cell signaling. *J. Biol. Chem.* 283: 30385-30400.
27. Anumula, K.R., and P.B. Taylor. 1992. A comprehensive procedure for preparation of partially methylated alditol acetates from glycoprotein carbohydrates. *Anal. Biochem.* 203: 101-108.
28. Zaragoza, O., and A. Casadevall. 2004. Experimental modulation of capsule size in *Cryptococcus neoformans*. *Biol Proced Online* 6: 10-15.

29. Wopereis, S., D.J. Lefeber, E. Morava, and R.A. Wevers. 2006. Mechanisms in protein *O*-glycan biosynthesis and clinical and molecular aspects of protein *O*-glycan biosynthesis defects: a review. *Clin. Chem.* 52: 574-600.
30. Wells, L., and G.W. Hart. 2003. *O*-GlcNAc turns twenty: functional implications for post-translational modification of nuclear and cytosolic proteins with a sugar. *FEBS Lett.* 546: 154-158.
31. Nishikawa, S., A. Hirata, and A. Nakano. 1994. Inhibition of endoplasmic reticulum (ER)-to-Golgi transport induces relocalization of binding protein (BiP) within the ER to form the BiP bodies. *Mol. Biol. Cell* 5: 1129-1143.
32. Levine, T.P., C.A. Wiggins, and S. Munro. 2000. Inositol phosphorylceramide synthase is located in the Golgi apparatus of *Saccharomyces cerevisiae*. *Mol. Biol. Cell* 11: 2267-2281.
33. Gemmill, T. R., and R. B. Trimble. 1999. Overview of *N*- and *O*-linked oligosaccharide structures found in various yeast species. *Biochim. Biophys. Acta* 1426: 227-237.
34. Jars, M.U., S. Osborn, J. Forstrom, and V.L. MacKay. 1995. *N*- and *O*-glycosylation and phosphorylation of the bar secretion leader derived from the barrier protease of *Saccharomyces cerevisiae*. *J. Biol. Chem.* 270: 24810-24817.
35. Trimble, R.B., C. Lubowski, C.R. Hauer 3rd, R. Stack, L. McNaughton, T.R. Gemmill, and S.A. Kumar. 2004. Characterization of *N*- and *O*-linked glycosylation of recombinant human bile salt-stimulated lipase secreted by *Pichia pastoris*. *Glycobiology* 14: 265-274.

36. Jigami, Y., and T. Odani. 1999. Mannosylphosphate transfer to yeast mannan. *Biochim. Biophys. Acta* 1426: 335-345.
37. Mulder, H., F. Dideberg, H. Schachter, B.A. Spronk, M. De Jong-Brink, J.P. Kamerling, and J.F. Vliegthart. 1995. In the biosynthesis of *N*-glycans in connective tissue of the snail *Lymnaea stagnalis* of incorporation GlcNAc by beta 2GlcNAc-transferase I is an essential prerequisite for the action of beta 2GlcNAc-transferase II and beta 2Xyl-transferase. *Eur. J. Biochem.* 232: 272-283.
38. Stoeva, S., K. Idakieva, C. Betzel, N. Genov, and W. Voelter. 2002. Amino acid sequence and glycosylation of functional unit Rth2-e from *Rapana thomasiana* (gastropod) hemocyanin. *Arch. Biochem. Biophys.* 399: 149-158.
39. De Stefano, J.A., J.D. Myers, D. Du Pont, J.M. Foy, S.A. Theus, and P.D. Walzer. 1998. Cell wall antigens of *Pneumocystis carinii* trophozoites and cysts: purification and carbohydrate analysis of these glycoproteins. *J. Eukaryot. Microbiol.* 45: 334-343.
40. Xu, J., R. Vilgalys, and T.G. Mitchell. 2000. Multiple gene genealogies reveal recent dispersion and hybridization in the human pathogenic fungus *Cryptococcus neoformans*. *Mol. Ecol.* 9: 1471-1481.
41. Nielsen, K., G.M. Cox, P. Wang, D.L. Toffaletti, J.R. Perfect, and J. Heitman. 2003. Sexual cycle of *Cryptococcus neoformans* var. *grubii* and virulence of congenic alpha and alpha isolates. *Infect. Immun.* 71: 4831-4841.

42. Baker, L.G., C.A. Specht, M.J. Donlin, and J.K. Lodge. 2007. Chitosan, the deacetylated form of chitin, is necessary for cell wall integrity in *Cryptococcus neoformans*. *Eukaryot Cell* 6: 855-867.
43. Warren, R.L., Y.S. Butterfield, R.D. Morin, A.S. Siddiqui, M.A. Marra, and S.J. Jones. 2005. Management and visualization of whole genome shotgun assemblies using SAM. *BioTechniques* 38: 715-716, 718, 720.
44. Fraser, J.A., S.S. Giles, E.C. Wenink, S.G. Geunes-Boyer, J.R. Wright, S. Diezmann, A. Allen, J.E. Stajich, F.S. Dietrich, J.R. Perfect, and J. Heitman. 2005. Same-sex mating and the origin of the Vancouver Island *Cryptococcus gattii* outbreak. *Nature* 437: 1360-1364.
45. Kwon-Chung, K.J., J.C. Edman, and B.L. Wickes. 1992. Genetic association of mating types and virulence in *Cryptococcus neoformans*. *Infect. Immun.* 60: 602-605.

CHAPTER IV

MULTIMERIZATION OF A XYLOSYLPHOSPHOTRANSFERASE IN *CRYPTOCOCCUS NEOFORMANS*

Morgann C. Reilly

Department of Molecular Microbiology, Washington University School of Medicine,
St. Louis, MO 63110, USA.

ABSTRACT

The capsule of *Cryptococcus neoformans* is unique among pathogenic fungi and is considered to be the organism's primary virulence factor. In addition to the polysaccharide elements of the capsule, *C. neoformans* generates a number of other glycans and glycoconjugates. The composition of some of these structures has been studied in great detail; the enzymes responsible for their synthesis, however, remain largely unexplored. We recently identified and characterized the first described xylosylphosphotransferase, Xpt1p of *C. neoformans*, and determined its involvement in protein glycosylation. Here, we present preliminary evidence that suggests Xpt1p may act as part of a larger protein complex, multimerizing either with itself or other, heterologous proteins.

INTRODUCTION

Cryptococcus neoformans is an environmental yeast and an opportunistic fungal pathogen. Our laboratory is interested in studying the xylosyltransferase activity of this basidiomycete because previous studies determined that a mutant strain of *C. neoformans* that was unable to generate UDP-xylose (UDP-Xyl, the sole donor of all Xyl residues in the cell) was also no longer able to cause disease in a murine model of cryptococcal infection (1). In order to identify xylosyltransferases, we developed an activity assay using an UDP-[¹⁴C(U)]xylose (UDP-[¹⁴C]Xyl) donor and an α -1,3-D-mannobiose (α -1,3-Man₂) acceptor; the radiolabeled UDP-[¹⁴C]Xyl allows us to track any xylosylated products generated in our assay while the α -1,3-Man₂ corresponds to structures found in cryptococcal glycolipids, glycoproteins, and the capsule polysaccharides that may be linked to Xyl. Using membrane proteins prepared from a wild-type *C. neoformans* strain as the source of enzyme activity in this assay, we see the formation of two distinct products. One of these is Man- α (1→3)[Xyl- β (1→2)]-Man and is generated by the xylosyltransferases Cxt1p and Cxt2p (2).¹ The other is Xyl-P-Man- α (1→3)-Man (where P represents phosphate; (3)), formed by a second and highly unusual activity that is the focus of the studies detailed in this dissertation.

When we discovered the enzyme responsible for the formation of the Xyl-P-Man- α (1→3)-Man product, we named it Xpt1p, for xylosylphosphotransferase 1 (3). Our studies, reported in Chapter II of this thesis, determined that this glycosyltransferase specifically utilizes UDP-Xyl as the activated sugar donor. The enzyme also prefers to

transfer Xyl-P to a Man acceptor molecule, although this may be in multiple configurations. Finally, Xpt1p requires a metal ion cofactor for its activity, preferably manganese. Our report of Xpt1p and its product represented the first indication that a Xyl-P-Man modification existed in nature and we went on to investigate its function within the cryptococcal cell. In studies detailed in Chapter III of this thesis, we showed that Xpt1p xylosylates protein substrates found in preparations of cryptococcal cell lysates. We further verified the presence of Xyl-P-Man moieties in the *O*-linked glycans of wild-type cells that were absent in an *xpt1Δ* cell line.

Our studies outlined here suggest that Xpt1p functions as part of a larger protein complex. Similar complexes have been observed with the glycosyltransferase activities of other organisms. In some instances, a single catalytic protein may require the presence of one or more scaffolding proteins in order to function. This is the case with the oligosaccharyltransferase (OST) protein complex, which transfers GlcNAc₂Man₉Glc₃ from Dol-PP-GlcNAc₂Man₉Glc₃ to a particular asparagine residue of a nascent polypeptide as part of the *N*-linked protein glycosylation pathway. In *S. cerevisiae*, the OST is comprised of at least eight proteins: the highly conserved Stt3p harbors the transferase activity of the complex while the other seven proteins mediate the association of the diverse reaction substrates (4). In other instances, the formation of a polysaccharide structure involves the activities of several glycosyltransferases working in tandem and these enzymes exist in single complex of proteins. An example of this is when the ‘core’ structure of *N*-glycans in *S. cerevisiae* is modified by the actions of the

¹ J.S. Klutts and T.L. Doering, manuscript in preparation

mannan polymerase complexes I and II (M-Pol I and M-Pol II), which can extend a linear branch of α -1,6-linked Man up to sixty residues in length (5, 6). In this chapter we present several pieces of evidence suggesting that Xpt1p multimerizes either with itself or other, heterologous proteins.

EXPERIMENTAL PROCEDURES

Materials. UDP-[¹⁴C(U)]xylose (UDP-[¹⁴C]Xyl; 151 mCi/mmol) was from PerkinElmer and α -1,3-D-mannobiose (α -1,3-Man₂) was from Carbohydrate Synthesis (Oxford, United Kingdom). Unless specified, all other chemicals or reagents were obtained from Sigma Aldrich. Protease inhibitor cocktail I (PIC-I) included 1 mg/ml leupeptin, 2 mg/ml antipain, 0.1 M TLCK, 10 mg/ml Benzamidine, and 10,000 units/ml Traysylol (aprotinin) in water; protease inhibitor cocktail II (PIC-II) included 1mg/ml chymostatin and 1 mg/ml pepstatin in DMSO.

Strains and cell growth. *C. neoformans* strains (Table 1) were grown in liquid culture at 30°C in YPD medium (1% w/v yeast extract, 2% w/v peptone, 2% w/v dextrose) with shaking (230 rpm) or at 30°C on YPD agar plates (YPD medium with 2% w/v agar). As appropriate, media included 100 μ g/ml nourseothricin (NAT; from Werner BioAgents) and/or Geneticin[®] (G418; from Invitrogen).

Table 1. *C. neoformans* strains used in these studies.

Name ^{a,b}	Origin
CAP67 <i>ctx1</i> Δ	Klutts <i>et al.</i> 2007 (1)
CAP67 <i>ctx1</i> Δ <i>ctx2</i> Δ	J.S. Klutts and T.L. Doering, manuscript in preparation
KN99 α	Kwon-Chung <i>et al.</i> 1992 (13)
KN99 α <i>xpt1</i> Δ	Reilly <i>et al.</i> 2009 (3)
KN99 α <i>xpt1</i> Δ p <i>XPT1</i>	Reilly <i>et al.</i> 2009 (3)
KN99 α <i>xpt1</i> Δ p <i>XPT1-HA</i>	Reilly <i>et al.</i> 2009 (3)

^a All strains are MAT α

^b All KN99 strains are serotype A; all CAP67 strains are serotype D

Total membrane preparation and detergent extraction. *C. neoformans* membranes and their detergent extracts were prepared as in (3). Briefly, cells from an overnight culture were washed in Tris-EDTA Buffer (100 mM Tris-HCl pH 8.0, 0.1 mM EDTA), broken with glass beads, and the resulting lysate subjected to a clearing centrifugation step. Total membranes were isolated from the resulting supernatant fraction by ultracentrifugation and resuspended in Tris Buffer (100 mM Tris-HCl pH 8.0). For protein purification studies only, the membranes were again resuspended in the same buffer and sedimented by ultracentrifugation in a wash step. The membranes were then treated with 1% Triton X-100, subjected to ultracentrifugation, and the resulting supernatant stored at 4°C. Protein concentration of the total or washed membranes was determined using the Bio-Rad Protein Assay (Bio-Rad Laboratories) while protein concentration of the Triton X-100 extract of membranes was determined using the Bio-Rad Detergent Compatible Protein Assay (Bio-Rad Laboratories). For some studies, the protease inhibitor cocktails PIC-I and PIC-II were added to the samples prior to cell lysis at a dilution of 1:1000.

Xylosyltransferase activity assays. Enzyme activity was assayed by monitoring the transfer of [¹⁴C]Xyl from a UDP-[¹⁴C]Xyl donor to an α -1,3-Man₂ acceptor as in (3). Briefly, reactions containing 625 μ g protein (from *C. neoformans* total membranes or Triton X-100-extracts), 1 μ M UDP-[¹⁴C]Xyl, 8.8 mM α -1,3-Man₂, and 7.5 mM MnCl₂ in 100 mM Tris-HCl pH 6.5 were incubated overnight at 20°C. Unincorporated radiolabel was removed using AG[®] 2-X8 resin (Bio-Rad) and the xylosylated products were resolved by thin layer chromatography (TLC) on Silica Gel 60 plates (EM Sciences), and

developed in a solvent system of 5:4:1 1-propanol:acetone:water. TLC plates were sprayed with En³Hance[®] Spray (PerkinElmer) and the radiolabeled reaction products visualized by autoradiography.

Protein purification studies. All steps were performed at 4°C and using pre-chilled buffers. Triton X-100 extracts (2-4 ml; ~15 mg/ml) of washed membranes were prepared from a 1 L culture of CAP67 *cxt1Δ cxt2Δ* as above. The sample was filtered using a CoStar[®] Spin-X[®] Centrifuge Tube Filter (0.22 μm cut-off; from Corning) and loaded onto a 20-ml HiPrep 16/10 Q-Sepharose Fast Flow column (GE Healthcare) that had been pre-equilibrated with Q1 Buffer (20 mM Tris-HCl pH 8.0, 0.1 mM EDTA, 0.05% TritonX-100, and 100 mM NaCl). The column was first washed with 200 ml Q1 Buffer and then eluted with a 200-ml gradient from Q1 Buffer to Q2 Buffer (20 mM Tris-HCl pH 8.0, 0.1 mM EDTA, 0.05% TritonX-100, and 2 M NaCl) that was collected in 4-ml fractions. Aliquots (40 μl) from each fraction were assayed for xylosyltransferase activity as above; reaction products were quantified using ScintiSafe[™] Econo 1 (Fisher) and an LS 6000 CI Scintillation Counter (Beckman). Those fractions corresponding to the peak of xylosyltransferase activity were pooled and concentrated to 0.5-1 ml using an Amicon[®] Ultra-15 Centrifugal Filter Device (30,000 MWCO; from Millipore).

The concentrated Q-Sepharose peak activity fractions sample was filtered using a CoStar[®] Spin-X[®] filter and applied to a 316-ml HiPrep 26/60 Sephacryl S-300 Gel Filtration Column (GE Healthcare) that was pre-equilibrated with S1 Buffer (100 mM Tris-HCl pH 8.0, 0.1 mM EDTA, 0.05% TritonX-100, and 500 mM NaCl) and had been previously calibrated using a Gel Filtration HMW Calibration Kit (GE Healthcare). The

column was eluted with 253 ml (0.8 column volume) of S1 Buffer, with the first 95 ml going to waste (void volume) and the remaining 158 ml collected into 4-ml fractions. As the high salt content of the S1 Buffer interferes with the ability of the AG[®] 2-X8 resin to remove unincorporated UDP-[¹⁴C]Xyl label from the reactions, aliquots from the Sephacryl S-300 column fractions were transferred to Slide-A-Lyzer Mini Dialysis Units (10 kDa MWCO; from Pierce) and dialyzed against Tris Buffer for 1 hr prior to being assayed for xylosyltransferase activity by scintillation counting as above. Fractions corresponding to the peak of xylosyltransferase activity were pooled, concentrated to 0.5-1 ml, diluted 10-fold with Tris Buffer, and again concentrated using an Amicon[®] Ultra-15 Centrifugal Filter Device (30,000 MWCO).

The concentrated Sephacryl S-300 peak activity fractions sample was brought up to a volume of 5 ml using M1 Buffer (20 mM Tris-HCl pH 8.0, 0.1 mM EDTA, and 0.01% TritonX-100) and applied to a 5-ml column of a custom-synthesized α -1,3-Man₂-agarose resin (Carbohydrate Synthesis) that was pre-equilibrated with M1 Buffer. The column was capped and allowed to rock overnight at 4°C. The column was then washed with 40 ml M1 Buffer, followed by 50 ml M2 Buffer (20 mM Tris-HCl pH 8.0, 0.1 mM EDTA, 0.01% TritonX-100, and 5 mM NaCl), and eluted with a 25-ml gradient of M2 Buffer to M3 Buffer (20 mM Tris-HCl pH 8.0, 0.1 mM EDTA, 0.01% TritonX-100, and 250 mM NaCl) collected in 0.8-ml fractions. Fractions were assayed by scintillation counting as above and those corresponding to the peak of xylosyltransferase activity were pooled and concentrated to 0.5-1 ml using an Amicon[®] Ultra-15 Centrifugal Filter Device (30,000 MWCO).

Immunoprecipitation studies. Detergent-extracts of total membranes from KN99 α *xpt1* Δ p*XPT1* and KN99 α *xpt1* Δ p*XPT1-HA* were prepared as above. Each sample (5 mg total protein) was rotated for 1 hr at 4°C with 50 μ l Anti-HA MicroBeads from the μ MACS™ HA Epitope Tag Protein Isolation Kit (Miltenyi Biotec) in a total of 500 μ l Tris-EDTA Buffer. The sample was then applied to a μ Column placed in the magnetic field of a μ MACS Separator and the column washed with 200 μ l Tris Buffer five times. To prepare the material associated with the Anti-HA MicroBeads for elution, 20 μ l CAPS Buffer (100 mM CAPS pH 11.9, 0.1% Triton X-100) was applied to the column and incubated for 5 min. Then 100 μ l CAPS Buffer was applied to the column and the eluate was collected in a tube containing 6 μ l MES Buffer (1 M MES pH 2.9).

Half of each μ Column eluate was assayed for xylosyltransferase activity by TLC as above. The remainder of each eluate was resolved by SDS-PAGE on a 10% gel according to standard methods (7) and then transferred to a 0.2 μ m nitrocellulose membrane using the Transblot SD Semi-dry Transfer Cell (BioRad). The blot was developed using the primary antibody Anti-HA High Affinity Rat Monoclonal IgG (Roche) at 50 ng/ml in 3% dry milk in TBS pH 8.0, the secondary antibody Anti-RAT Goat Polyclonal IgG-Peroxidase (Sigma Aldrich) at 1 ng/ml in 3% dry milk in TBS, and the Western Lightning®-ECL Kit (PerkinElmer) according to standard methods (8).

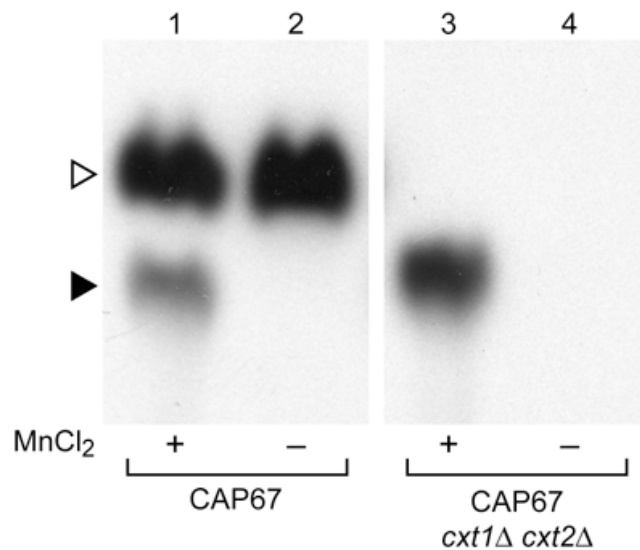


Figure 1. Xylosyltransferase activities of *C. neoformans*. Total membranes prepared from CAP67 and CAP67 *cxt1*Δ *cxt2*Δ cells were assayed as described in the Experimental Procedures with UDP-[¹⁴C]Xyl and α-1,3-Man₂ in the presence (+) or absence (-) of MnCl₂ as indicated. Only a portion of an autoradiograph of the products resolved by TLC is shown: no signal was detected in other regions beyond minor amounts of free Xyl and no signal was detected in the absence of the α-1,3-Man₂ acceptor. In this and subsequent figures, the filled arrowhead indicates the product of Xpt1p and the open arrowhead indicates the products of the unrelated Cxt1p and Cxt2p. This figure is adapted from (3).

RESULTS

Protein purification of the manganese-dependent activity. Our studies of Xpt1p began when, using the xylosyltransferase assay outlined in the Experimental Procedures, we detected a manganese-dependent xylosyltransferase activity that generated a product distinct from that of the previously identified manganese-independent xylosyltransferases Cxt1p and Cxt2p (Figure 1, tracks 1-2) (9).¹ We initially attempted to identify the protein responsible for this activity by isolating it using traditional protein purification methods. In order to do this, we took advantage of an available CAP67 *cxt1*Δ *cxt2*Δ strain in which the manganese-dependent xylosyltransferase product was the only one visible in our xylosyltransferase assay (Figure 1, tracks 3-4), allowing us to track the activity by scintillation counting. Our initial purification scheme used a combination of detergent extraction, ion exchange chromatography, and gel filtration (see Experimental

Table 2. Partial purification of the manganese-dependent xylosyltransferase activity from CAP67 *cxt1*Δ *cxt2*Δ.

	Total protein (mg)	Total units^a	Specific activity (units/mg)	Purification factor (-fold)	Recovery (%)
1. Total membranes	102.3	51.3	0.5	---	---
2. Detergent extract	45.9	30.3	0.7	1.3	59
3. Anion exchange	6.5	3.6	0.6	1.1	7
4. Gel filtration	1.4	12.2	8.99	17.7	24
5. α -1,3-Man ₂ affinity resin	0.6	7.4	12.9	25.7	14

^a A unit is defined as the amount of enzyme that transfers 100 cpm of [¹⁴C]Xyl from UDP-[¹⁴C]Xyl to α -1,3-Man₂ per minute.

Supplemental Table 1. Affinity resins tested during protein purifications studies.

Resins
Hydrophobic interaction resins (GE Healthcare): butyl, octyl, low-substitution phenyl, high-substitution phenyl
Reactive dye-ligands (Sigma Aldrich): Blue 3GA, Blue 4, Brown 10, Green 19, Red 120, Yellow 86
α -1,3-Man ₂ coupled to agarose (Carbohydrate Synthesis)
Concanavalin A coupled to sepharose (GE Healthcare)
UDP coupled to agarose (Sigma Aldrich)
UDP-hexanolamine coupled to agarose (Sigma Aldrich)
Immobilized affinity chromatography select gel (Sigma Aldrich) charged with: CaCl ₂ , CoCl ₂ , CuCl ₂ , Fe(II)Cl ₂ , MgCl ₂ , MnCl ₂ , NiCl ₂ , ZnCl ₂

Procedures), but only enriched the activity of interest ~20-fold (Table 2). In an attempt to improve upon the initial isolation protocol, various affinity resins were tested (see Supplemental Table 1); of these materials, only the α -1,3-Man₂-agarose resin consistently enhanced purification of the manganese-dependent xylosyltransferase activity and this only modestly. Ultimately, the greatest improvements to the preliminary purification scheme were associated with the optimization of sample preparation and column operating conditions, including the buffer, pH, detergent, and salt concentrations of the extraction, wash, elution, and storage conditions used throughout the protocol. Unfortunately, the maximal enrichment of ~25-fold achieved in our studies was not enough to allow for the successful identification of a protein band whose concentration in a given fraction varied in correspondence with the detected levels of manganese-dependent xylosyltransferase activity.

Sizing of the manganese-dependent activity. Although purification studies did not identify the protein associated with the manganese-dependent xylosyltransferase activity,

we were able to garner other information regarding our activity of interest. Most importantly, the volume in which the manganese-dependent xylosyltransferase activity eluted from the Sephacryl S-300 gel filtration column allowed us to calculate an approximate molecular mass for the our activity of interest. Using commercially available standards, we were able to estimate the mass for the manganese-dependent

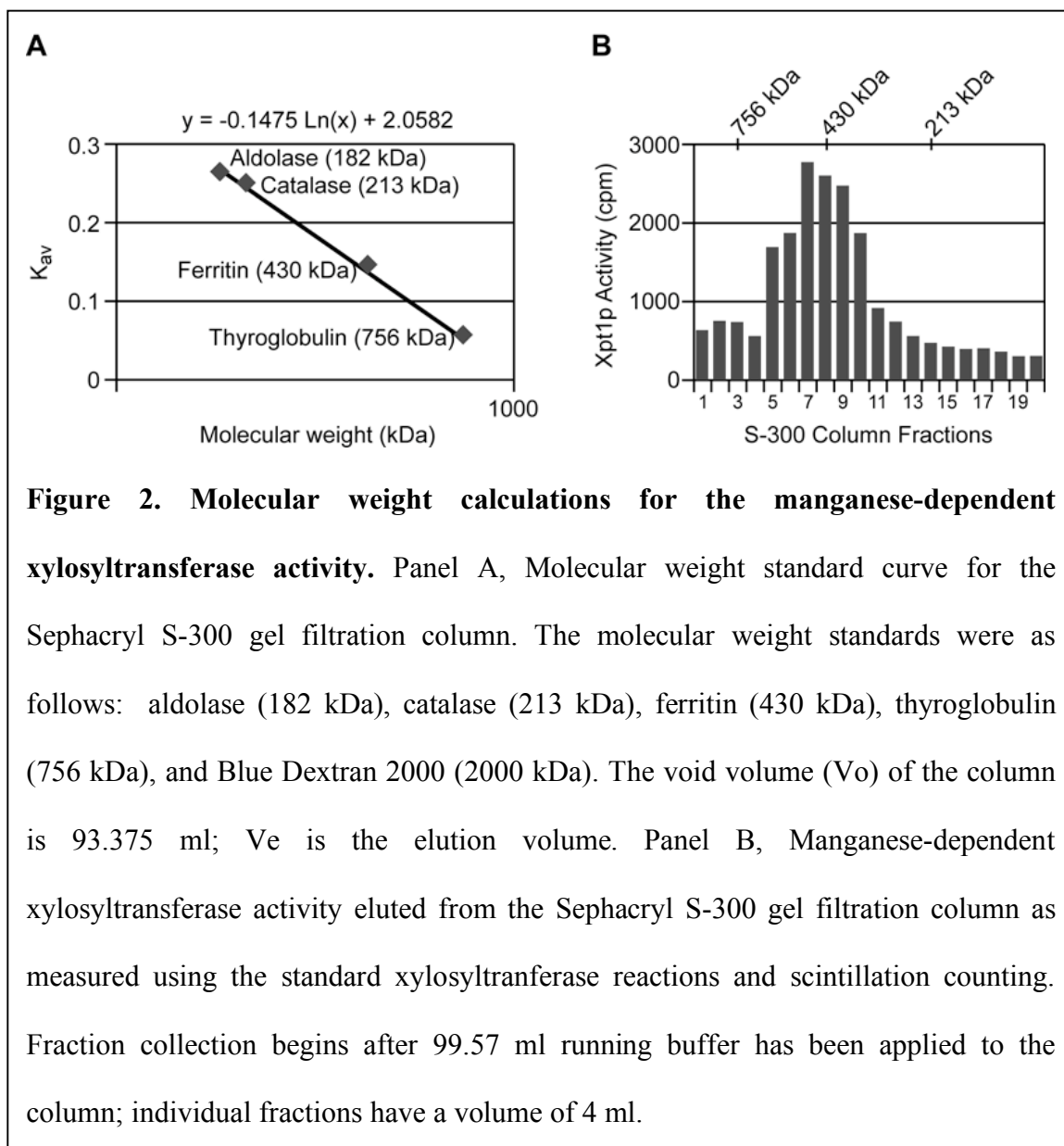


Figure 2. Molecular weight calculations for the manganese-dependent xylosyltransferase activity. Panel A, Molecular weight standard curve for the Sephacryl S-300 gel filtration column. The molecular weight standards were as follows: aldolase (182 kDa), catalase (213 kDa), ferritin (430 kDa), thyroglobulin (756 kDa), and Blue Dextran 2000 (2000 kDa). The void volume (V_o) of the column is 93.375 ml; V_e is the elution volume. Panel B, Manganese-dependent xylosyltransferase activity eluted from the Sephacryl S-300 gel filtration column as measured using the standard xylosyltransferase reactions and scintillation counting. Fraction collection begins after 99.57 ml running buffer has been applied to the column; individual fractions have a volume of 4 ml.

xylosyltransferase activity at ~440 kDa (Figure 2). This was unexpectedly large (see Discussion for further explanation).

Identification and analysis of Xpt1p. In the course of the purification studies described above, we determined the product of the manganese-dependent xylosyltransferase activity to be Xyl-P-Man- α (1 \rightarrow 3)-Man (3). The protein responsible for its formation was finally identified based on its homology to known glycosylphosphotransferases and named Xpt1p; this identity was confirmed by gene deletion and complementation studies (Figure 3). The mRNA transcript of *XPT1* was confirmed by analysis of cDNA sequence in combination with 5' and 3' RACE studies; this allowed us to predict the amino acid sequence of Xpt1p. When entered into several publicly available prediction programs, the Xpt1p sequence was estimated to generate a protein ~100 kDa in size. Given that the Sephacryl S-300 gel filtration column studies of the manganese-dependent xylosyltransferase activity had predicted a protein more than four times that size, we considered the possibility that Xpt1p might exist as either a homo- or hetero-oligomer.

Affinity purification of Xpt1p by epitope-tagging. In an effort to isolate Xpt1p, and possibly any binding partners, we took advantage of a strain engineered to express an HA-tagged form of the protein (KN99 α *xpt1* Δ p*XPT1-HA*). The C-terminal addition of the epitope tag (3) did not interfere with the strain's Xpt1p activity (Figure 3, compare lanes 5 and 7). Detergent-extracts of membrane material prepared from KN99 α *xpt1* Δ p*XPT1-HA* and KN99 α *xpt1* Δ p*XPT1* (as a control) were immunoprecipitated as in the Experimental Procedures. When the eluted material was run out on an SDS-PAGE gel

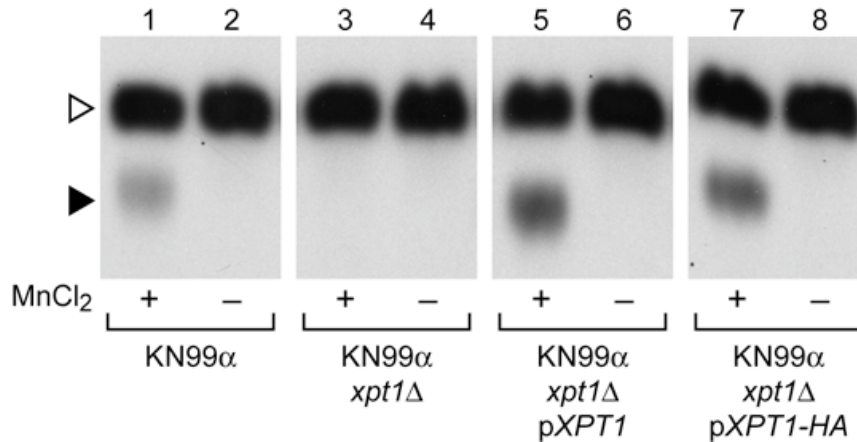


Figure 3. Deletion and complementation of *XPT1*. Xylosyltransferase activity assays were performed as in Figure 1 using total membranes from the wild-type (KN99 α), mutant (KN99 α *xpt1* Δ), or complemented mutant (KN99 α *xpt1* Δ *pXPT1* and KN99 α *xpt1* Δ *pXPT1-HA*) strains indicated. Symbols are as in Figure 1. This figure is from Chapter III.

and developed by immunoblot using an anti-HA antibody, bands were visible in the KN99 α *xpt1* Δ *pXPT1-HA* sample that were absent in the KN99 α *xpt1* Δ *pXPT1* sample (Figure 4). These bands ran at ~65 kDa, ~70 kDa, and ~100 kDa (Figure 4, lanes 2-3); the largest of these was close to the predicted size of the Xpt1p polypeptide. The addition of protease inhibitors during preparation of the membrane material did nothing to alter the observed banding pattern (data not shown). Because the Sephacryl S-300 gel filtration studies had indicated the manganese-dependent xylosyltransferase activity eluted as if it were ~440 kDa, the stacker portion of the gel and the wells were also transferred to the immunoblot, but there was no evidence of high molecular weight anti-HA antibody-reactive material (data not shown).

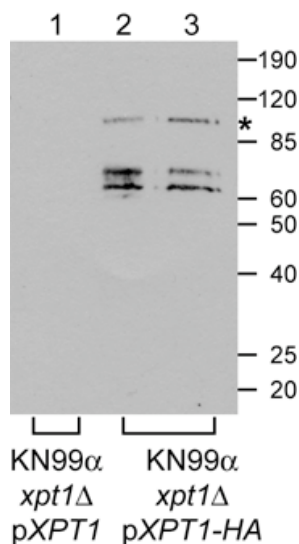
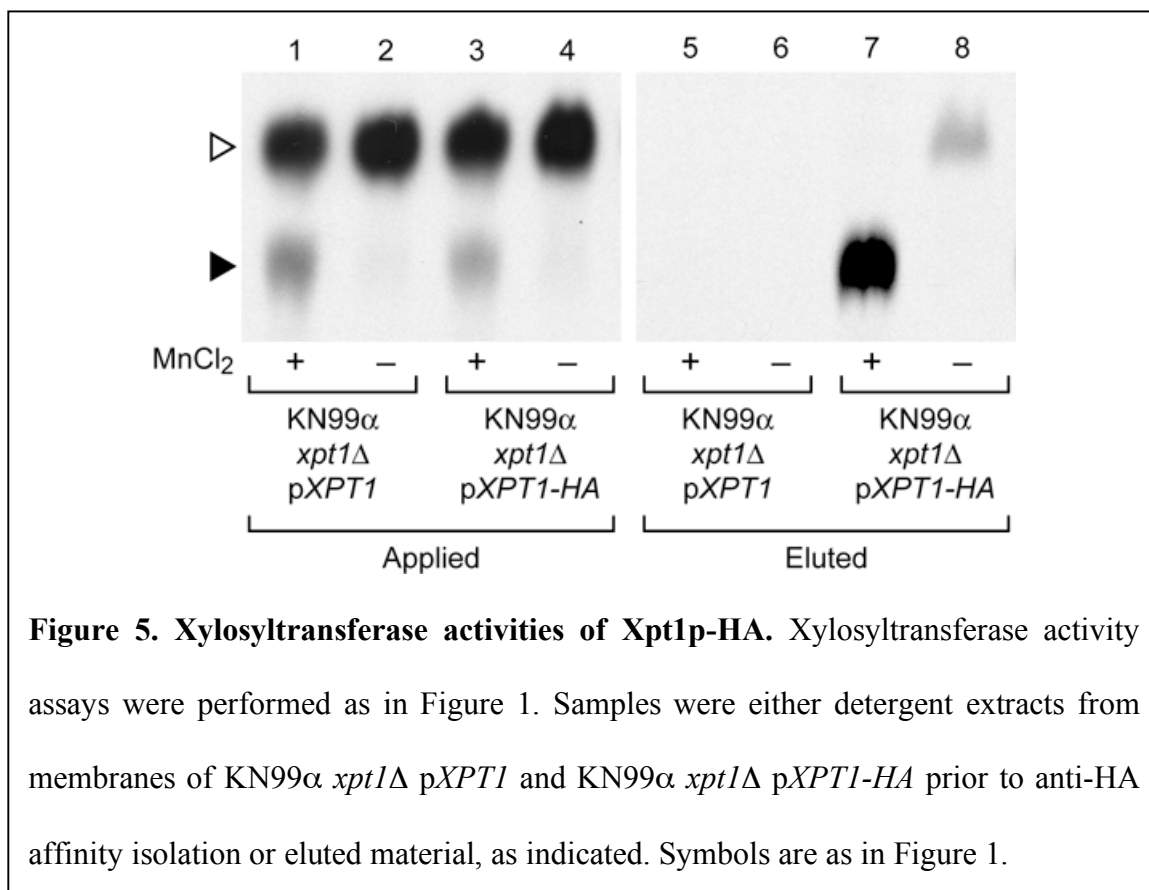


Figure 4. Immunoblot of Xpt1p-HA. Detergent extracts from membranes of KN99 α *xpt1* Δ *pXPT1* or KN99 α *xpt1* Δ *pXPT1-HA* were subjected to anti-HA affinity isolation as outlined in the Experimental Procedures. Material eluted from the columns was run on a 10% SDS-PAGE gel, transferred to nitrocellulose, and developed by immunoblot using an anti-HA antibody. Molecular weight standards (kDa) are indicated at the right. * indicates the predicted size of Xpt1p (100 kDa).

Finally, material eluted from both the control KN99 α *xpt1* Δ *pXPT1* and the tagged KN99 α *xpt1* Δ *pXPT1-HA* samples was evaluated by TLC for xylosyltransferase activity. Although both Cxt1p/Cxt2p and Xpt1p activity was visible in the detergent-extracts applied to the μ Columns (Figure 5, tracks 1-4), only the eluate from KN99 α *xpt1* Δ *pXPT1-HA* sample retained the Xpt1p activity (Figure 5, compare tracks 5 and 7). Unexpectedly, however, there was a trace of manganese-independent activity associated with the isolated material (Figure 5, track 8). This activity was not the result of non-



specific binding to the column material as it was present only in the KN99α *xpt1Δ* p*XPT1-HA* sample and not in the KN99α *xpt1Δ* p*XPT1* sample (Figure 5, compare tracks 6 and 8).

DISCUSSION

Data generated using a Sephacryl S-300 gel filtration column indicated that the manganese-dependent xylosyltransferase activity eluted at ~440 kDa (Figure 2). This was surprisingly large as most glycosyltransferases average around 50 kDa in size (as calculated using information obtained from the CAZy database). When we identified Xpt1p as the protein behind the manganese-dependent xylosyltransferase activity, we predicted the enzyme to be ~100 kDa given the amino acid sequence encoded by the *XPT1* transcript (3). Together, these data suggest to us that Xpt1p may function as part of a larger protein complex, multimerizing either with itself (forming a homo-oligomer) or with other proteins (forming a hetero-oligomer). This would not be unprecedented, as glycosyltransferases in other systems have been found in multi-protein complexes, like the OST complex (4) and M-Pol I/M-Pol II complexes (5, 6) of *S. cerevisiae*. Interestingly, the glycosylphosphotransferase whose sequence initially identified Xpt1p (the GlcNAc-1-phosphate transferase) itself has an $\alpha_2\beta_2\gamma_2$ subunit structure, with the catalytic portion contained in the α and β subunits while the γ subunits are thought to perform a regulatory function for the activity (10-12).

Immunoprecipitation studies performed using protein preparations from a KN99 α *xpt1* Δ *pXPT1-HA* strain provided additional insights into the possibility of Xpt1p interacting with other proteins. In assaying the immunoprecipitate samples for xylosyltransferase activity, we detected a second, manganese-independent activity in conjunction with Xpt1p-HA. As noted above, the enzyme responsible for this activity did not associate with the column material non-specifically as it was absent from the

untagged Xpt1p control samples. We do not believe this unexpected xylosylated product was synthesized by Xpt1p as it has never been observed in any *cxt1Δ cxt2Δ* strain preparations (Figure 1, tracks 3-4), regardless of variation in the temperature, pH, or other reaction components (data not shown). Interestingly, the product of this mystery activity migrates on the TLC at roughly the same position as the product of the Cxt1p/Cxt2p activities, though additional studies are needed to verify this possibility. Together, these data suggest that at least one other protein associates with Xpt1p in the cell.

Finally, we observed three distinct protein bands on the immunoblot of material isolated by immunoprecipitation of Xpt1p-HA from cell membranes (Figure 4). The largest band, at ~100 kDa, is most likely full-length Xpt1p-HA given its amino acid sequence and predicted size. We do not think the two smaller bands, at ~65 kDa and ~70 kDa, are non-specific degradation products of Xpt1p as their presence is not impacted by the inclusion of protease inhibitors during the experiment (data not shown). These data raise the possibility that Xpt1p may undergo some kind of processing following translation. At this time we cannot conclude which of the three bands might be responsible for the manganese-dependent xylosyltransferase activity.

The experiments presented here support the possibility that Xpt1p acts as part of a larger protein complex, either associating with other enzymes that perform distinct functions (as suggested by the data in Figure 5) or multimerizing with itself, potentially following processing of the protein (as suggested by the data in Figure 4). Additional studies are needed to directly address each of these possibilities. Approaches to these questions are outlined in detail in the Future Directions section of Chapter V.

ACKNOWLEDGEMENTS

The author thanks J. Stacey Klutts and David Haslam for technical assistance and thoughtful discussions on this project.

ABBREVIATIONS USED

GlcNAc, N-acetylglucosamine; GXM, glucuronoxylomannan; GXMGal, glucuronoxylomannogalactan; G418, geneticin; HA, hemagglutinin; Man, mannose; M-Pol, mannan polymerase complex; NAT, nourseothricin; OST, oligosaccharyltransferase; P, phosphate; RACE, rapid amplification of cDNA ends; TLC, thin layer chromatography; Xyl, xylose.

REFERENCES

1. Moyrand, F., B. Klaproth, U. Himmelreich, F. Dromer, and G. Janbon. 2002. Isolation and characterization of capsule structure mutant strains of *Cryptococcus neoformans*. *Mol. Microbiol.* 45: 837-849.
2. Klutts, J.S., S.B. Levery, and T.L. Doering. 2007. A beta-1,2-xylosyltransferase from *Cryptococcus neoformans* defines a new family of glycosyltransferases. *J. Biol. Chem.* 282: 17890-17899.
3. Reilly, M.C., S.B. Levery, S.A. Castle, J.S. Klutts, and T.L. Doering. 2009. A novel xylosylphosphotransferase activity discovered in *Cryptococcus neoformans*. *J. Biol. Chem.* [online].
4. Lennarz, W.J. 2007. Studies on oligosaccharyl transferase in yeast. *Acta Biochim. Pol.* 54: 673-677.
5. Jungmann, J., and S. Munro. 1998. Multi-protein complexes in the *cis* Golgi of *Saccharomyces cerevisiae* with alpha-1,6-mannosyltransferase activity. *EMBO J.* 17: 423-434.
6. Jungmann, J., J.C. Rayner, and S. Munro. 1999. The *Saccharomyces cerevisiae* protein Mnn10p/Bed1p is a subunit of a Golgi mannosyltransferase complex. *J. Biol. Chem.* 274: 6579-6585.
7. Gallagher, S.R. 2006. One-dimensional SDS gel electrophoresis of proteins. *Curr. Protoc. Mol. Biol.* Chapter 10: Unit 10.2A.
8. Gallagher, S., S.E. Winston, S.A. Fuller, and J.G. Hurrell. 2008. Immunoblotting and immunodetection. *Curr. Protoc. Mol. Biol.* Chapter 10: Unit 10.8.

9. Klutts, J.S., and T.L. Doering. 2008. Cryptococcal xylosyltransferase 1 (Cxt1p) from *Cryptococcus neoformans* plays a direct role in the synthesis of capsule polysaccharides. *J. Biol. Chem.* 283: 14327-14334.
10. Kudo, M., M. Bao, A. D'Souza, F. Ying, H. Pan, B.A. Roe, and W.M. Canfield. 2005. The alpha- and beta-subunits of the human UDP-N-acetylglucosamine:lysosomal enzyme N-acetylglucosamine-1-phosphotransferase are encoded by a single cDNA. *J. Biol. Chem.* 280: 36141-36149.
11. Raas-Rothschild, A., V. Cormier-Daire, M. Bao, E. Genin, R. Salomon, K. Brewer, M. Zeigler, H. Mandel, S. Toth, B. Roe, A. Munnich, and W.M. Canfield. 2000. Molecular basis of variant pseudo-hurler polydystrophy (mucopolidosis IIIC). *J. Clin. Invest.* 105: 673-681.
12. Pohl, S., S. Tiede, M. Castrichini, M. Cantz, V. Gieselmann, and T. Braulke. 2009. Compensatory expression of human N-Acetylglucosaminyl-1-phosphotransferase subunits in mucopolidosis type III gamma. *Biochim. Biophys. Acta.* 1792: 221-225.
13. Kwon-Chung, K.J., B.L. Wickes, L. Stockman, G.D. Roberts, D. Ellis, and D.H. Howard. 1992. Virulence, serotype, and molecular characteristics of environmental strains of *Cryptococcus neoformans* var. *gattii*. *Infect. Immun.* 60: 1869-1874.

CHAPTER V

FUTURE DIRECTIONS AND CONCLUSIONS

Morgann C. Reilly

Department of Molecular Microbiology, Washington University School of Medicine,
St. Louis, MO 63110, USA.

FUTURE DIRECTIONS

I have identified a novel xylosylphosphotransferase activity in the fungal pathogen *Cryptococcus neoformans* and determined the enzyme responsible for it (Chapter II). Additional characterization of the protein is needed in terms of identifying those regions and residues necessary for its enzymatic activity and, possibly, processing. I am also intrigued by the possibility that Xpt1p acts as part of a larger protein complex, multimerizing either with itself or other proteins while in the cell (Chapter IV). Furthermore, I have shown that Xpt1p is involved in the synthesis of *O*-linked protein glycans (Chapter III). I am interested in determining if Xpt1p plays any role in the synthesis of *N*-linked protein glycans and identifying those proteins targeted by its activities. I would also like to explore the hypothesis that this unusual enzyme is required for survival of this organism in the environment.

Activity of Xpt1p

In Chapter II, I determined the preferred donor of Xpt1p by testing a panel of nucleotide sugars: GDP-[³H]mannose, UDP-[³H]glucose, UDP-[³H]galactose, UDP-[³H]glucuronic acid, UDP-[³H] N-acetylglucosamine, and UDP-[¹⁴C]xylose. Of these, I found that only UDP-xylose (UDP-Xyl) functioned as a substrate of Xpt1p in my transferase activity assay. As noted in the Discussion of Chapter II, however, I cannot exclude the possibility that my enzyme of interest utilizes an uncommon nucleotide sugar donor that I did not test. To address this, I propose analyzing the nucleotide sugars present in wild-type KN99 α cells by mass spectrometry using methods similar to those in (1). If *C. neoformans* is found to generate any unusual nucleotide sugars, it would be prudent to then test them in my transferase assay. I recognize that the pool

of nucleotide sugars generated by the cell can change depending on growth conditions; therefore, should later studies determine that Xpt1p is preferentially expressed under a given growth condition, I would need to repeat this nucleotide sugar analysis.

I used the results of an immunoprecipitation experiment (Chapter II, Figure 9) as evidence that UDP-Xyl serves as the source of both the phosphate and sugar moieties of the Xpt1p product, Xyl-P-Man (where P represents phosphate and Man represents mannose). A more direct means of addressing the source of the phosphate residue would require the generation of a radiolabeled UDP-Xyl in which the phosphate was radioactive: UD[³²P]-Xyl. This nucleotide sugar is not commercially available and would have to be synthesized from UD[³²P]-Glc as in Figure 10 of Chapter I, using the cryptococcal UDP-Glc dehydrogenase (Ugd1; (2)) and UDP-GlcA decarboxylase (Uxs1; (3)), both of which have been purified in their active forms in the Doering laboratory. If UD[³²P]-Xyl could be generated, I would then include it in my transferase assays to demonstrate the source of the phosphate moiety in the Xpt1p product.

Necessary regions and residues.

As mentioned in Chapter I, DXD motifs have been implicated in the binding of metal ions by those glycosyltransferases that require cofactors for their activity (4). I am interested in determining which of several potential DXD sites in the amino acid sequence of Xpt1p is necessary for activity of the enzyme. To do this would require expression of p*XPT1* with the necessary point mutations introduced into a KN99α *xpt1Δ* background. The DXD sites would be selected in part based on their conservation among the predicted protein sequence encoded by *XPT1* in the genomes of serotype A (locus *CNAG_04860*; from the *C. neoformans* var. *grubii* H99 database main-

tained by the Broad Institute), serotype B (locus *CNBG_5687*; from the *C. gattii* R265 Database maintained by the Broad Institute), and serotype D (locus *CNJ02890*; from the *C. neoformans* var. *neoformans* JEC21 Database maintained by TIGR). The activity of the DXD mutant proteins would be compared to wild-type using my standard xylosyltransferase assay.

There is also the intriguing idea of a conserved phosphate transfer region, the region described by Kudo (5) in relation to the α/β subunit of UDP-GlcNAc phosphotransferase and by Sperisen (6) in relation to various glycosyltransferases with a role in capsule production. Similarly to the selection of possible DXD sites in Xpt1p, residues potentially involved in the transfer of phosphate would be selected based on the alignment of predicted Xpt1p sequence from Serotypes A, B, and D for conserved residues in conjunction with comparisons to the protein sequences examined in the aforementioned papers. I would then proceed to express a p*XPTI* construct with the desired point mutations in a KN99 α *xpt1* Δ background and assess xylosyltransferase activity.

Multimerization of Xpt1p

I have some intriguing data to suggest that Xpt1p may act as part of a larger protein complex, multimerizing either with itself or other proteins in the cell. Although the manganese-dependent xylosyltransferase activity of Xpt1p elutes from a gel filtration column at a volume indicative of a ~440 kDa protein (Chapter IV, Figure 2), the amino acid sequence of the *XPTI* transcript predicts a ~100 kDa protein (Chapter II, Discussion). The results of an immunoprecipitation experiment only furthered my speculation that Xpt1p may not function as a monomer: immunoprecipita-

tion of Xpt1p-HA led to the isolation of three distinct anti-HA reactive protein bands, running at ~65 kDa, ~70 kDa, and ~100 kDa (Chapter IV, Figure 4). Furthermore, when assayed for xylosyltransferase activity, these samples generated not only the expected product of Xpt1p but also a second, manganese-independent product (Chapter IV, Figure 5).

The immunoprecipitated material should be run on a native gel to see if I have been able to isolate anything close to the ~440 kDa size indicated by the gel filtration column. This could also tell me whether Xpt1p is associated with other proteins. I am interested in scaling-up the immunoprecipitation reactions such that any isolated protein can be visualized by staining an SDS gel and then submitted for identification by mass spectrometry and N-terminal sequencing. The largest band seen on the immunoblot in Figure 4 of Chapter IV runs under denaturing conditions near the size predicted for full-length Xpt1p. It seems unlikely that the two smaller bands are non-specific degradation products as the inclusion of proteases in the reactions had no impact on their formation. If Xpt1p does undergo some kind of processing, it could be interesting to explore if this cleavage is necessary for the xylosylphosphotransferase activity, possibly by targeting conserved residues immediately adjacent to the cleavage site to prevent this activity. Generation of a strain expressing a C-terminally epitope-tagged Xpt1p would allow us to determine if both halves of the processed protein are maintained. Alternatively, expression of two differentially tagged forms of Xpt1p in the same cell could let us explore the possible self-oligomerization of the protein.

The second, manganese-independent xylosyltransferase product that was isolated in association with Xpt1p-HA migrates on the TLC plate similarly to the product

of Cxt1p and Cxt2p (Chapter IV, Figure 5). In order to determine if either Cxt1p or Cxt2p is responsible for generating this second product, I can introduce the p*XPT1-HA* plasmid into available strain backgrounds lacking *CXT1* and/or *CXT2*. If the formation of the second product corresponds with either of these proteins, I would proceed to express Xpt1p-HA in a strain engineered to express (non-HA) epitope-tagged forms of Cxt1p and/or Cxt2p. This would allow me to track both Xpt1p and Cxt1p/Cxt2p in a series of co-immunoprecipitation studies. Should the activities of Cxt1p and Cxt2p not prove responsible for the manganese-independent xylosyltransferase activity I have observed, scaling up the immunoprecipitation assays might allow for the isolation of interacting protein(s) that, if visible by staining an SDS gel, could then be identified mass spectrometry.

I am also interested in expressing the cDNA of *XPT1* in a heterologous system such as *Saccharomyces cerevisiae*. This would allow me to determine if Xpt1p requires other proteins for activity, either because it is processed by another protein or because its activity requires association with other proteins. If Xpt1p can function in a heterologous system, this may also be useful for isolating pure protein and determining the kinetics of this unusual enzyme.

Protein glycosylation

While trying to identify the biological role of Xpt1p, I determined that the enzyme is capable of glycosylating polypeptide substrates (Chapter III, Figure 4). With collaborators, I subsequently evaluated the *O*-linked glycan modifications of *C. neoformans* and found that there was a broad and significant decrease in the amount of *O*-glycans isolated from *xpt1*Δ cells compared to wild-type (Chapter III, Figure 5). In an

extension of this work, I would like to more fully characterize the major *O*-linked glycan structures of *C. neoformans*, which has not been done before. Although the mass spectrometry work we have already done (Chapter III and data not shown) indicates the overall pattern of this glycosylation, full characterization of the structures will require composition and linkage analysis of some of the observed species. I am also interested in evaluating the structures of *N*-linked glycans, both in order to determine if Xpt1p plays any role in their synthesis, and to generate a profile of the major *N*-glycans of *C. neoformans*, which are currently unexplored. In depth analysis of both the *N*- and *O*-linked glycans of *C. neoformans* will require significant input from our collaborators.

I am interested in identifying the *C. neoformans* proteins that carry this unusual Xyl-P-Man modification generated by Xpt1p. In some of the gels looking at protein modifications by Xpt1p (Chapter III, Figure 4), individual bands can be seen. I have not yet explored the possibility that these proteins are abundant enough among the total membranes samples used that they could be visualized on SDS-PAGE by staining and subsequently identified by mass spectrometry. Of course, it is possible that Xpt1p is only targeting these proteins because they are present in my assay and they do not represent the native targets of its activity. In this case, I would consider attempting to generate an antibody specific to the Xyl-P-Man modification. This could then be used to pull-down Xpt1p-modified proteins by immunoprecipitation or to follow the modification in fractionations of total membrane samples.

Biological role of Xpt1p

From our studies using an inhalation murine model of cryptococcal infection (Chapter III), I know that Xpt1p is not required by the organism to survive in the lungs of mice for short periods of time. I could expand our studies to see if Xpt1p is needed during longer periods of infection, perhaps for dissemination of *C. neoformans* from the lungs to the brain. I would also like to explore the hypothesis that this enzyme (possibly by means of its target proteins) is required for survival of this organism in the environment. Xpt1p has been maintained among all four members of the *C. neoformans* species complex and has homologs in the genomes of two other environmental yeasts, the basidiomycete plant pathogens, *Postia placenta* (brown wood rot) and *Ustilago maydis* (corn smut). I would like to see if I could detect a similar xylosyltransferase activity to Xpt1p in *P. placenta* and *U. maydis*. I can also explore the expression pattern of *C. neoformans* *XPT1* using microarray data that have been generated for other projects in our laboratory and is available for analysis. Preliminary examination indicates that *XPT1* is expressed at very low levels under all conditions tested so far,¹ though I do know that the Xpt1p activity is detectable in most of these conditions.

¹ B.C. Haynes, personal communication

CONCLUSIONS

Cryptococcosis is an AIDS-defining illness and the causative agent, *C. neoformans*, is a fascinating example of an opportunistic pathogen. The organism is able to survive for extended periods of time in the environment, in association with soil, trees, and avian excreta, as well as within the human body. Studies of glycosynthetic pathways in *C. neoformans* began because the organism possesses an extensive polysaccharide capsule that is absolutely required for its virulence in the host. The field has since grown to encompass the biosynthesis of numerous glycans and glycoconjugates within the cell, many of which are unique to *C. neoformans* compared to its human host and are needed for full virulence in models of infection. Here, I have explored the role of a single glycosyltransferase whose activity, the transfer of Xyl-P to a Man substrate, appears to be completely novel. In my efforts to identify the function of this unusual enzyme within the cell, I have initiated a survey of the many protein-linked glycan structures of *C. neoformans* and have already noticed both intriguing similarities to and differences from other model yeast organisms and humans. I have only begun to elucidate the function of this unusual enzyme and look forward to seeing its role in cryptococcal biology further defined.

ACKNOWLEDGEMENTS

The author thanks Aki Yoneda for many thoughtful discussions over the years on this project.

ABBREVIATIONS USED

Man, mannose; P, phosphate; Xyl, xylose.

REFERENCES

1. Griffith, C.L., J.S. Klutts, L. Zhang, S.B. Levery, and T.L. Doering. 2004. Dec 3. UDP-glucose dehydrogenase plays multiple roles in the biology of the pathogenic fungus *Cryptococcus neoformans*. *J. Biol. Chem.* 279: 51669-51676.
2. Bar-Peled, M., C. L. Griffith, J. J. Ory, and T. L. Doering. 2004. Jul 1. Biosynthesis of UDP-GlcA, a key metabolite for capsular polysaccharide synthesis in the pathogenic fungus *Cryptococcus neoformans*. *Biochem. J.* 381: 131-136.
3. Bar-Peled, M., C.L. Griffith, and T.L. Doering. 2001. Functional cloning and characterization of a UDP-glucuronic acid decarboxylase: the pathogenic fungus *Cryptococcus neoformans* elucidates UDP-xylose synthesis. *Proc. Natl. Acad. Sci. U.S.A.* 98: 12003-12008
4. Qasba, P.K., B. Ramakrishnan, and E. Boeggeman. 2005. Substrate-induced conformational changes in glycosyltransferases. *Trends Biochem. Sci.* 30: 53-62.
5. Kudo, M., M. Bao, A. D'Souza, F. Ying, H. Pan, B.A. Roe, and W.M. Canfield. 2005. The alpha- and beta-subunits of the human UDP-N-acetylglucosamine:lysosomal enzyme N-acetylglucosamine-1-phosphotransferase are encoded by a single cDNA. *J. Biol. Chem.* 280:3 6141-36149.
6. Sperisen, P., C.D. Schmid, P. Bucher, and O. Zilian. 2005. Stealth proteins: *in silico* identification of a novel protein family rendering bacterial pathogens invisible to host immune defense. *PLoS Comput. Biol.* 1: e63.